AD-A195 118 SOME EFFECTS OF NITRATES ON THE TENSILE PROPERTIES OF 1/2
AL 7075-T7351(U) ARMY BELVOIR RESEARCH DEVELOPMENT AND
ENGINEERING CENTER FORT BELVOIR VA D HARRIS ET AL.
UNCLASSIFIED MAR 88 BRDEC-2461 F/G 11/6.1 NL

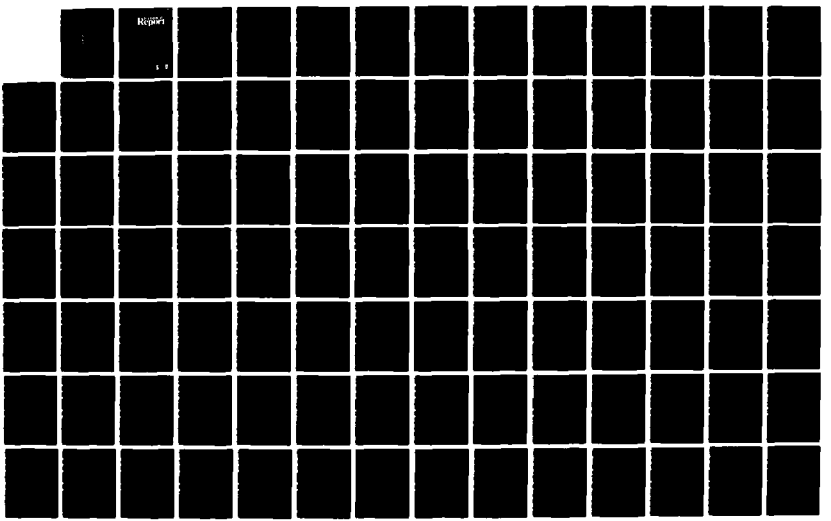

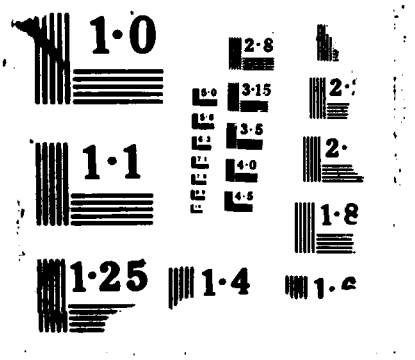
1·0
1·1
1·25
1·4
2·8
3·15
3·5
4·0
2·
2·
1·8

technical Report

United States Army
Belvoir Research, Development & Engineering Center
Fort Belvoir, Virginia 22060 5606

Report 2461

Some Effects of Nitrates on the Tensile Properties of Al 7075-T7351

Authored By: Donovan Harris
Chris Miller
Dario Emeric

Report Date: March 1988

Destroy this report when it is no longer needed.
Do not return it to the originator.

The citation in this report of trade names of commercially available products does not constitute official endorsement or approval of the use of such products.

Unclassified
SECURITY CLASSIFICATION OF THIS PAGE

ADA195118

REPORT DOCUMENTATION PAGE

Form Approved
OMB No 0704 0188

1a REPORT SECURITY CLASSIFICATION Unclassified	1b RESTRICTIVE MARKINGS None
2a SECURITY CLASSIFICATION AUTHORITY	3 DISTRIBUTION AVAILABILITY OF REPORT Approved for public release; distribution unlimited.
2b DECLASSIFICATION / DOWNGRADING SCHEDULE	
4 PERFORMING ORGANIZATION REPORT NUMBER(S) Report No. 2461	5 MONITORING ORGANIZATION REPORT NUMBER(S)
6a NAME OF PERFORMING ORGANIZATION Chemistry Research Group Materials, Fuels, and Lubricants 6b OFFICE SYMBOL (If applicable) STRBE-VC	7a NAME OF MONITORING ORGANIZATION
6c ADDRESS (City, State, and ZIP Code) Belvoir RD&E Center Fort Belvoir, VA 22060-5606	7b ADDRESS (City, State, and ZIP Code)
8a NAME OF FUNDING / SPONSORING ORGANIZATION 8b OFFICE SYMBOL (If applicable)	9 PROCUREMENT INSTRUMENT IDENTIFICATION NUMBER
8c ADDRESS (City, State, and ZIP Code)	10 SOURCE OF FUNDING NUMBERS PROGRAM ELEMENT NO / PROJECT NO / TASK NO / WORK UNIT ACCESSION NO

11 TITLE (Include Security Classification)
SOME EFFECTS OF NITRATES ON THE TENSILE PROPERTIES OF AL 7075-T735 (U)

12 PERSONAL AUTHOR(S)
Donovan Harris, Chris Miller, and Dario A. Emeric

13a TYPE OF REPORT	13b TIME COVERED	14 DATE OF REPORT (Year, Month, Day)	15 PAGE COUNT
Final	FROM Aug 85 TO Oct 86	March 1988	160

16 SUPPLEMENTARY NOTATION

17 COSATI CODES			18 SUBJECT TERMS (Continue on reverse if necessary and identify by block number)
FIELD	GROUP	SUB-GROUP	Intergranular corrosion; tensile properties; aluminum alloy Al 7075-T7351

19 ABSTRACT (Continue on reverse if necessary and identify by block number)

This report is the first of three related to the effects of nitrates on the chloride corrosion of Al 7075-T7351 alloy. Laboratory work was performed from March 1983 through February 1987 at the Belvoir RD&E Center. This report highlights research performed between August 1985 and October 1986. It details experimental testing efforts and results of a study on the effects of nitrates on the mechanical and physical properties of aluminum alloy Al 7075-T7351 when exposed in a chloride environment. The results show that changes in the tensile properties of unstressed Al 7075-T7351 followed exposure to a nitrate-chloride environment in four instances. . . .

20 DISTRIBUTION / AVAILABILITY OF ABSTRACT	21 ABSTRACT SECURITY CLASSIFICATION
☒ UNCLASSIFIED/UNLIMITED ☐ SAME AS RPT ☐ DTIC USERS	Unclassified
22a NAME OF RESPONSIBLE INDIVIDUAL Donovan Harris	22b TELEPHONE (Include Area Code) 703 664-1127 22c OFFICE SYMBOL STRBE-VC

DD Form 1473, JUN 86 Previous editions are obsolete SECURITY CLASSIFICATION OF THIS PAGE

PREFACE

This report is the first of three in a series relating to the effects of nitrates on the chloride corrosion of Al 7075-T7351 alloy, covering laboratory work performed at the Belvoir Research, Development and Engineering Center during the period of March 1983 through February 1987. The research effort reported herein covers the timeframe of August 1985 through October 1986 and details experimental testing and results of studies on the effects of nitrates on mechanical and physical properties of aluminum alloy Al 7075-T7351 when exposed in a chloride environment. In four instances, changes in tensile properties of unstressed Al 7075-T7351 followed exposure to a nitrate-chloride environment.

Standard Test Methods

ASTM B 577 *Standard Methods of Tension Testing Wrought and Cast Aluminum and Magnesium-Alloy Products*

ASTM G 1 *Standard Practice for Preparing, Cleaning, and Evaluating Corrosion Test Specimens*

ASTM G 16 *Standard Practice for Applying Statistics to Analysis of Corrosion Data*

ASTM G 38 *Standard Practice for Making and Using C-Ring Stress-Corrosion Test Specimens*

ASTM G 44 *Standard Practice for Alternate Immersion Stress Corrosion Testing in 3.5% percent Sodium Chloride Solution*

References

MIL-HDBK-5D Military Standardization Handbook: *Metallic Materials and Elements for Aerospace Vehicle Structures*

MIL-S-81733 Military Specification: *Sealing and Coating Compound, Corrosion Inhibitive*

Symbols and Abbreviations

ASTM	American Society for Testing and Materials
% elong	Elongation in percent, a measure of ductility of a material based on a tension test
gm	Gram
ksi	Kips (1,000 pounds per square inch)
L	Longitudinal: parallel to the direction of principal metal product manufacture; the rolling direction
L-T	Long Transverse: perpendicular to the longitudinal; in products whose grain structure clearly shows directionality, it is that perpendicular which is parallel to the major grain dimension/direction
N	Normal
S-T	Short Transverse: perpendicular to the longitudinal direction and parallel to the minor dimension of the grains in products with significant grain directionality
TUS	Tensile Ultimate Strength
TYS	Tensile Yield Strength
wt	Weight

TABLE OF CONTENTS

Figures

Section I. BACKGROUND

While working with a series of formulations designed to inhibit crack growth from corrosion fatigue, we experienced what seemed to be anomalous results with one solution. This particular formulation was being run as a control and had been well tested previously,[1] at which time it was shown to be an effective inhibitor for fatigue crack growth in a chloride environment. But when we used the formulation, the fatigue life was markedly reduced. At this time we were also reviewing several incidents of sudden accelerated corrosion occurring at various sites along the West Coast of the United States. The rates of corrosion experienced could not be reconciled with the physical causes of the corrosion. Articles by Byrne and Miller,[2] and by Maitra and English[3] showed that the chloride/nitrate environment found in the Los Angeles area produced an accelerated attack on aluminum alloy series Al 7075-T6, T73, and T7351. The descriptions of some results were very similar to our laboratory and field experiences. Of particular interest and concern was the severe intergranular attack reported by Maitra and English[3] on unstressed Al 7075-T7351. The chemistry of these experimental environments,[2,3] was very similar to the chemistry of the exhausts from tactical vehicles,[4] due to the absence of exhaust abatement systems and to the effects of nitrates on stress corrosion cracking (SCC) of Al 7075-T651.[5-8]

The ability of exhaust gases to create a localized sub-environment has been well established in air pollution research literature.[9-17] Navy researchers have shown that these effects can extend over an area larger than was originally thought could be affected.[18] The same type of an effect occurs in the immediate vicinities of a convoy, motor pool, and depot. Artillery and armored units in the field have this same capacity to create a localized sub-environment which is chemically different from the surrounding general environment.

The synergistic attack of chlorides and nitrates on aluminum alloys was well established[19-22] prior to the work of Byrne and Miller[2] who related this type of attack to actual existing environments and, in combination with Maitra and English[3] attempted to provide an explanation of the initial failures reported by Lifka.[23] All three studies stress the apparent isolated nature of the results and the chemical environments which generate them. The argument at that time was that conditions, which would induce this type of behavior, rarely occur in the general environment. The tenuous nature of this argument has been demonstrated[9-17] primarily due to the lack of this type of environmental data.

Another factor is the dynamic nature of any environment as demonstrated in Figures 1 and 2 which document the change in the average pH of the rainfall over a 10-year period for the regions shown. The last 10 years have seen a global increase of chlorides and nitrates in the environment of both local and regional areas. The sources of these

changes are increased use of road salts for deicing and nitrate-based agricultural chemicals on the farm and around the home. These agricultural chemicals are found worldwide, since the US exports its technology to the world community. In North African and Middle Eastern regions, the native soils have large natural concentrations of chlorides. In Egypt, the soils contain up to 3.5% sodium chloride. As actual experience has shown the nightly formation of a condensate on metal objects, the lack of rainfall does not eliminate the corrosion potential. The area which is potentially affected by the presence of nitrates is far greater than conceived in the studies cited.[2,3,23]

In corrosion, as in economics, we are able to develop excellent models for what occurred in the past. Unlike economics, corrosion science is unable to recover all the pertinent data leading to a field failure, since that data rarely exists for field failures and it is incomplete when it does exist. Better than in economics, these field failures can be recreated both in the laboratory and in the field, thus building an accurate model in time. To establish design limits in testing, test methods such as those promulgated in Military Standarization Handbook 5D, *Metallic Materials and Elements for Aerospace Vehicle Structure,* rely on the accuracy of the developed models. With 7xxx series aluminum alloys, the tests expect that neutral 3.5% sodium chloride solution is an accurate predictor of field behavior. Navy studies have shown this was not the case in the area of a task force.[19] The same possibility exists for these nitrate driven/controlled environments.

If the end items are painted and the reactions discussed are on a bare metal surface, the relevance of the behavior of Al 7075-T751 in the environment described relies on the following facts:

1. Every painted surface has holidays or holes.
2. On many air mobile items, the paint thickness is minimal due to weight considerations.
3. The same environment corrosion attack at a holiday can be more severe than on a bare metal surface.
4. Items in depot or forwardly deployed are not washed down nor cleaned until deployed to the field.
5. On fielded items, the paint surfaces are broken by stones, impact with another piece of equipment, and the very act of deployment or redeployment in the field.
6. When inspecting for signs of corrosion, troops tend to look for the tell-tale red stains which mark ferrous corrosion.
7. Prior to Maitra and English,[3] there were no reports of intergranular attack on unstressed Al 7075-T7351.

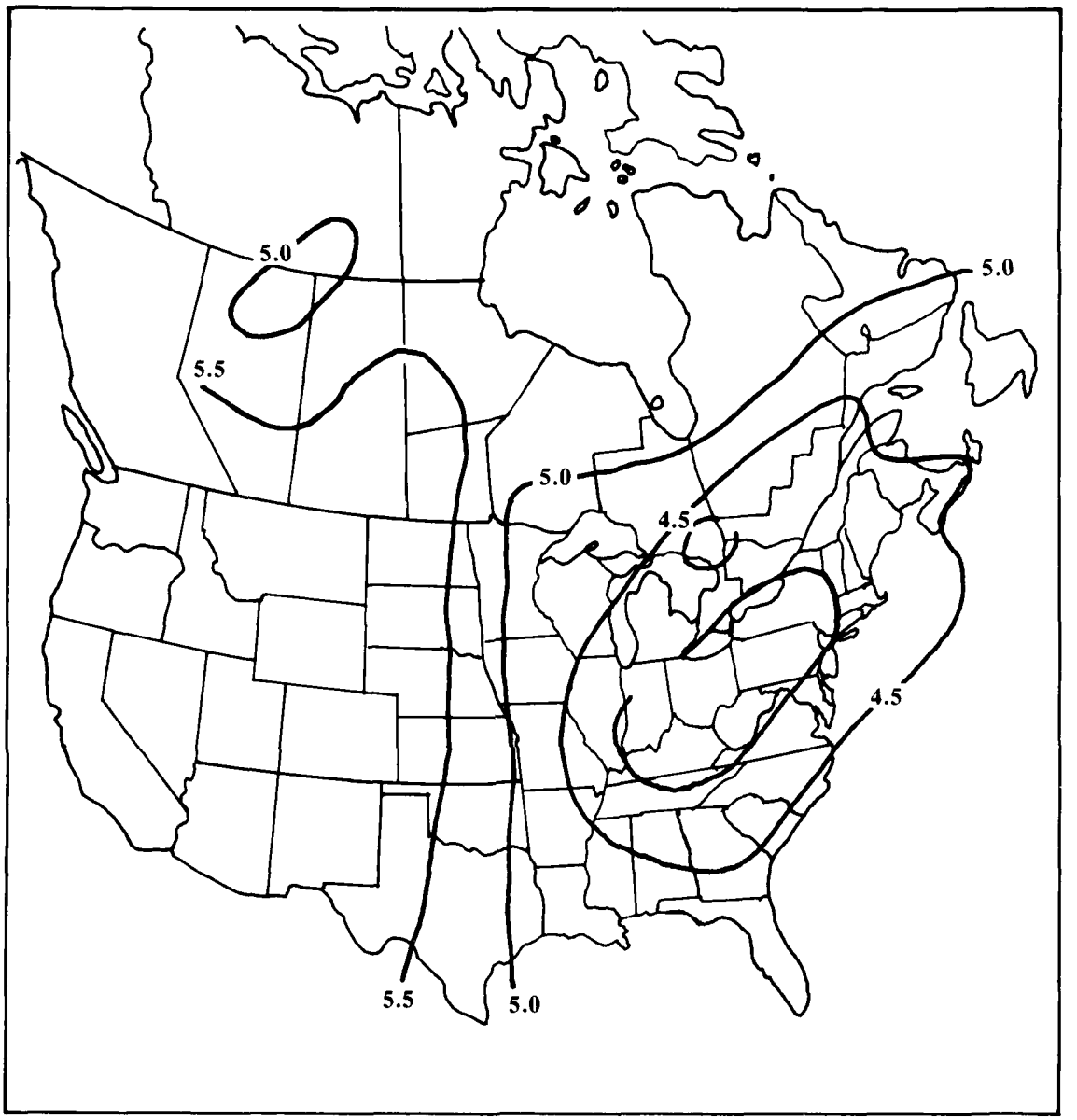

Figure 1. Remote monitoring pH rain values

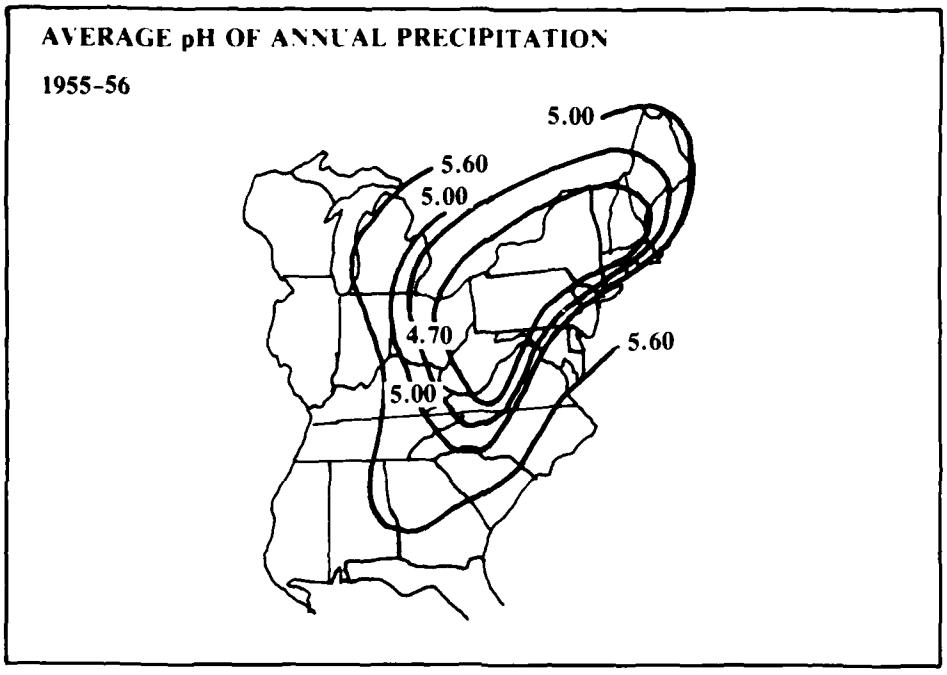

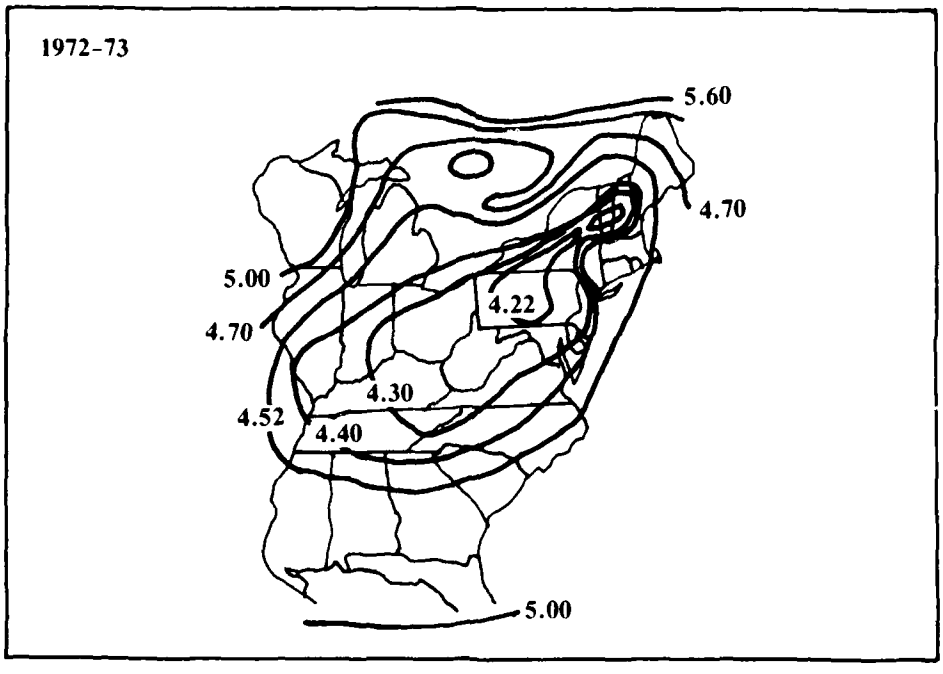

Figure 2. Trends in precipitation acidity in eastern North America (Adapted from *Chemical and Engineering News*, 1976)

This is not the building of a worst case model, but a simple statement of what is. Painting is good to excellent for minimizing general corrosion attack, but that protection can become illusionary where intergranular corrosion, stress corrosion cracking, and fatigue corrosion cracking are concerned. These three types of corrosion are due to corrosion of localized cells, and can be envisioned as point defect failures. Painting does reduce the number of available sites which can develop into these point defects due to attack by the environment. The very fact that an item operates in a military environment increases the number of sites available to corrosion attack.

In the aircraft industry, the 7xxx series alloys, which are widely used as structural support members and for which application they were developed, are usually covered by alclad aluminum sheets or if in sheet form, used as an alclad product depending on the heat treatment. In turn, they are generally painted. When the end part is used where it will have direct exposure to the environment, it is subject to regular replacement and to visual and instrumental inspection, such as in landing gear assemblies. Overall, aircraft operate in a less abusive environment and are better maintained than ground equipment. In fact, aircraft are at their greatest risk to corrosion or corrosion-promoting damage when on the ground or the carrier deck.

The findings of Maitra and English[3] are important when coupled with the findings of Byrne and Miller[2] because the two studies establish naturally occurring conditions under which unstressed Al 7075-T7351 is subject to intergranular attack. Due to the world-wide use of nitrate-based agricultural chemicals, there is an increased likelihood of exposure to these conditions. The lack of abatement equipment on tactical vehicles leads to the generation of exhaust gases which have chemistries very similar to the previously referenced environmental types. Our own laboratory and field experiences have shown unexpected corrosion behavior in aluminum alloys when nitrates have been present. The increased use of 7xxx series alloys—particularly Al 7075—in ground support roles requires clarification of nitrate's role in the chloride-induced corrosion of these alloys.

SECTION II. EXPERIMENTAL TESTING

Approach

It was decided to combine and essentially repeat the studies done by Maitra and English [3] and Byrne and Miller,[4] measure the tensile properties, document the microstructure's condition, and then see what changes had taken place and if further work was needed.

Funding changes, personnel availability, funding's timing, and time available forced the use of a cyclic salt spray in place of alternate immersion as per ASTM G-44, *Standard Practice for Alternate Emersion Stress Corrosion Testing in 3.5% Sodium Chloride Solution,* and a 45-day exposure in place of the 90-day exposure time.

Specimen Configuration

Control and exposure specimens were two basic configurations: a flat-type and a C-ring type. All the tensile test specimens were subsize rectangular tension test specimens per ASTM B-557, *Standard Methods of Tension Testing Wrought and Cast Aluminum and Magnesium-Alloy Products,* except that the grip section width was 1/2" and not the specified 3/8".

While all flat-type specimens came from the same 1/4" sheet of Al 7075-T7351, the size and the shape of the exposure pieces varied (See Appendix A). Initially, 4" x 6" panels were exposed, then 4" x 1/2" bars were cut out using an abrasive cutting wheel. These bars were then cut to form the subsize tension specimens. Since none of the available abrasive cutters were capable of making the 4" cut in a single pass, the 4" x 1/2" bars had to be made by cutting from both ends of the 4" x 6" plates. The resulting bars usually had steps along the newly cut edges, which had to be removed by wet grinding so the bars would fit the tensile cutting jig. These specimens were tensile tested in the L-T orientation, long transverse; however this process used too much time and materials. Therefore, we changed to using 4" x 1/2" bars, which were cut out on a hydraulic shear. The subsize tension specimens, per ASTM B-557, were used for exposure in Test IV only. All the 4" x 1/2" specimens were exposed and tensile tested in the L orientation (rolling direction) due to a misunderstanding at the time of manufacture.

The C-rings were supposed to have been made in accordance with ASTM G-38, *Standard Practice for Making and Using C-Ring Stress-Corrosion Test Specimens,* but the wall thickness was 0.028" and not the 0.056" required. The 0.028" was used for the applied stress calculations. C-rings with the correct wall thickness were used in Tests IV through VIII. All the C-rings were made in the short transverse direction from the same 1 1/2" plate of Al 7075-T7351. The nominal applied stress was 31 ksi (1,000 pounds per square inch) for all but the November 1985 Baseline Test, where the applied stress was 3.1 ksi due to human error.

To stress the C-rings, 316 stainless steel machine screws and nuts were used. Polysulfide sealant per Military Specification MIL-S-81733, *Sealing and Coating Compound, Corrosion Inhibitive,* was used in the Baseline Tests as protection against galvanic corrosion. The later test used teflon bushings in place of the MIL-S-81733.

Test Environments

The exposure environments in Appendix B were made from reagent grade chemicals in tap water which had been treated by a reverse osmosis system. Except for the Test II environment, the Baseline Test solution served as the concentrate for making all the other exposure solutions, using either sodium salts or dilute acids. Details of the exposure environments are in Appendix C.

The Baseline Test was repeated due to the appearance of a growth, which choked off the flow of fogging solution through the fog generator by clogging the reservoir filter and solution-aspirating ports. Acetic acid was used to acidify the fogging solution for the Baseline retest in place of the acid rain analog. A different growth appeared after only 10 days, so the reservoir was dumped, cleaned, and recharged with fresh solution using the original acid rain analog. This last solution was, in turn, replaced 23 days later with another fresh solution. While no further growth was seen in the reservoir system, it was evident on the surfaces of the specimens.

The Test II solution was replaced on the 23rd day of exposure with no signs of any growth. By the 38th day of the exposure, the growth seen in the first Baseline Test had reappeared, and the solution was again replaced.

The growth seen in the reservoir systems of both the first Baseline Test and Test II resembled a dust ball covered by clear gelatin. The growth seen in the repeat Baseline Test was snow white in color and resembled fine iron particles attached to one of the poles of a magnet. The surface growth seen on all the specimens was grey-brown in color, had no shape of its own, and visually could not be discerned as a growth. Rather, it appeared to be a simple chemical discoloration of the metal. The reason we know there was a growth there was the slippery condition of the surface when touched or handled. It is interesting to note that the exterior surface of all the C-rings appeared to be more heavily affected.

The Test III solution was found to be very unstable. The pH would shift from 4.2 to 6.5 over 8 hours. Thus, starting with the 4th day of exposure, the test solution was made fresh daily using the baseline stock solution, acidified to pH 4.2, placed into the system reservoir, and drained 4 hours later. The volume of solution prepared and used was 4 liters, which was the limit of our mixing and handling capabilities. This method was used for the remainder of the tests. The frequency of preparing the stock solutions was changed to every 3 weeks for the sodium salts solution, and every 6 weeks for acid mixture solution.

The solution for Test IV was made by using only the acid rain analog II and acidifying to pH 4.2. The new analog had the acids in the same concentrations as their sodium salt counterparts in the Baseline Test. The new analog was also used in Tests VI and VII so as not to disturb the normality ratios at the low concentrations used.

The Baseline Tests through Test III were strictly cyclic salt fog type exposures. Tests IV, VI, and VII were a mixed exposure of acid gases and a fogging solution. The solution ion concentrations and the chamber concentration of the acid gases were nominally the same. Tests V and VIII were acid gas exposures in high humidity.

Test IV was designed to simulate a West Coast environment, and Tests V through VIII simulated unabated diesel exhausts from tactical vehicles. All the exposures were to include the use of ozone, but the ozone generator was not on hand for the start of Test IV. It was decided to run the simulated diesel environment without the ozone at this time, rather than delay the tests any further. This decision was made because the ozone should have less of an effect on the simulated diesel environment than on the simulated West Coast environment.

Only the ozone concentration was actually measured in the test cabinets. The concentration of the other gases was calculated using the flow rate measured over a series of five points using a wet test meter; the total time gas was introduced into the cabinets, the cylinder concentration; and the cabinet volumes—300 liters. Table 1 presents exposure test cycles.

Table 1. Exposure Test Cycles

I. Baseline Tests, Test II, Test III

Salt Spray	8 Hours (Mon-Fri)
Purge Air	16 Hours (Mon-Thurs)
Hot Soak (35 °C/95 °F)	28 Hours (Fri-Sat)
Condensing Soak (20 °C/68 °F)	35 Hours (Sat-Mon)

II. Tests IV through VII

*Salt Spray	8 Hours (Mon-Fri)
**Purge Air	4 Hours (Mon-Fri)
Hot Soak (35 °C/95 °F)	16 Hours (Mon-Fri)
	28 Hours (Fri-Sat)
Condensing Soak (20 °C/68 °F)	35 Hours (Sat-Mon)

*Tests V and VIII were not subject to salt spray.
**Includes 15 minute charging of cabinets with acid gases

The change in the test cycle was due to the limits imposed by the solenoid control timers, 150 seconds charging time. The cabinets were charged using four 150-second cycles, then allowed to sit for 16 hours; the only exception was the ozone which ran continously for 10 1/2 minutes.

A cabinet heater failed during the repeat of the Baseline Test so the test cabinet was at 20 °C/68 °F for 9 days. The cold period was repeated for all the remaining tests, in order to avoid repeating the Baseline Test a third time.

Initially specific ion electrodes (Cl^-, SO_2, NO_3^-, and pH) were used in an attempt to monitor the daily changes in the various solution chemistry. This proved to be impractical due to time and personnel constraints, so only the pH was done on a daily basis. The specific ions were measured over a 2 day period on a biweekly basis. The solutions to be analyzed were kept stoppered and refrigerated in the intervening time span.

Both Baseline Tests consisted of two types of exposures: a cyclic salt fog and a total immersion. The other difference (besides the previously discussed fogging solution problem) was the immersion test. The first immersion test made use of the same solution for the entire 45 days, with only periodic additions to maintain the fluid level of the covered vessel. For the second Baseline immersion test, fresh solution was added daily, Monday through Friday, to maintain a pH of 4.4 to 4.5. Approximately a quarter of the container solution volume was replenished daily. The replenishment reservoir had a pH of 4.4 in the first week, which was lowered to 3.3 by the fifth week and held there for the remainder of the test. Ninety percent of the volume in the replenishment system was replaced weekly. The stock solution used was taken from the salt fog reservoir, then acidified to the desired pH before being placed into the replenishment system.

As stated earlier, it is important to us whether or not the results of Maitra and English[3] were anomalous. To achieve this end, the test program as originally designed had ten 90-day exposures with the possibility of an additional two exposures if needed. The program as run consisted of eight 45-five day exposures, including the two Baseline Tests; and one 90-day exposure (Test IV). The two exposures dropped from the program were: a salt fog exposure in which the chloride concentration ratio to the nitrate and sulfate concentrations was double that of the Baseline Test environment, and another inhibitor exposure test in which the inhibitor was applied on a weekly and biweekly basis instead of daily.

The Baseline Test, in combination with Test III, served as the control for the reproducibility of Maitra and English's results.[3] The two tests also served to measure the effects due to absolute concentration changes in the solution chemistry.

The purpose of Test II was to demonstrate the effects of change in the chloride/nitrate ratio. The 0.344 normal (N) nitrate ion concentration used lies halfway between the Baseline Test concentration, 0.229 N, and the theoretical inhibiting concentration of 0.459 N.[20,21]

Test IV was designed to simulate the Los Angeles ambient high weekly average concentration for gaseous pollutants.[4] The test was also designed to measure the effects of the time of wetness by having a sample population removed after 45, 67, and 90 days of exposure.

Tests V through VIII were designed to simulate the exhaust gases from tactical vehicles.[4]

Tests VII and VIII tested for the effects of using a nitrate/nitrite corrosion inhibitor. The inhibitor was applied using a spray bottle so as to produce conditions similar to those experienced during the corrosion fatigue experiments.

Surface Preparation

All the test specimens were degreased using reagent grade 1,1,1 trichloroethane and stored in desiccators. The specimens were recleaned just prior to exposure and also prior to being measured or weighed. Except for the second Baseline Test, all the flat specimens were exposed with as-received surfaces. The second Baseline Test used both as-received plates and plates which had been polished down, using a 5-micron silica slurry as the final polishing step. The plates used in the immersion retest were polished only on one face. All this was done in effort to measure any effects of surface finish on the corrosion attack and tensile properties.

SECTION III. TEST RESULTS

The test results are presented as two separate parts; the first covers testing for changes in the physical and mechanical properties, and the statistical analysis of those test results, and the second part details the microscopic examination of the surfaces and the microstructural analysis of the specimens.

Properties

The tensile properties were measured using a 60,000 pound capacity tensile test machine. The stress-strain curves were recorded in autographic form, and the yield load determined using the 0.2% offset method. The entire test procedure was performed in accordance with ASTM B-557.

Specimen weights from the two Baseline Tests, August 1985 and November 1985, were not taken primarily due to the method of preparing the 4" x 6" specimen plates. It was originally thought, and subsequently proven, that the machine shearing and hydraulic hole punching would promote localized areas of general corrosion unrelated to any possible tensile effects, and therefore not relevant to the study. Examination of the surface of the plates showed that 90% of the general corrosion, which was 80% of the visible surface corrosion, was associated with the cold worked areas.

See Appendices B and C for detailed test data. A summary of the test results is presented in tabular form in Tables 2 and 3, and in graphic form in Figures 3 through 12. The data from the two Baseline Tests is shown both as the sum for all the individual tensile tests for that sub-group, and as if each 4" x 6" plate was an individual test by itself.

Table 2. Test Averages for L-T Grain Orientation

Test Designation	% Elong	TUS ksi	TYS ksi	mg WT Loss	% WT Loss
L-T Control	15.5	70.1	58.5	*	*
8/85 Baseline	16.6	68.8	56.0	—	—
LT	18.2	69.6	56.0	*	*
LU	15.6	68.3	56.0	*	*
LB	15.8	68.4	55.9	*	*
11/85 Baseline					
Immersed	15.4	70.3	59.0	—	—
LM	15.9	69.4	57.6	*	*
LP	15.0	71.2	60.3	*	*
Polished	17.2	69.8	57.1	—	—
LN	16.9	68.3	55.9	*	*
LO	18.6	70.1	56.9	*	*
LQ	16.0	71.0	58.5	*	*
As Received	15.2	70.2	59.1	—	—
LV	13.0	69.8	58.3	*	*
LX	16.9	71.2	60.4	*	*
LW	15.5	70.0	58.8	*	*

* weights not taken

Table 3. Test Averages for L Grain Orientation

Test Designation	% Elong	TUS ksi	TYS ksi	mg WT Loss	% WT Loss
L-Control	15.5	69.7	58.8	—	—
Test II	14.0	70.5	58.8	3.33	.015
Test III	18.0	70.8	60.6	1.67	.008
Control IV/45	16.2	70.3	58.2	0.00	.000
Test IV/45	16.0	70.5	57.5	6.25	.028
Control IV/67	12.6	70.2	59.2	0.00	.000
Test IV/67	15.4	69.1	58.8	11.0	0.52
Control IV/90	17.3	69.5	58.8	10.0#	.052#
Test IV/90	16.4	68.3	58.1	16.4	.073
t-Controls	16.6	70.3	58.8	—	—
Control IV/45t	15.7	70.7	57.8	0.00	.000
Test IV/45t	14.2	72.6	59.8	3.75	.021
Control IV/67t	16.3	69.6	60.4	0.00	.000
Test IV/67t	16.0	70.8	58.9	17.5	.097
Control IV/90t	17.0	71.0	58.6	0.00	.000
Test IV/90t	17.0	69.6	59.1	19.1	.105
Test V	15.1	70.2	59.2	7.25	.032
Test VI	15.6	69.4	57.8	27.8	.123
Test VII	15.1	69.7	58.2	14.5	.064
Test VIII	15.7	69.9	58.5	12.3	.055

* weights not taken
# single sample
t subsize tensile specimen configuration

Looking at the L-T orientation results, the value which seems most out of place is the LV % elongation value; otherwise, the data appears tightly grouped. The August 1985 TYS data as a whole is slightly lower than the other data sets, but it is not that much different from the polished data set for the November 1985 Baseline Test. In graphic form (see Figure 5) these differences are more clearly seen though the changes are only 2.4% to 4.3%.

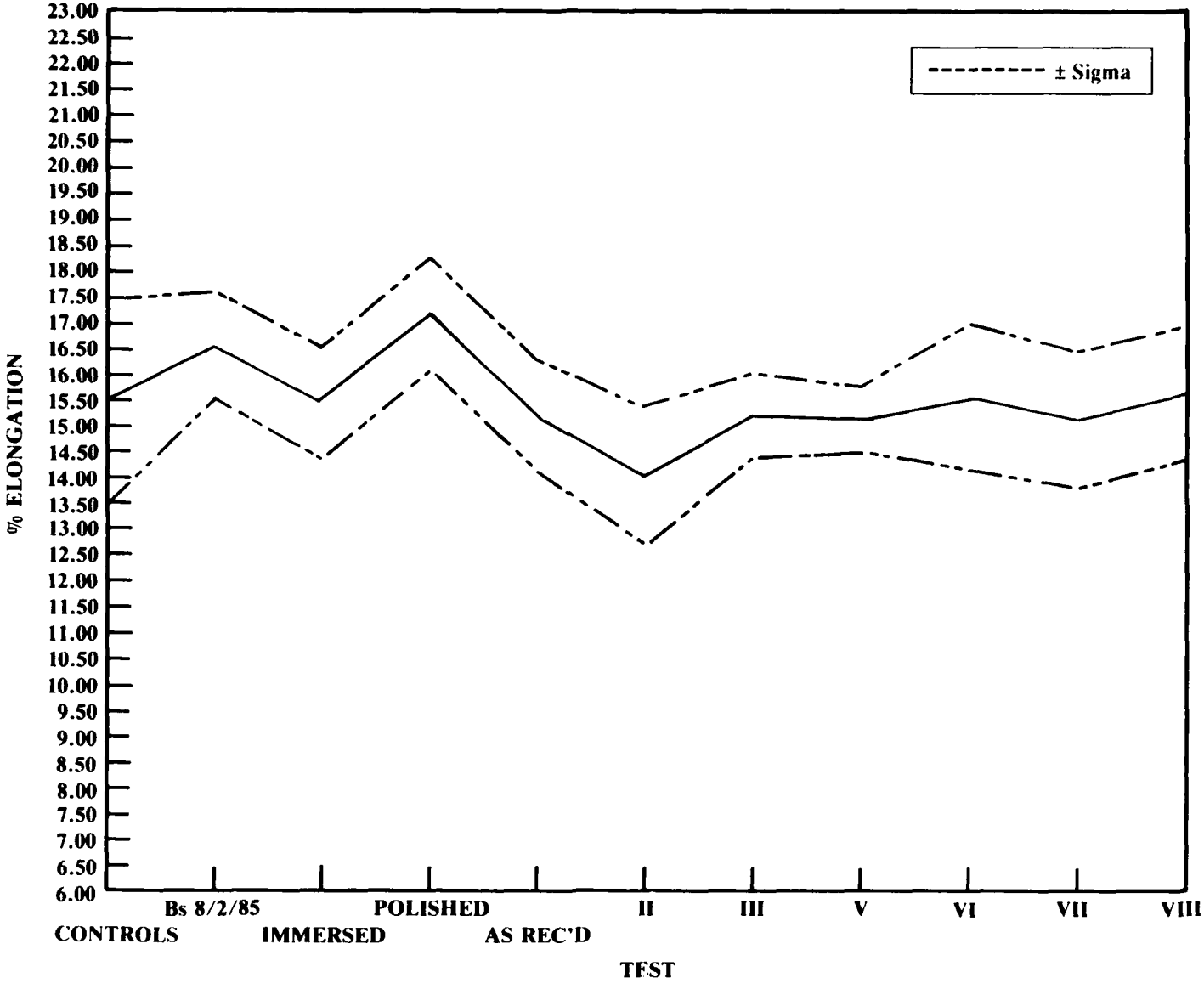

Figure 3. Averages: percent elongation, tensile data: IG 45-day test

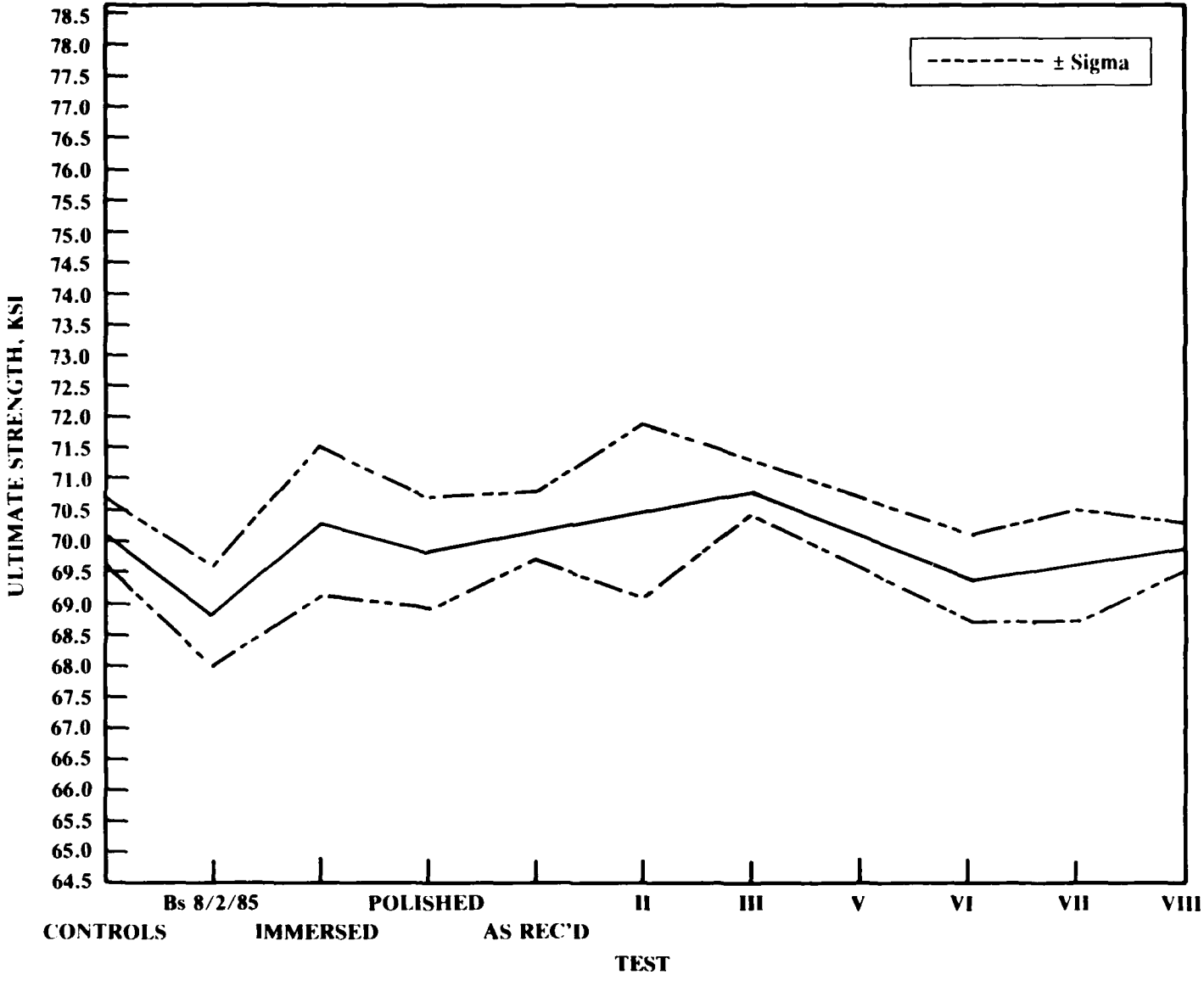

Figure 4. Averages: ultimate strength, TUS: IG 45-day test

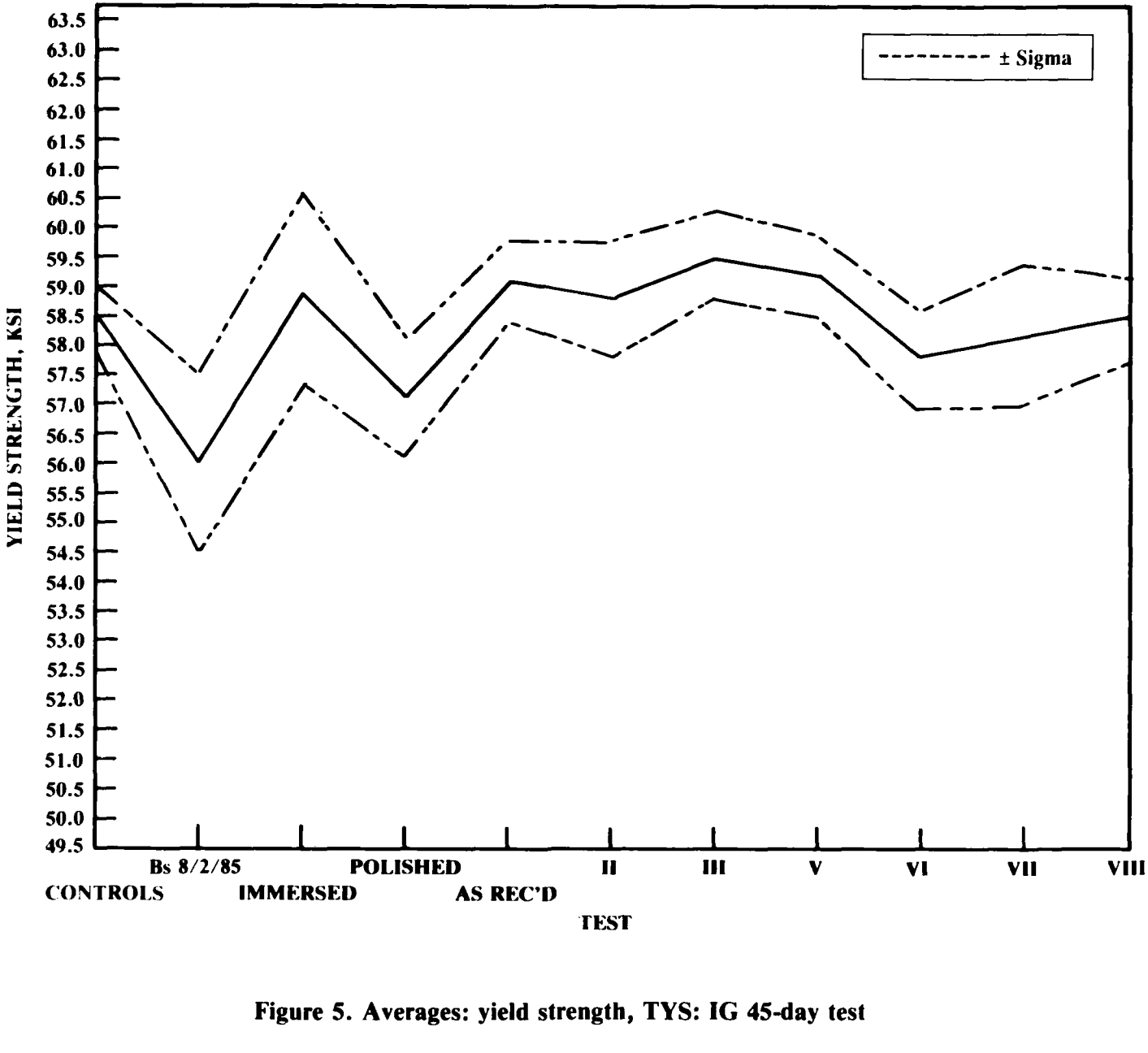

Figure 5. Averages: yield strength, TYS: IG 45-day test

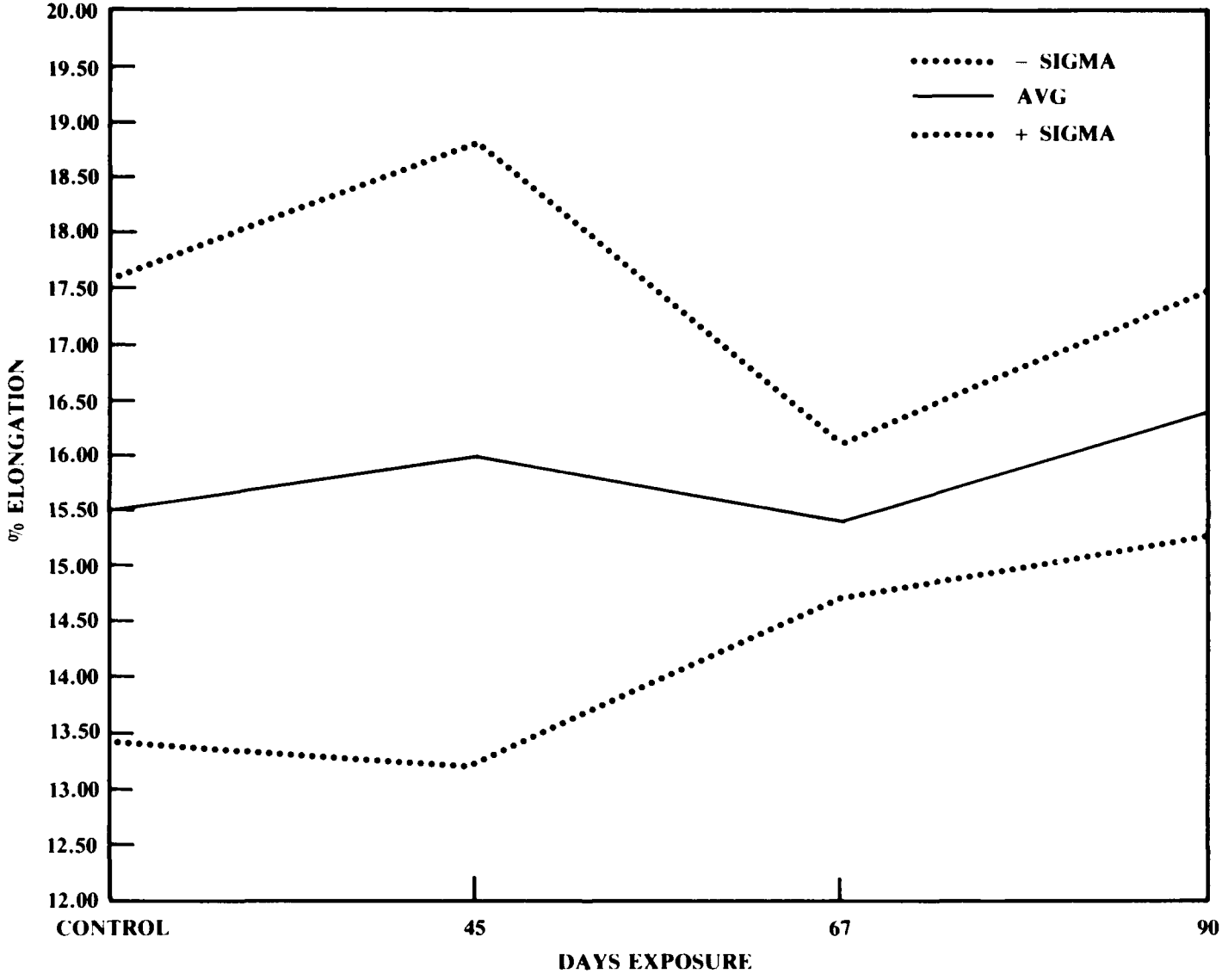

Figure 6. IG Test IV: solid bars: percent elongation

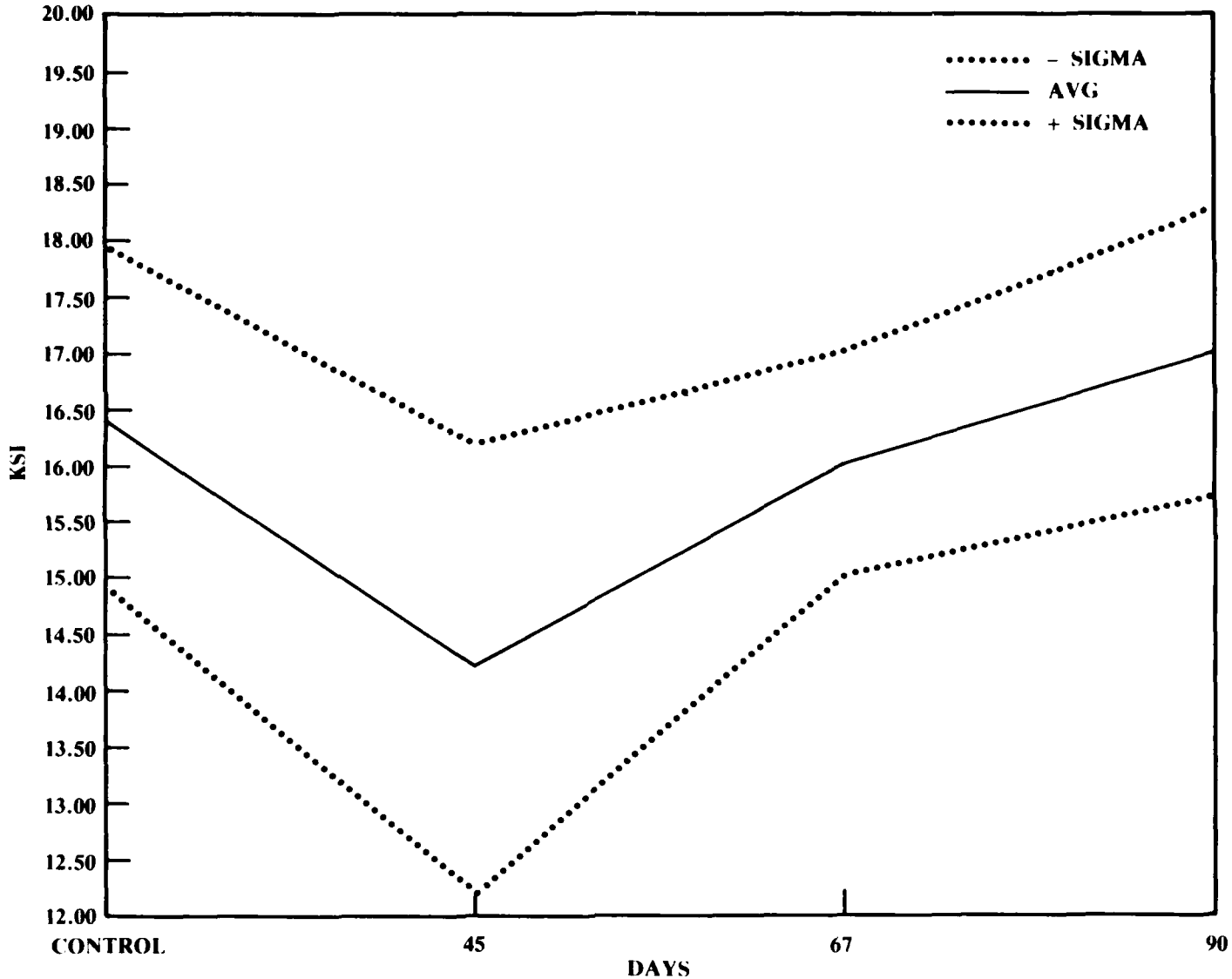

Figure 7. IG Test IV: tensile bars: percent elongation

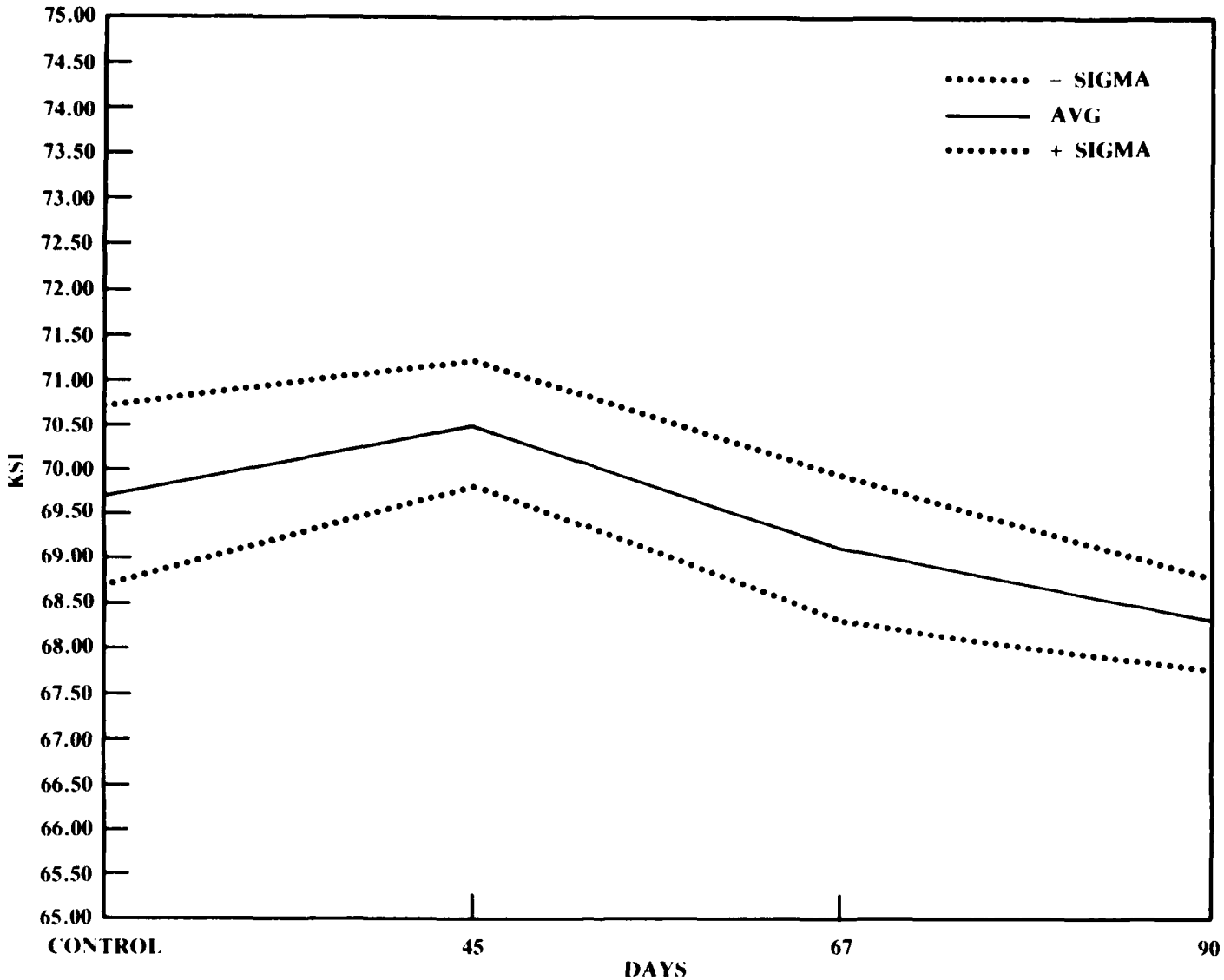

Figure 8. IG Test IV: solid bars, ultimate strength: TUS

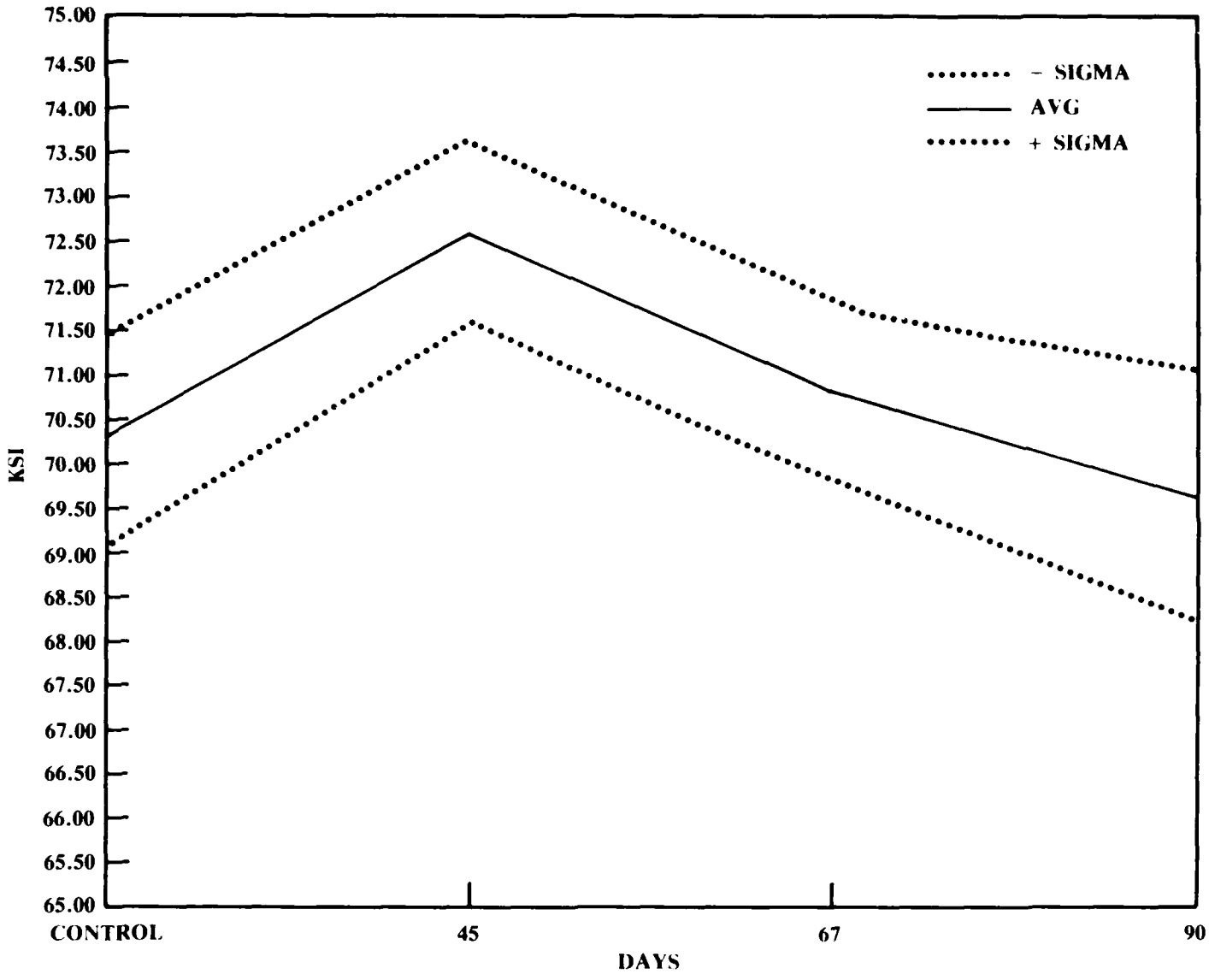

Figure 9. IG Test IV: tensile bars, ultimate strength: TUS

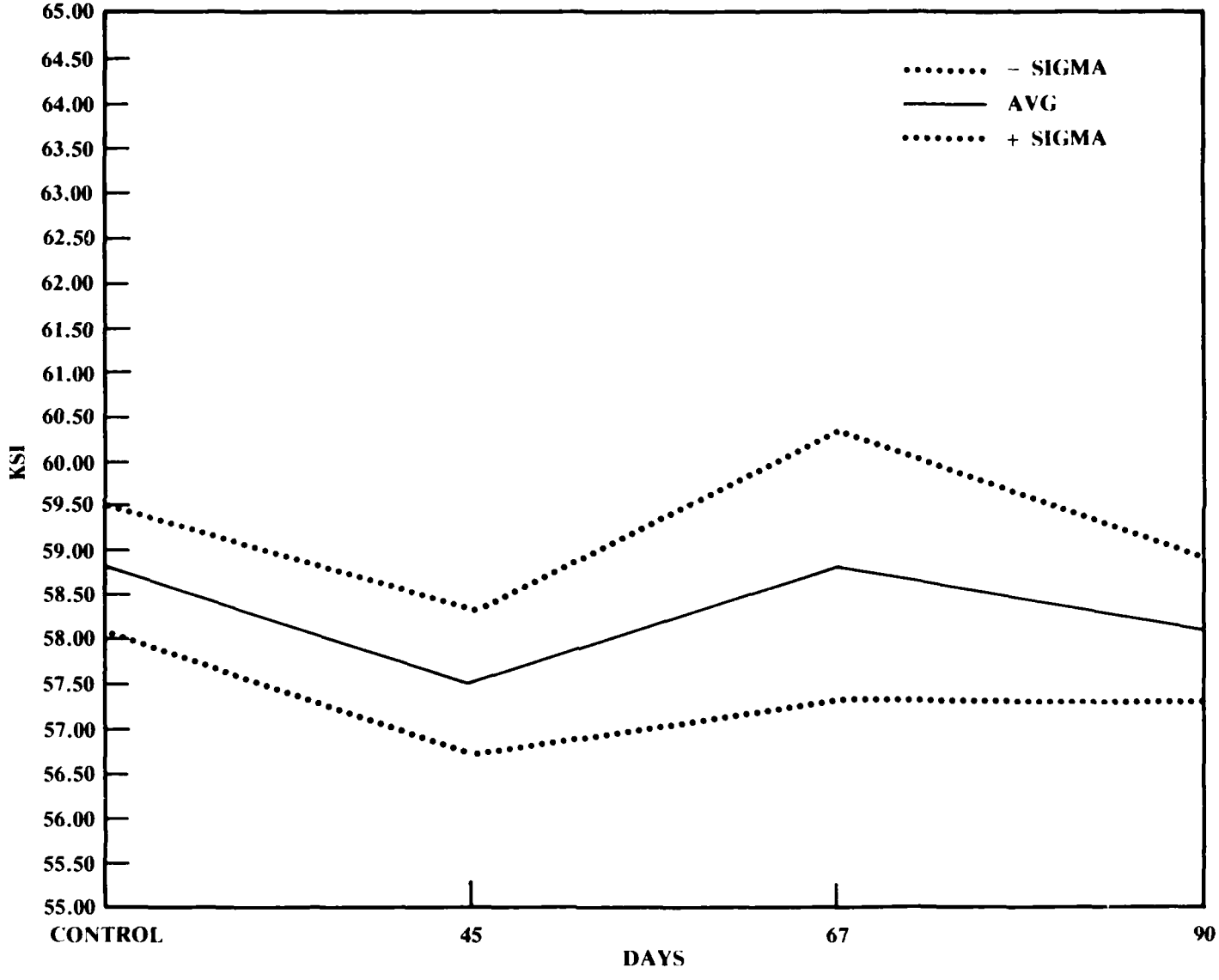

Figure 10. IG Test IV: solid bars, yield strength: TYS

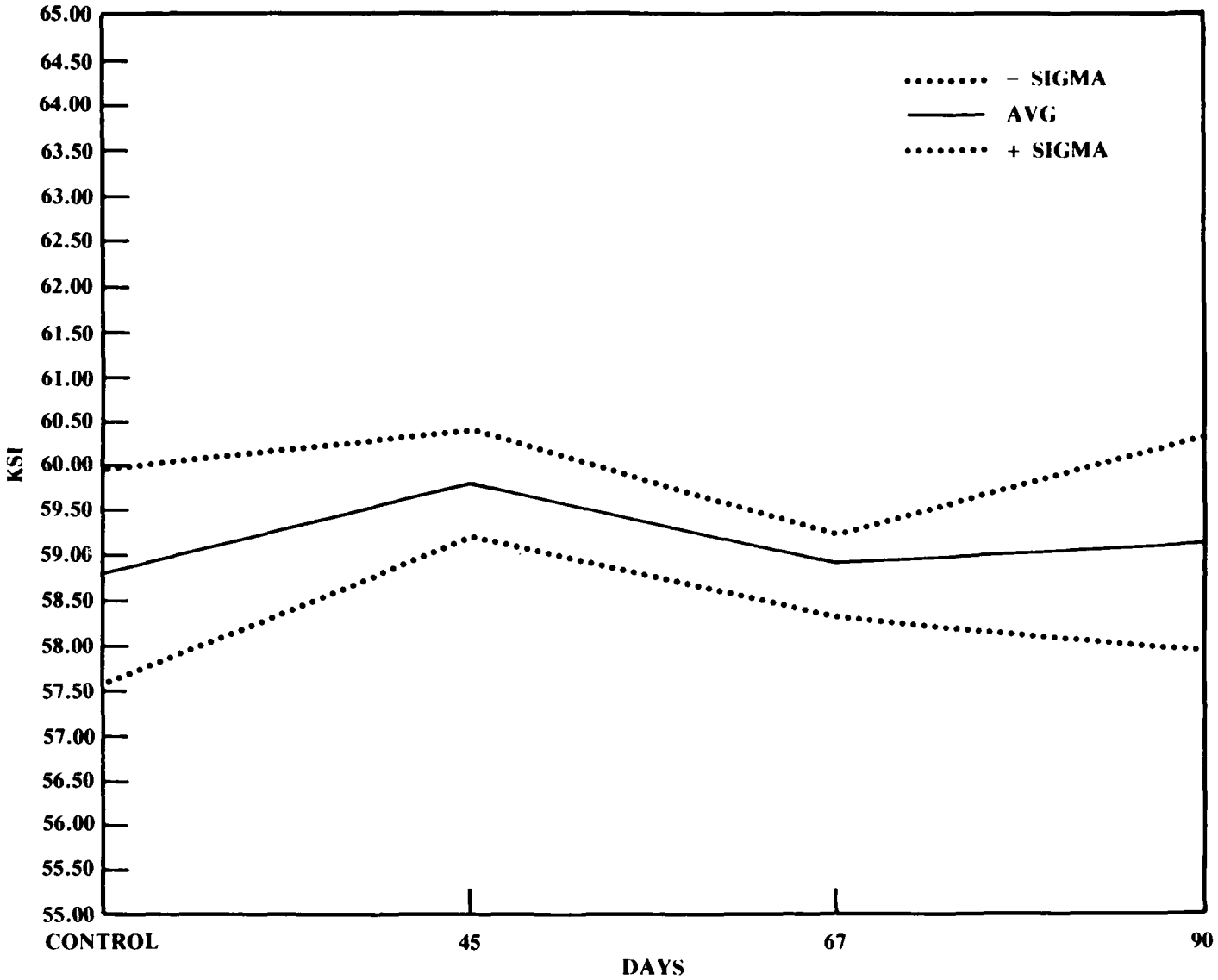

Figure 11. IG Test IV: tensile bars, yield strength: TYS

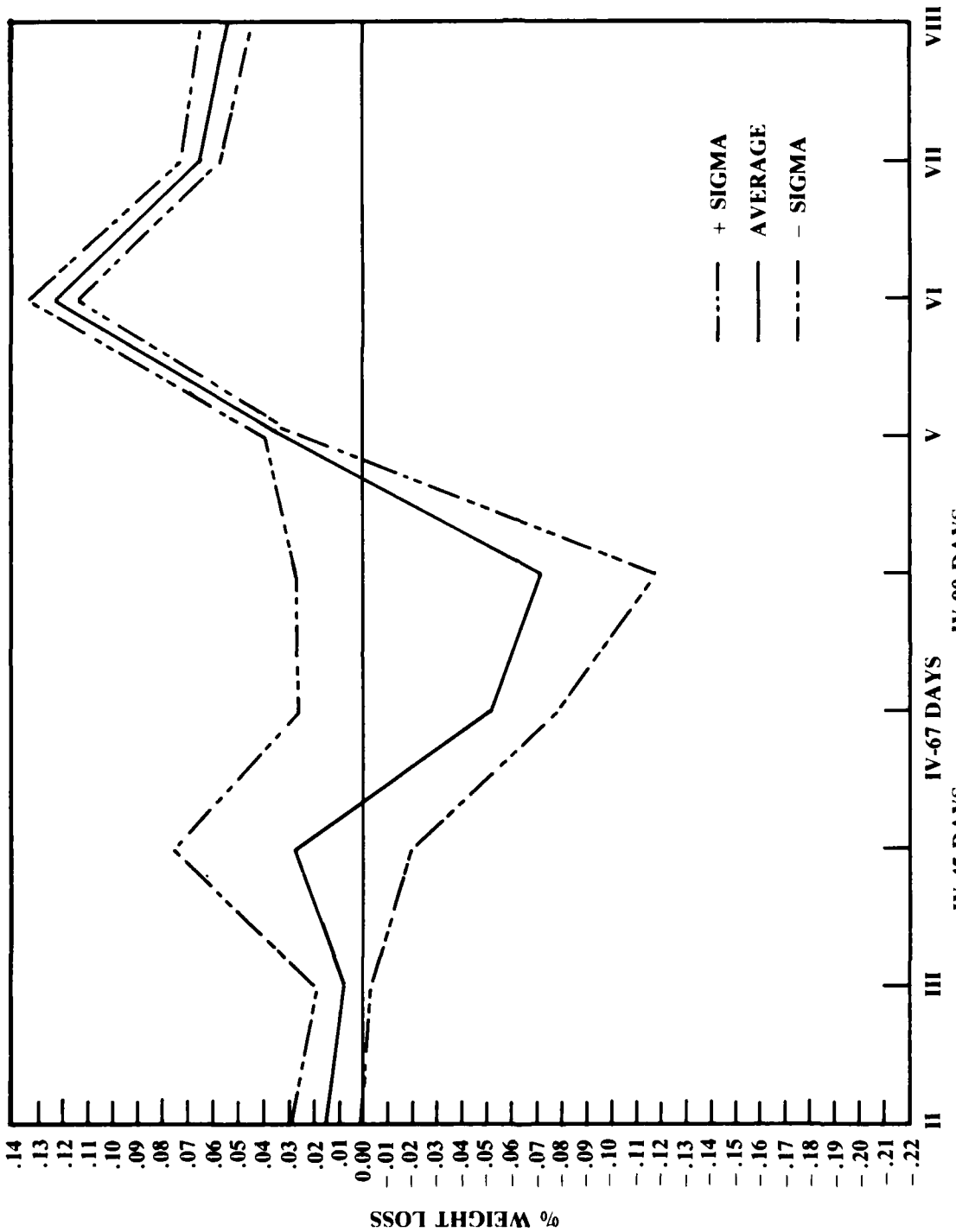

Figure 12. Percent weight loss, Tests II through VIII

For the L oriented samples, the weight data shows the most dramatic change in values, and with the exception of the 12.6 value for the % elongation of Control set IV/t, no other variable shows much of a deviation within its data set. The weight data in graphic form is given in Figure 12. In Figure 4, TUS averages, and Figure 5, TYS averages, the Test VI values appear to be lower than the rest of the values for Tests II through VIII. Similarly, the Test IV/90 values appear to be lower than the rest of the field in Figure 8, TUS averages, and Figure 9, TYS averages. For the TYS averages, the changes are 1.7% and 1.2%, respectively, less than half the value of the largest change seen in the L-T data set.

The test exposure tensile data was statistically compared to the appropriate control data set, L-T, L, t, using both one-way analysis of variance, the f-statistic, and the pooled estimate of variance for the difference between two means, the t-statistic. In the statistical analysis, the null hypothesis, $A = B$, was not rejected unless the probability of the f-statistic was $\leq 4.99\%$ and that of the t-statistic was $\leq 2.49\%$. The tensile data from this study forms our entire data base for subsize tensile specimens of Al 7075-T7351 alloy. The Galvanic Corrosion portion of this research program contains the remainder of our data base regarding subsize tensile specimens. Therefore, there is no foundation for interpreting those values which lie adjacent to the probability limits. In all those cases where the null hypothesis, $A = B$, was rejected, the case probability was half or less of the limiting probability value.

The results from both sets of Baseline Tests were evaluated against the control data on the basis of individual plate results, and as the sum of all the plate results within a sub-group. Additionally, the results of the individual plates within a sub-group were cross compared, as were the results between sub-groups. Table 4 presents the results of the analysis of the L-T specimen tensile data, and Table 5 presents L specimen data.

Both tables document only those instances where there are statistically significant differences between the test set and the control set for the TUS and TYS properties; that is, the null hypothesis can be rejected. Only in the case of the November 1985 Polished Baseline data is there a failure of both statistical procedures to track one another. Rejection of the null hypothesis by either method is sufficient to establish a change in the tensile property under test.

Table 4. Statistical Analysis Results — L-T Specimen Orientation

Test	Tensile Property	Statistic
8/85 Baseline	TUS, TYS	f&t
LT	TYS	f&t
LU	TUS, TYS	f&t
11/85 Baseline		
Polished	TUS	t
	TYS	f&t
LN	TUS, TYS	f&t
LO	TYS	f
As Received		
LX	TUS, TYS	f&t
Immersed		
LP	TYS	f&t

Considering each 4'' x 6'' plate as an individual test and only the TYS tensile property produces a 60% rate of effect on the tensile property. When the data is summed into subgroups, the same analysis changes the rate of effect to 50%; so, a change in the tensile properties of unstressed A1 7075-T7351 has been demonstrated for the L-T specimens.

Table 5. Statistical Analysis Results — L Specimen Orientation

Test	Tensile Property	Statistic
III	TUS	f&t
IV/45	TYS	f&t
IV/45t	TUS	f&t
IV/90	TUS	f&t
VI	TYS	f&t

The L specimens' rolling direction indicate changes in 16.7% of the test for the TYS tensile property. Again, change is seen in a tensile property of unstressed Al 7075-T7351. And while the time of exposure is still 45 days, the total fogging time for the two tests in question is one half that of the L-T specimens. The orientation least susceptible to the effects of a corrosive environment shows changes in unstressed samples.

A case could be made for ignoring the results of the August 1985 Baseline results as being due to a biologically initiated attack. The latter argument has some substance if the samples had been under an applied stress, or if we had limited the study to only the chemically induced effects of nitrates. But the study was open to include all the effects, so that in at least four separate instances a change in the TYS tensile property has been demonstrated.

SECTION IV. MICROSTRUCTURAL ANALYSIS

The Intergranular Corrosion Program was established to determine whether or not the mechanical properties of unstressed aluminum alloy Al 7075-T73 are affected by the different concentration of nitrates in the environment. One basic method to accomplish this is to examine the microstructure of sectioned samples after exposure. The purpose of such an examination is to:

- correlate apparent surface damage to actual microstructural damage,
- measure the extent of corrosion damage, and
- compare the extent of damage to the tensile properties.

This section includes a brief explanation of sample preparation, an introduction to surfaces and microstructure, and results from the Baseline Tests through Test VIII.

Two different types of sample configurations, C-rings and flat tensile samples, were exposed to eight different environments (see Appendix B) within environmental test chambers. The C-rings in the Baseline, Test II, and Test III were in both the stressed and unstressed state. This was done so the unstressed rings could act as controls for corrosion damage caused by residual stresses from the fabrication process and due to sample geometry. Tests IV through VIII had thick (0.056" wall thickness) and thin (0.028" wall thickness) versions of the C-rings stressed to 31,000 psi; the balance of the tests used the thin version of the C-ring. The flat specimens were exposed at an angle of approximately 65° in a rack with no stresses applied.

After exposure to the environment and chemical cleaning, the surfaces were viewed under low magnification to choose the best area for section and photographing. The C-rings were sectioned in the plane perpendicular to the central axis in order to minimize the effect of machining on the surface of the microstructure being viewed. The flat specimens had two sections cut from the end of the sample which was within the specimen rack and two sections from the center of the bar. Sectioning was done on a Buehler Isomet, while grinding and polishing was done on a Buehler Ecomet with a Euromet polishing head. The final polish was with colloidal silica suspension. In the hope that a correlation could be drawn between the visible surface feature and the underlying damage, the polished microstructures were etched on Kellers's Reagent and then photographed. **NOTE:** Photographs corresponding to the text are in Appendix D. Upon microscopic surface observation, the C-rings that had been exposed to the test environments showed visible signs of corrosion in both control (Figure D-1) and stressed (Figure D-2) samples. In some cases the pitting was extensive and penetrated through the sample (Figure D-3). The flat specimens tended to have less visible corrosion except for the area that was within the specimen slot of the specimen rack, where the corrosion damage appeared to be rather severe. There were six surface features caused by corrosion that were observed. They are defined below.

Type A, Small Equiaxed Pits: Type A corrosion could be found anywhere on the sample, but was generally associated with the inner and outer surfaces of the C-ring. The two equiaxed pits in Figure D-4 occurred when water droplets formed on the underside of the ring and remained there for a significant amount of the test period.

Type B, Deep Elongated Pits: Type B corrosion was similar to the equiaxed pits except that it was found on the outer surface of the ring and was elongated in the direction perpendicular to the stress axis (Figure D-5).

Type C, Shallow Elongated Pits: Type C corrosion was found on the edges of the C-ring and was similar to the deep elongated pit, except that it was shallower and that all the pits on a sample ran in a single direction (Figure D-6), which was assumed to the grain direction.

Type D, Shallow Surface Corrosion: Shallow surface corrosion, Type D corrosion—the fourth and most prevalent corrosion surface feature—ranged in severity from the obscuring of the machine marks up to the removal of grains. The Type D corrosion was characterized by a pit with a diameter which was greater than the depth of the pit and by an erratic or irregular edge.

Type E, Cracks: Crack-like pits (Type E corrosion) were generally found at the surface-edge interface of stressed specimens (Figure D-7). However, these cracks were due more to the presence of the water and not directly to its chemistry.

Type F, Corrosion of Machine Marks: Type F corrosion usually occurred on the field specimens since the finish on these specimens is rough. This obscured some of the Type D corrosion which was also present.

Polishing and etching the sample sections showed the extent of damage caused by the pit under the surface and how the pit interacted with the microstructure. Damage by the pit itself varied from very shallow, lens-like surface removal to rod-like pitting with a narrow orifice. In addition, intergranular corrosion can leave behind a pit-like structure when grain removal occurs (Figure D-8). The pits which had orifices smaller than their depths corresponded to the equiaxed and elongated pits on the surface. The remaining pits, intergranular corrosion, and surface corrosion correspond to Type D corrosion. The shallow elongated pits were exclusive to the edge of the C-rings and have no corresponding microstructural damage. Type C corrosion—shallow elongated pits—was judged to present a much less serious threat than those detrimental features which were found on the outer and inner surfaces. Sectioning of the C-rings was performed so that the exterior/interior surface features were seen rather than edge surface features. The flat specimens tended to have shallow surface corrosion on the front and back surfaces. In addition, the edge surfaces had rod-like pitting which may have had accompanying grain removal. The corrosion damage found varied with the chemical compositions of the various tests, which are detailed in the following paragraphs.

BASELINE TEST

The surfaces of the C-ring in the Baseline Test were severely attacked by the environment. There was evidence of corrosion Types A, B, C, D, and E on both the unstressed control and the stressed specimens. These types of corrosion-related surface features were found on specimens from other tests as well. Generally, the severity of the attack in the other tests was less than that found in the Baseline. One feature which showed up only in Baseline was a deep pit which penetrated from the top surface through the bottom (Figure D-9). This kind of penetration would be especially detrimental to vessels containing pressurized fluids.

After sectioning, polishing, and etching, the full extent of the corrosion damage could be seen. The control, unstressed C-rings were characterized by small (Figure D-10) and shallow (Figure D-11) surface pits. The surfaces were smooth with occasional patches of surface roughness. The control set also had several large deep pits which followed in the grain direction (Figure D-12), and pits with intergranular corrosion in the bottom. The pit seen in Figure D-13 was unique to the Baseline tests.

When stress was applied, the corrosion damage became more severe. The small pits tended to be larger (Figure D-14) and the large deep pits became more abundant. More

intergranular corrosion and intergranular cracks were seen in the pits than on the surface. The main difference between the control and stressed rings was the presence of narrow deep pits (Figure D-15) (depth of penetration 0.06mm-0.71mm) on the stressed C-rings.

The surface of the flat tensile specimens generally contained more machined imperfections than did the material for the C-rings. The streaks (Figure D-16), inclusions (Figure D-17), and the gull-wing-like cracks (Figure D-18) were a direct result of the rolling operation on the plate from which the flat tensile bars were cut. These machine marks were the initiation sites for the Type F corrosion (Figure D-19). The remaining portion of each specimen had patchy areas of shallow surface attack.

Sectioning, polishing, and etching revealed that corrosion on the Baseline flat specimens tended to be shallow (Figure D-20), if not superficial (Figure D-21). Generally, this shallow corrosion did not penetrate more than one or two grain depths below the surface. A further complication of this form of attack was the shallow grain corrosion (Figure D-22). These areas corresponded to the deeper areas under encrustation where exfoliation took place. There were also pits present (Figure D-23) on the Baseline flat specimens. These pits were shallower and had wider mouths than those formed on the corresponding pits on the C-ring. The Baseline flat specimens suffered more damage overall than did specimens in most of the other tests.

TEST II

The surface examination revealed that the corrosion damage on the C-rings consisted mostly of Type B (deep elongated pits) and Type D (shallow surface) corrosion. The edge surfaces had shallow striation-like corrosion lines which were akin to the Type C (shallow elongated pits) corrosion found in the Baseline. Pits were occasionally found on the sides as well. The interior surfaces suffered from shallow crack-like surface corrosion (Figure D-24) which was sometimes serious. The control sample exhibited the same surface features as the stressed rings, but to a lesser degree. The polished sections exhibited a variety of pits. These pits varied from the shallow surface corrosion to the regular and deep pits (Figure D-25). These pits were neither as abundant nor as deep as on the Baseline C-rings. There was a significant amount of intergranular corrosion on these samples (Figure D-26). The depth of the corrosion was mainly dependent upon the angle the grain direction made with the surface. The closer this angle was to 90°, the deeper the corrosion. An unusual case of intergranular attack occurred in the bottoms of small pits where a single narrow finger of corrosion proceeded along the grain boundary. The control sample had the same basic corrosion features as did the stressed samples, except the intergranular corrosion was not as prevalent.

The surfaces of the flat specimens in Test II were much the same as those in the Baseline. It was noticed that there were colonies of algae/bacteria growing on the metal specimens in most of the tests. The areas under the colonies tended to have a slightly deeper version of the shallow surface attack (Figure D-27) than those exposed directly to the test environment (Figure D-28).

The polished sections revealed that Test II flats were less severely attacked than the Baseline flats. Most of the corrosion took place on the front and back surfaces in the form of shallow under-surface corrosion (Figure D-29). The under-surface corrosion was generally less than 0.7mm wide and 0.1mm deep. There was no grain removal associated with this corrosion as had occurred in the Baseline. A second and more rarely observed form of corrosion (Figure D-30) resembled some of the transgranular and intergranular attacks seen in the C-rings which became pits (Figure D-31) with further attack. This form of corrosion attained the same depth as the shallow under-surface corrosion, but did not cover the same amount of area. The edges of these specimens did not exhibit as much corrosion as did the exterior and interior surfaces. This observation was mostly due to rough machining which made the discerning of corrosion difficult. When it did occur, the corrosion consisted of pits traveling along the grain direction. The center section arc exhibited no signs of corrosion.

TEST III

The surfaces of the edges of the Test III C-rings appeared essentially the same as those of Test II. The main difference was the presence of several shallow elongated pits and larger pits on the interior surface which were not seen in Test II. Furthermore, the surface of the unstressed sample had the same surface phenomena as the stressed rings. This indicates that the presence of a stress did not affect the types of corrosion in this environment.

Areas of localized corrosion were observed on the polished sections of this test, and many areas had shallow or nearly shallow pits (Figure D-32). Intergranular corrosion also took place, but did not penetrate into the samples as deeply as in the Baseline or Test II. The unstressed sample in Test III exhibited the same types of corrosion as were found on the stressed rings. However, there was more pitting found in Test III than intergranular corrosion, and the intergranular corrosion was somewhat less distinct. In all specimens of Test III, corrosion began at and followed along the grain boundaries. There was also very little of the shallow surface corrosion that had occurred in the Baseline and Test II.

The surfaces of the Test III flat specimens had the same general corrosion (Figure D-33) and corrosion initiated at machine marks found on the flat specimens of the Baseline and Test II. There were also some deeper pits which were not seen on the Baseline or Test II specimens.

The polished sections had large amounts of shallow under-surface corrosion with some grain removal and some surface roughness. The under-surface corrosion was much more severe than that found in Test II. There was also some grain removal associated with the severest under-surface corrosion. The grain removal may have caused some of the losses in mechanical properties of the tensile specimens in this test. Finally, there was a good deal of surface roughness on these samples which is indicative of general corrosion.

TEST IV

Test IV was run using three different exposure intervals: 45 , 67, and 90 days. The 45-day exposure C-rings generally had small pits on the surface (Figure D-34). However, the edge surfaces had damage which ranged from minimal pitting to very severe pitting. The thin rings (0.028" thickness) seemed to have had more severe attack on the sides than did the thick rings (0.056" thickness). In this test, two C-rings were kept in a desiccator for each time period and surface features consisted entirely of machine marks (Figure D-35).

After 67 days, the shallow elongated pits (Figure D-36) were only slightly larger than after 45 days. The small equiaxed pits (Type A corrosion) on the front surface (Figure D-37) grew significantly during that span of 22 days and, in addition, appeared on the edge surfaces. In the same time span, a few large pits developed on the surface of the C-rings (Figure D-38). The specimens that were kept in the desiccator showed no perceptible changes after 67 days.

The surfaces of the 90-day exposure C-rings were noticeably more affected by the environment than either the 45- or 67-day exposure. The exterior surface was severely attacked by Type A corrosion (Figure D-39). The edges also had more severe versions of the elongated shallow pits and equiaxed pits (Figure D-40) that were seen on the 67-day exposure. The desiccator specimens showed no change in microstructure nor signs of corrosion after 90 days.

The polished C-ring sections from the 45-day exposure had smaller versions of the pits found in the Baseline and Tests II and III specimens. These pits were neither as severe nor as numerous as those previously seen. However, these pits did have one feature that was not often seen in the other tests—the larger pits tended only to have small intergranular cracks or corrosion, and were sometimes found on the exterior surface.

The pits on the interior surface, while smaller, were more numerous and the cracks within the pits were significantly more severe. Intergranular cracks (Figure D-41) were usually found in the deeper pits where the grain direction was nearly perpendicular to the surface, but there was some intergranular crack initiation at the sites of the shallow surface attack. Transgranular cracks tended to initiate from the smaller shallow pits (Figure D-42) and, in some cases, the surface pit was only barely visible (Figure D-43). The specimens which were kept in the desiccator had no signs of any corrosion attack (Figure D-44) and had smooth surfaces with no cracks after 45 days.

While the outer surface of the polished 67-day exposure C-ring sections had very little in the way of cracks or pits with cracks at the bottoms of them, the pits associated with cracks on the inner surface were larger after 67 days than they were after 45 days. The large pits with intergranular cracks, which were observed after 67 days, consisted of further corrosion and coalescence of those intergranular cracks observed after 45 days (Figure D-45). The transgranular cracks had larger pits after 67 days, indicating that pit growth occurred after cracking. In some cases, a narrow deep pit seemed to follow the path of a transgranular crack (Figure D-46). There was an increase of pitting and intergranular cracks. Many of the intergranular cracks appeared to have been initiated at the smaller surface pits (Figure D-47) indicating that these were formed between the 45th and 67th day. The presence of both trans- and intergranular cracks in the same region of the specimen was seen on the polished specimens of the 67-day exposure, but not on any of the 45-day exposure. Figure D-48 shows how the crack changed mode at some time in its life. Like the 45-day desiccated samples, the 67-day desiccated samples showed no sign of corrosion.

The polished sections from the 90-day exposure again revealed that most of the corrosion damage occurred on the inner surface rather than on the outer surface. In some instances, the large pits in these specimens rivaled the size of those seen in the Baseline Test (Figure D-49). These large 90-day pits evolved from 45-day pits with intergranular cracks in them. There were still signs of intergranular cracking within some pits, but not as severe as in the 67-day exposure. Most of the cracks stopped growing when the stresses were relieved. The pits then grew along the cracks causing the cracks to disappear. There was also a decrease in the amount of transgranular cracks. It was believed that the transgranular cracks seen in the C-rings after 67 days of exposure became the transgranular pits seen in the C-ring after 90 days of exposure. However, not enough transgranular pits (Figure D-50) were found to account for the disappearance of the transgranular cracks. Since most of the transgranular cracking was relatively shallow, many of the transgranular cracks were probably swallowed up by large, shallow pits. The deeper cracks could have been removed through substantial intergranular corrosion resulting in grain loss as is seen in Figure D-51. The samples which were kept in the desiccator for 90 days exhibited no changes from those which were stored for shorter time intervals.

The surfaces of Test IV flat's samples were variegated. The 67-day samples had an abundance of small, shallow pits (Figure D-52). The pits found on the 90-day exposure specimens were somewhat larger (Figure D-53). The corrosion also obscured the rolling machine marks. In this test, some of the flat specimens were tensile cut before, rather than after, exposure. The machine marks from tensile cutting were obscured by the corrosion that took place. Figure D-54 shows how the side appeared after the tensile cutting operation, while Figure D-55 shows the bar after 67- and 90-day exposures.

The polished sections of the flat specimens from Test IV's 67- and 90-day exposures, were very similar to each other. The 90-day samples suffered only a litte more in the way of damage than did the 67-day samples. The corrosion on the front and back surfaces was almost exclusively the shallow under-surface corrosion. Figure D-56 shows how the shallow under-surface corrosion can eventually lead to grain removal. There were also several small surface pits (Figure D-57). On the edge surfaces, which were within the rack, there were some large pits which usually followed the grain direction. The pits which were found in the tensile pre-cut sections were significantly smaller than those sections from within the rack (Figure D-58) because the specimen rack did not create a crevice with this particular sample configuration.

TEST V

The surfaces of the Test V C-rings suffered only light to moderate amounts of Type A (small equiaxed pits) corrosion. The edges of these samples only had minor amounts of shallow surface corrosion. The surfaces of these specimens were affected by the environment less than in any other test, except for Test VIII.

The polished C-ring sections of Test V showed only minor damage due to corrosion. Most of this damage was because of shallow surface corrosion (Figure D-59) and small surface pits. There was some intergranular corrosion as well. As the surface analysis seemed to indicate, there was very little sub-surface corrosion damage.

The surfaces of the flat specimens in Test V also showed very little damage from environmental attack. There was almost no evidence of Types D or F corrosion, although there were a few small pits. The flat specimens in this test were not sectioned.

TEST VI

The surface examination of Test VI's thick C-rings (0.056'' wall thickness) revealed that there were two types of surface features present: Type C and Type D. Type D corrosion varied on the outer surface from cosmetic (where machine marks were slightly obscured) to moderate (where the area had several large shallow pits (Figure D-60)). Sometimes the latter version may have had cracks associated with it. Surface corrosion on the edges

was somewhat more severe (Figure D-61). The edges also had Type C (shallow elongated pits) corrosion (Figure D-62), and a feature that can best be described as directionally oriented shallow corrosion (a combination of Types C and D). The thin ring (0.028" thick) exhibited the same features as those found on the thick rings.

The polished sections of the thick rings had shallow pits, deep pits, and pits with associated intergranular corrosion (Figure D-63). The damage found on the exterior of the rings was significantly greater and deeper than that found on the interior, indicating that the greater effect was on areas directly exposed to the environment and under applied tensile stress. The thin ring specimen had traces of all the previously mentioned forms of attack but was predominantly damaged by shallow surface corrosion. Figure D-64 shows how corrosion left the surface in good shape while quite a bit of the metal had been removed from underneath.

The surfaces of the flat specimens in this test typically had a variegated appearance (Figure D-65) which indicated that corrosion took place in adjacent patches over the sample's area. It is believed that the brighter areas were spots where microbiological colonies grew (Figure D-66) and where the damage was more severe. There was also a substantial number of pits on the samples in this test.

The polished sections revealed large amounts of corrosion damage. As with the previous tests, shallow under-surface corrosion was the predominant form of attack. This form did not penetrate more than two grain layers into the sample. There was significant surface roughness, which indicated general corrosion but not grain removal. Shallow pits with short, narrow channels at their bottoms (Figure D-67)—like those seen in Test III—mainfested themselves in this test as well, but these narrow channels were deeper. As was indicated by the surface analysis, there was more pitting (Figure D-68) than in the Baseline, Test II or Test III. Some of the pits were serious (Figure D-69), penetrating into the sample more than six grain layers deep. This penetration was more than three times the depth of anything previously observed. Additionally, the sides had deep pitting which followed in the grain direction (Figure D-70). This was the only test in which the flat specimens were more severely attacked than the Baseline test.

TEST VII

Test VII was run concurrently with Test VI with only one change—all the specimens in Test VII were sprayed with Air Force Inhibitor 7. The surface analysis showed that the thick C-rings had elongated shallow pits, elongated pits, and shallow pits. These various forms of pitting were also found on the thin C-ring. The differences between Test VI and Test VII were fewer pits in Test VII and certain areas of the Test VII sample suffered only minimal corrosion damage.

The polished sections reflected what was seen in the surface anlaysis. There was significantly less intergranular corrosion than on Test VI C-rings and it was less severe. There were also fewer deep pits (Figure D-71). Shallow pits were the prevalent form of corrosion, varying from shallow-normal pits to shallow-surface corrosion. The outer surface had less deep pits and intergranular corrosion than was found in Test VI, whereas the decrease on the interior was less dramatic. This would seem to indicate that the inhibitor worked by preventing the shallow pitting from penetrating and forming into intergranular cracks rather than by preventing corrosion altogether. For some reason, the thin C-rings did not enjoy the same benefits of the inhibitor as did the thick C-rings. The thin ring had more of the severe forms of corrosion (Figure D-72) than were found on the thick rings.

The use of Air Force Inhibitor 7 on the Test VII flat specimens reduced the number and severity of the features seen in the surface analysis of the C-rings. The variegated surface was still present, but there was less distinction between the dark and light areas. Even those areas covered by microbiological colonies showed less corrosion damage. There were still a few pits, but they were smaller and less severe than in Test VI.

The polished sections from Test VII showed signs of significantly less internal damage than did those from Test VI, which can be attributed to the use of the inhibitor. The predominant form of corrosion was the shallow under-surface corrosion which did not penetrate to more than one grain layer. There were fewer instances of the narrow pits within shallow pits, which were shallower than in Test VI.

There was virtually no surface roughness nor pitting. Also, the edges of these samples showed no signs of the attack which was seen in Test VI. In addition, the face of the sample receiving the greater dose of inhibitor exhibited less corrosion damage than the opposite face.

TEST VIII

The specimens for Test VIII were run in the same environmental chamber concurrently with the specimens for Test V. The only difference was that the specimens of Test VIII were sprayed daily with Air Force Inhibitor 7. The surface of the C-rings in Test VIII showed no visible difference in corrosion of the sides from the specimens in Tests V, but the pitting of the exterior surface seemed to be less severe.

The polished ring sections of Test VIII showed much of the same kind of damage (Figure D-73) as was seen in Test V, but not to the same degree. The corrosion damage did not go as deep, and the shallow surface corrosion was virtually nonexistent. The damage seen in Test V and VIII was much less severe than that seen in any of the other

tests. As was the case in Test V, the flat specimens in Test VIII exhibited almost no signs of environmental damage, and there was very little in the way of biological attack. The flat specimens from this test were not sectioned.

SUMMARY FEATURE ANALYSIS

While the surface analysis was particularly effective in tracking the changes in corrosion due to variations of the test environment, it generally did not reflect nor predict the microstructural damage found. This damage was usually far worse than was suggested by the surface corrosion damage. The most serious corrosion feature in Test IV—cracks—was not seen on any of the surfaces analyzed. Once again, the surface condition of aluminum alloys did not accurately indicate potential corrosion problems due to the localized nature of the corrosion attack on these alloys.

Although the surface analysis was not a good indicator of specific microstructural damage, it accurately reflected the differences in relative amounts of corrosion between Tests V and VIII, and Tests VI and VIII. Each pair of tests was run concurrently in the same environmental chamber, but one set of the samples from each chamber was sprayed with Air Force Inhibitor 7[1] and the other was not treated. In each case, the inhibitor sprayed set (Tests VII and VIII) had less surface corrosion than its untreated counterpart. This observation was sustained in the examination of the microstructure of the polished and etched specimens. The inhibitor prevented cracks of intergranular corrosion and caused the pitting and shallow surface corrosion damage to be less severe.

The type and severity of corrosion differed between the flat specimens and the C-rings. The flat specimens generally had very shallow surface attack with some under-surface corrosion, which did not penetrate more than one or two grain depths on both the front and back surfaces. Aside from several intrusions by pits along the grain boundaries (depth of 0.040mm maximum), there was very little in the way of corrosion of the edges. This may have been due to rougher surfaces on the sides which made some forms of corrosion difficult to discern, even on the polished sections and shallow surface corrosion. The C-ring had a considerable amount of pitting, which occurred on all surfaces and varied in depth from > 0.002mm to complete penetration of the sample. The width of the pits also varied widely. On some of the stressed rings, cracks were also present. The unstressed C-rings behaved in much the same way as their stressed counterparts. On both sets, there was damage on the interior surface due to water droplets collecting and remaining there through the hot soak. The difference between the stressed and the unstressed C-rings was that corrosion damage was shallower and there were no cracks on the unstressed C-ring. The initiation of most of the dissimilarities in the corrosion behavior was attributed to configurational differences with the exception of cracking, which was not seen on the flat specimens or unstressed C-rings and was attributed to the presence of an applied stress.

SECTION V. CONCLUSIONS

The statistical analysis of the tensile data establishes a probable linkage between the exposure to nitrates and a change in tensile properties of unstressed Al 7075-T7351. The word "probable" is used due to the limited number of samples tested, and as a result of some of the seemingly contradictory results, such as those occurring in Test IV between the solid bar exposure results and the tensile bar exposure results. The use of a single lot and a single heat for the test material hampers interpreting the apparent contradictions seen in the results of the tensile test data. The analysis of the microstructure, while showing that real differences did occur in the type and extent of corrosion between the different tests, revealed no differences to explain the different tensile test results between the two Baseline Tests or within the November 1985 Baseline Test. The basic statistics of data from those tests which showed no effects of the exposure on the tensile properties validates the technique of those performing the tests, and the reliability of the test system. In all but two cases, the f-statistic and the t-statistic tracked one another when a test was compared to its control set. The mass of evidence is sufficient to warrant further study of these effects.

In terms of the microstructural analysis, we achieved our original goal to block out the parameters of the synergistic effects of chlorides and nitrates. The Baseline environment proved to be the most detrimental to both C-rings and flat specimens. The flat specimens were most affected by the environment in Test VI, and the C-rings by the environment in Test IV. The C-ring and flat specimens of Test V sustained the least amount of corrosion-related damage without the use of an inhibitor. The high concentration of nitrates and other salts in the Baseline environment, as against the Test III concentration, indicates that the concentrations may have been responsible for the amount of damage in this test. The results from Test V and the C-rings of Test VI support this hypothesis. Each had lower salt concentrations than the Baseline and lower incidence of corrosion. The severe attack of the flat specimens of Test VI showed that the combination of dilute salts and concentrated gases can be worse than the presence of concentrated salts alone. The acid gases, however, require the presence of the salts for accelerated corrosion to occur. This was illustrated by Test V, where no fogging solution was used and very little corrosion damage was sustained.

The samples in Test IV were exposed to an environment similar to the one used in Test VI, except the concentrations of SO_2, NO_2, NO, and CO_2 were lower, and ozone—which was not used in Test VI—was present. The lower concentrations of acid gases should have lessened the extent of damage on the specimens and, as would be expected after 90 days of exposure, the flat specimes of Test IV showed less damage (i.e., the surface attack was shallower) than was seen on the flats of Test VI.

On the other hand, the ring specimens of Test IV behaved differently than expected. Although the pits were of normal size and quantity there was, after 45 days, a substantial number of pits which had cracks and pits emanating from them. The cracks in the stressed material (C-ring) can be attributed to the presence of ozone in the test environment. Crack growth continued until the stresses were relieved and further exposure to the environment eventually lead to corrosion damage, which after 90 days, looked like severe pitting. The cracks were unusual in that crack initiation occurred at the bottoms of pits on the interior surface and grew towards the exterior surface. Usually, crack initiation occurs on a surface in tension. The exterior surface was subjected to a tensile stress of 31,000 psi and exhibited no sign of cracking.

Our fogging solutions for exhaust and West Coast-simulated environments proved to be rather benign when compared to the actual thing. Unabated exhaust condensates have a pH range of 2.3-3.0, or 30 times more acid than our pH of 4.2-4.5.[24-27] Environmental data for southern California, 1982-1984, shows some portions of that area were subjected to acid fogs, pH 1.7-3.0,[28-36] and that the local daily ozone concentration could exceed 0.12ppm for up to 154 days per year,[37] making our simulated Los Angeles environment more benign than originally planned. This illustrates a generalized problem with most corrosion data today. The long term data represents a world that no longer exists except in a few isolated instances, so that while the trends are still valid, the actual rates are not. The 40-year compilation of data can no longer be relied on for design values. The problem is in the short term in keeping the system together long enough for the long term trend to take effect, as the short term rates are ever-changing in response to changes in the local environment. The rate of transfer of relevant environmental data needs to be greatly improved, as does the ability to collect that data, and general access to the data sources.

FOOTNOTES

1. C. E. Lynch and F. W. Vahldiek, "High Performance Multifunctional Corrosion Inhibitors," *AF INF 14985*, AF/JACPD, Wright-Patterson AFB, OH, 1982.

2. S. C. Byrne and A. C. Miller, "Effect of Atmospheric Polutant Gases on the Formation of Corrosive Condensate on Aluminum," *Atmospheric Corrosion of Metals, ASTM STP 767*, S. W. Dean, Jr. and E. C. Rhea, eds., Amercian Society for Testing and Materials, 1982, pp. 359-373.

3. S. Maitra and G. C. English, "Environmental Factors Affecting Localized Corrosion of 7075-T735 Aluminum Alloy," *Metall Trans Acta*, Vol. 13A, January 1982, pp. 161-166.

4. J. C. Tyler, J. T. Gray, and W. D., Weatherford, *An Investigation of Diesel Fuel Composition-Exhaust Emission Relationships,* Report AFLRL No. 42, US Army Fuels & Lubricants Research Laboratory, San Antonio, TX, October 1974.

5. A. H. Le, B. F. Brown, and R. T. Foley, "The Chemical Nature of Corrosion: IV Some Anion Effects on SCC of AA 7075-T651," *Corrosion*, Vol. 26, No. 12, December 1980, pp. 673-679.

6. T. H. Nguyen, B. F. Brown, and R. T. Foley, "On the Nature of the Occluded Cell in the Stress Corrosion Cracking of AA 7075-T651—Effect of Potential, Composition, Morphology," *Corrosion,* Vol. 30, No. 6, June 1982, pp. 319-326.

7. R. T. Foley, *Clarification of Environmental Effects in Stress Corrosion Cracking,* Technical Report AD-A138581, Office of Naval Research, Arlington, VA, 1984.

8. M. Khobaib, et al, "Accelerated Atmospheric-Corrosion Testing", *Atmospheric Corrosion of Metals, ASTM STP 767,* S. W. Dean, Jr. and E. C. Rhea, eds., ASTM, 1982, pp. 374-394.

9. F. H. Haynie, "Evaluation of the Effects of Microclimate Differences on Corrosion," *Atmospheric Corrosion of Metals, ASTM STP 767,* S. W. Dean, Jr. and E. C. Rhea, eds., ASTM, 1982, pp. 374-394.

10. R. M. Harrison and C. A. Pio, "A Comparative Study of the Ionic Composition of Rainwater and Atmospheric Aerosols: Implications for the Mechanism of Acidification of Rainwater," *Atmospheric Environment,* Vol. 17, No. 12, 1983, pp. 2,539-2,543.

11. G. T. Wolff, "On the Nature of Nitrate in Coarse Continental Aerosols," *Atmospheric Environment,* Vol. 18, No. 5, 1984, pp. 977-981.

12. C. Seigneur and P. Saxena, "A Study of Atmospheric Acid Formation in Different Environments," *Atmospheric Environment,* Vol. 18, No. 10, 1984, pp. 2,109-2,124.

13. J. H. Seinfeld, *Atmospheric Chemistry and Physics of Air Pollution,* John Wiley & Sons, New York, 1986, pp. 12-16, 93, 698-701.

14. S. Witz and R. D. MacPhee, "The Inverse Relationship and Diurnal Behavior of Sulfate and Nitrate," *Nitrogenous Air Pollutants,* David Grosjean, ed., Ann Arbor Science, 1979, pp. 243-257.

15. G. J. McRae and A. G. Russell, "Dry Deposition of Nitrogen Containing Species," *Deposition Both Wet and Dry,* Bruce Hicks, ed., Butterworth Pub., 1984, pp. 153-193.

16. F. W. Lipfert, *Effects of Acidic Deposition on Atmospheric Deterioration of Materials,* Conf. Paper 105, National Association of Corrosion Engineers, Houston, TX, March 1986.

17. W. H. Chan and D. H. S. Chung, "Regional Scale Precipitation Scavenging of SO_2, SO_4, NO_3, and HNO_3, *Atmospheric Environment*, Vol. 20, No. 7, 1986, pp. 1,397-1,402.

18. S. J. Ketcham, *Accelerated Laboratory Corrosion Test for Materials and Finishes Used in Naval Aircraft,* Report No. NADC-77252-30, Naval Air Development Center, September 1977.

19. H. Bohni and H. H. Uhlig, "Environmental Factors Affecting the Critical Pitting Potential of Aluminum," *J of Electrochem. Soc.,* Vol 116, No. 7, July 1969, pp. 906-910.

20. A. M. McKissick, A. A. Adams, and R. T. Foley, "Synergistic Effects of Anions in the Corrosion of Aluminum Alloys," *J of Electrochem. Soc.,* Vol. 117, No. 11, November 1970, pp. 1,459-1,460.

21. K. Sotoudeh, R. T. Foley, B. F. Brown, *The Chemical Nature of Aluminum Corrosion: I Activation of Aluminum Surfaces by Aluminum Salts,* Technical Report No. 10, The American University, Washington, DC, November 1979.

22. T. H. Nguyen and R. T. Foley, "The Chemical Nature of Aluminum Corrosion: III The Dissolution Mechanism of Aluminum Oxide and Aluminum Powder in Various Electrolytes," *J of Electrochem. Soc.,* Vol. 127, No. 12, December 1980, pp. 2,563-2,566.

23. B. W. Lifka, "SCC Resistant Aluminum Alloy 7075-T73 Performance in Various Environments," *Aluminum*, Vol. 53, 1977, pp. 750-752.

24. P. J. Boden, S. J. Harris, and B. R. Pearson, *Laboratory Simulation of Car Exhaust Corrosion,* UK National Corrosion Conference, 1982/1983.

25. R. L. Chance and R. G. Ceselli, *Corrosiveness of Exhaust Condensates,* Conf. Paper 830585, Society of Automotive Engineers, 1983.

26. J. E. Hunter, *The Effects of Emission Control Systems and Fuel Composition on the Composition of Exhaust Gas Condensate,* Conf. Paper 830584, Society of Automotive Engineers, 1983.

27. M. S. El-Shobokshy, "The Effect of Diesel Engine Load on Particulate Carbon Emission," *Atmospheric Environment*, Vol. 18, No. 11, 1984, pp. 2,305-2,311.

28. Waldman et. al., "Chemical Composition of Acid Fog," *Science*, 218, 1982, pp. 677-680.

29. J. L. Durham, H. M. Barnes, and J. H. Overton, Jr., "Acidification of Rain by Oxidation of Dissolved Sulfur Dioxide and Absorption of Nitric Acid," *Chemistry of Particles, Fogs, and Rain*, Jack L. Durham, ed., Butterworth Publishers, 1984, pp. 197-235.

30. A. W. Gerter, et. al., "Studies of Sulfur Dioxide and Nitrogen Dioxide Reactions in Haze and Cloud," *Chemistry of Particles, Fogs, and Rain*, Jack L. Durham, ed., Butterworth Publishers, 1984, pp. 197-235.

31. M. R. Hoffman and D. J. Jacob, "Kinetics and Mechanisms of the Catalytic Oxidation of Dissolved Sulfur Dioxide in Aqueous Solution: An Application to Nighttime Fog Water Chemistry," *So_2, NO and NO_2 Oxidation Mechanisms: Atmospheric Considerations,* Jack G. Calvert, ed., Butterworth Publishers, 1984, pp. 101-172.

32. J. W. Munger, et. al., "Fogwater Chemistry in an Urban Atmosphere," *J. Geophys. Res.*, 88, 1983, pp. 5,109-5,121.

33. M. R. Hoffman, "Acid Fog," *Engineering and Science,* September 1984, pp. 5-11.

34. W. T. Sturges and R. M. Harrison, "Bromine in Marine Aerosols and the Origin, Nature and Quantity of Natural Atmospheric Bromine," *Atmospheric Envirnoment,* Vol. 20, No. 7, 1986, pp. 1,485-1,496.

35. P. A. Mulawa, et. al., "Urban Dew: Its Composition and Influence on Dry Deposition Rates," *Atmospheric Environment,* Vol. 20, No. 7, 1986, pp. 1,389-1,396.

36. F. Mansfeld, et. al, "A New Atmospheric Corrosion Rate Monitor—Development and Evaluation," *Atmospheric Environment,* Vol. 20, No. 6, 1986, pp. 1,179-1,192.

37. *Gilian Instrument Company Newsletter,* December 1987, p. 4.

APPENDIX A
SPECIMEN CONFIGURATION

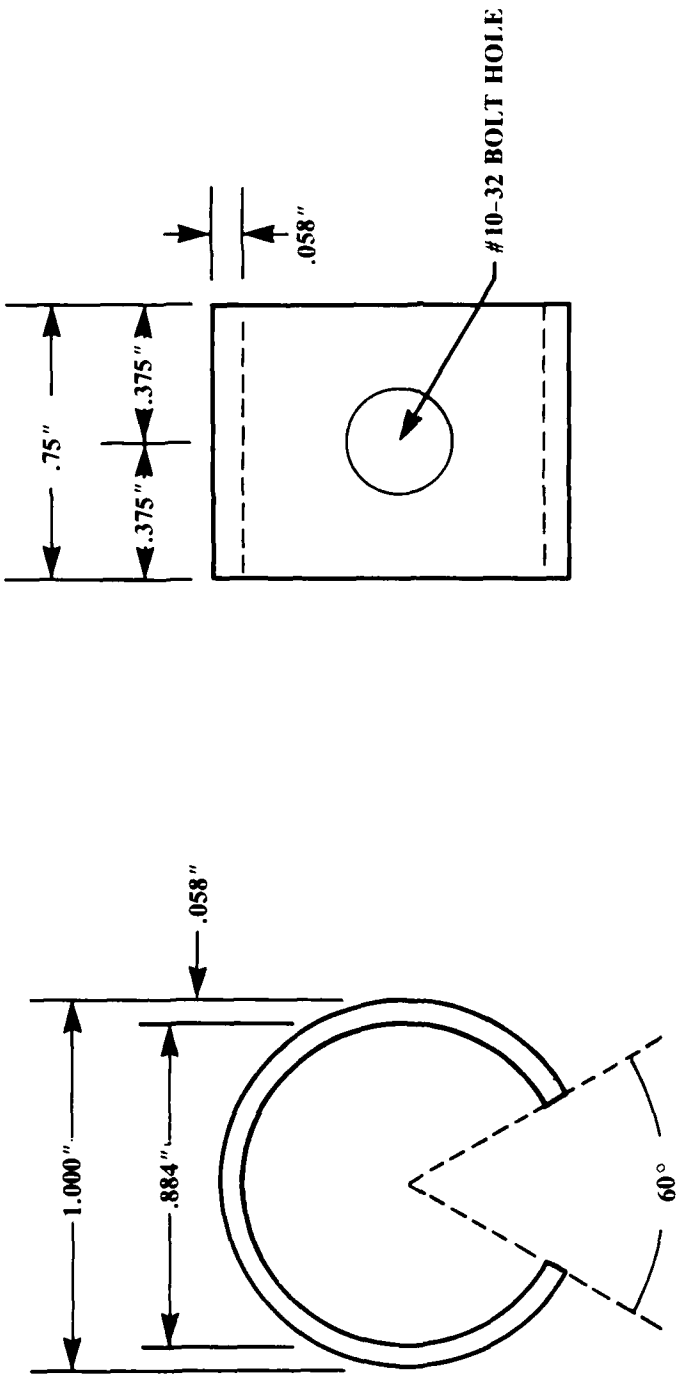

Figure A-1. C-Ring

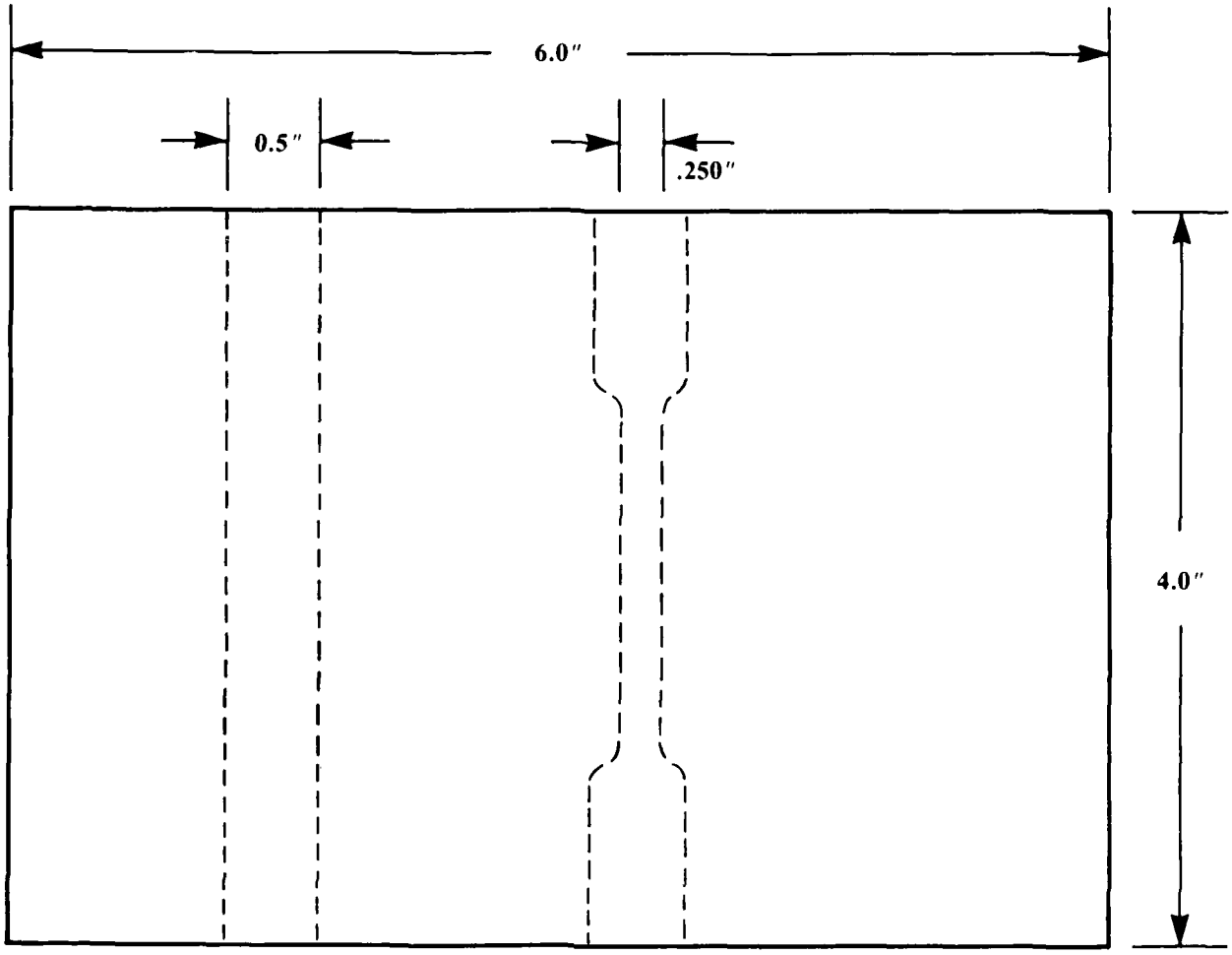

Figure A-2. Flat plates

APPENDIX B
CONTROL SETS — TENSILE TEST DATA

Contents

L-T CONTROLS

Tensile Specimens

REMARKS	Sample number	Thickness (inches)	Width (inches)	Area (sq. inch)	Gage Initial (inches)	Length: Final (inches)	Percent Elong-ation	Ultimate Force (pounds)	Ultimate Strength (ksi)	Yield Force (pounds)	Yield Strength (ksi)
CONTROLS	AL19	0.256	0.251	0.064	1.005	1.194	18.8	4505	70.4	3750	58.6
CONTROLS	AL20	0.247	0.250	0.062	0.998	1.160	16.2	4300	69.4	3650	58.9
CONTROLS	AL21	0.255	0.251	0.064	1.000	1.148	14.8	4515	70.5	3790	59.2
CONTROLS	AL22	0.256	0.250	0.064	1.000	1.155	15.5	4515	70.5	3725	58.2
CONTROLS	AL23	0.257	0.251	0.065	0.996	1.128	13.3	4520	69.5	3750	57.7
CONTROLS	AL24	0.255	0.251	0.064	0.999	1.142	14.3	4510	70.5	3725	58.2
average				0.064			15.5		70.1		58.5
std. dev				0.001			1.9		0.5		0.5

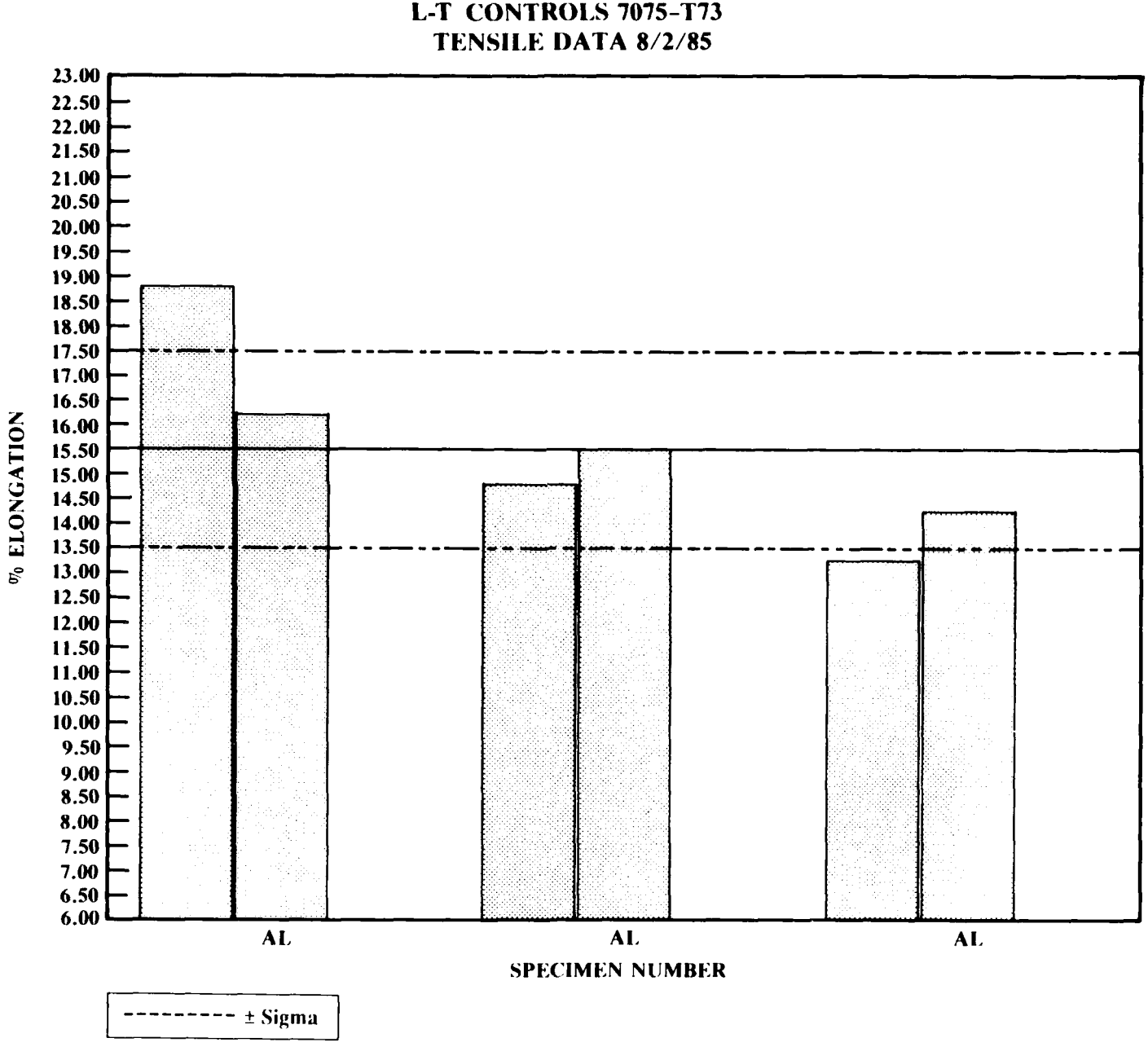
L-T CONTROLS 7075-T73
TENSILE DATA 8/2/85
% ELONGATION
23.00
22.50
22.00
21.50
21.00
20.50
20.00
19.50
19.00
18.50
18.00
17.50
17.00
16.50
16.00
15.50
15.00
14.50
14.00
13.50
13.00
12.50
12.00
11.50
11.00
10.50
10.00
9.50
9.00
8.50
8.00
7.50
7.00
6.50
6.00
AL
AL
AL
SPECIMEN NUMBER
± Sigma

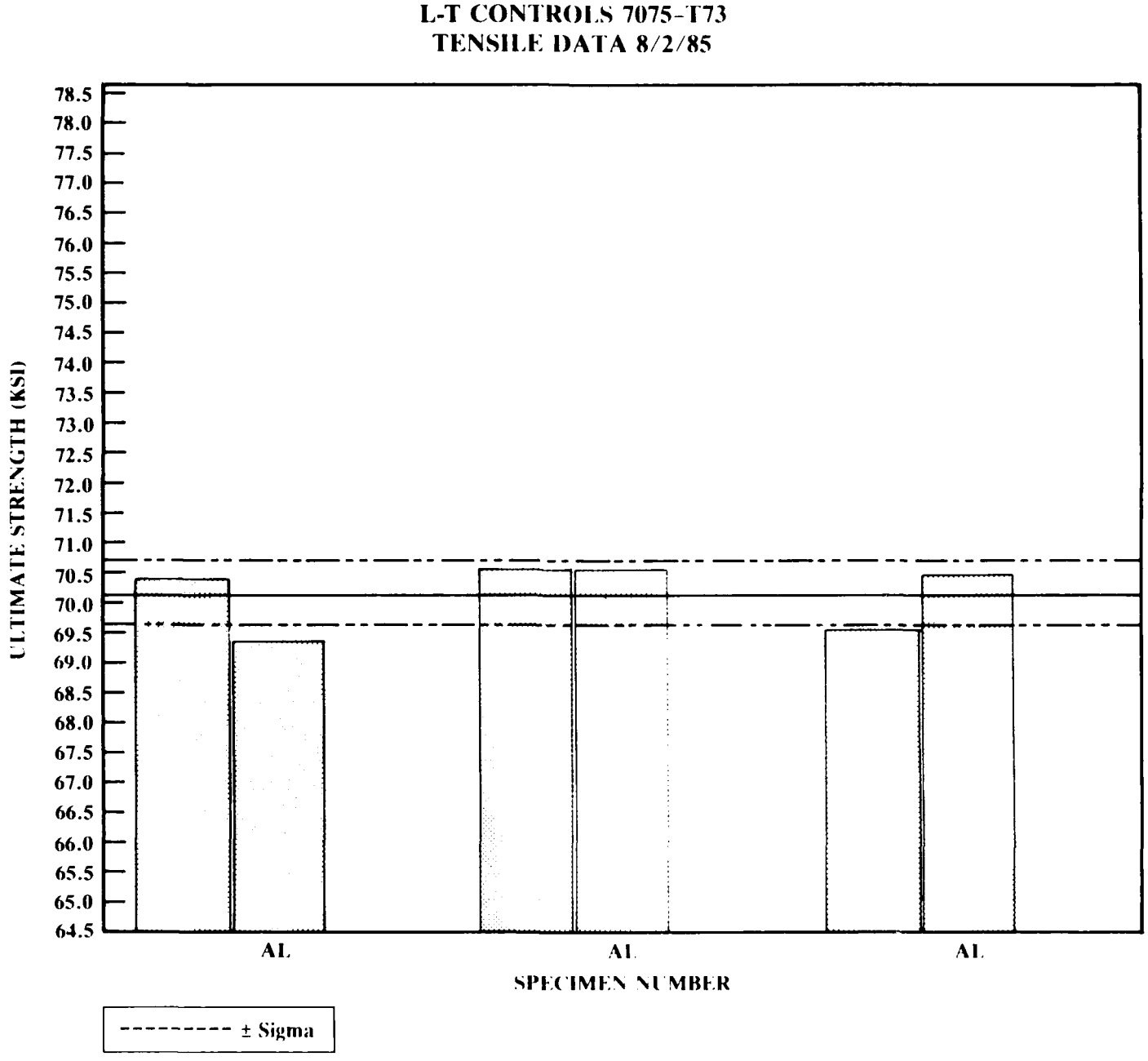
L-T CONTROLS 7075-T73
TENSILE DATA 8/2/85
ULTIMATE STRENGTH (KSI)
78.5
78.0
77.5
77.0
76.5
76.0
75.5
75.0
74.5
74.0
73.5
73.0
72.5
72.0
71.5
71.0
70.5
70.0
69.5
69.0
68.5
68.0
67.5
67.0
66.5
66.0
65.5
65.0
64.5
AL
AL
AL
SPECIMEN NUMBER
± Sigma

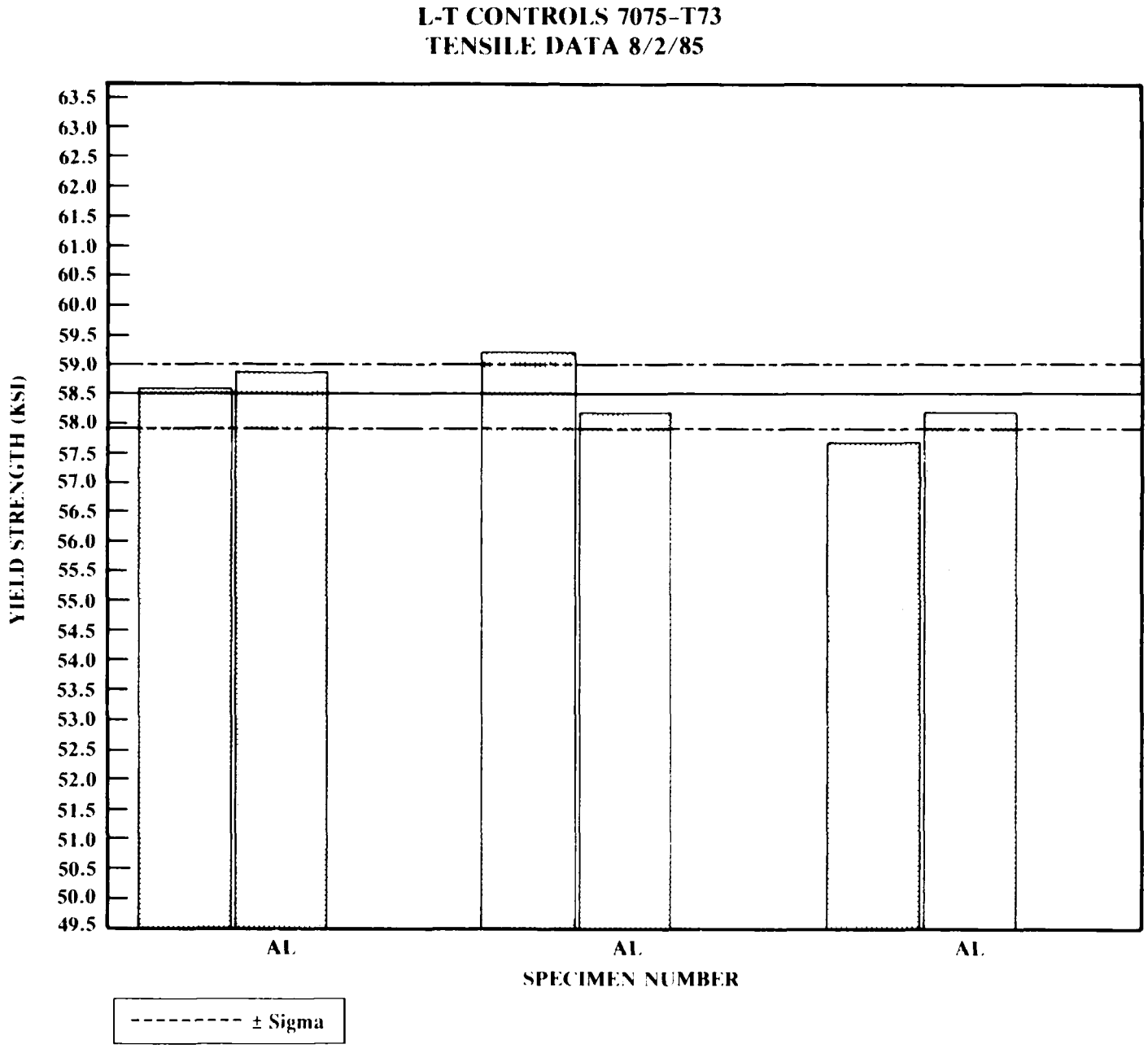
L-T CONTROLS 7075-T73
TENSILE DATA 8/2/85
YIELD STRENGTH (KSI)
63.5
63.0
62.5
62.0
61.5
61.0
60.5
60.0
59.5
59.0
58.5
58.0
57.5
57.0
56.5
56.0
55.5
55.0
54.5
54.0
53.5
53.0
52.5
52.0
51.5
51.0
50.5
50.0
49.5
AL
AL
AL
SPECIMEN NUMBER
± Sigma

C-RING PLATE MATERIAL

AL 7075-T7351
Tensile Specimens

REMARKS	Sample number	Thickness (inches)	Width (inches)	Area (sq. inch)	Gage Length: Initial (inches)	Final (inches)	Percent Elong-ation	Ultimate Force (pounds)	Ultimate Strength (ksi)	Yield Force (pounds)	Yield Strength (ksi)
ROLLING	I	0.249	0.247	0.062	1.000	1.116	11.6	4835	78.0	3955	63.8
ROLLING	II	0.248	0.247	0.061	1.000	1.140	14.0	4560	74.8	3760	61.6
ROLLING	III	0.249	0.248	0.062	1.000	1.132	13.2	4565	73.6	3780	61.0
ROLLING	IV	0.247	0.248	0.061	1.000	1.154	15.4	4630	75.9	3980	65.2
ROLLING	V	0.248	0.249	0.062	1.000	1.134	13.4	4595	74.1	3850	62.1
ROLLING	VII	0.249	0.253	0.063	1.000	1.134	13.4	4760	75.6	4010	63.7
ROLLING	VIII	0.248	0.249	0.062	1.000	1.122	12.2	4615	74.4	3970	64.0
AVERAGE				0.062			13.3		75.2		63.1
STDEV				0.001			1.2		1.5		1.5
SHORT	II	0.248	0.249	0.062	1.000	1.110	11.0	4750	76.6	4075	65.7
TRANSVERSE	III	0.248	0.245	0.061	1.000	1.112	11.2	4670	76.6	3910	64.1
	IV	0.245	0.245	0.060	1.000	1.113	11.3	4595	76.6	3850	64.2
	V	0.248	0.247	0.061	1.000	1.109	10.9	4450	73.0	3845	63.0
AVERAGE				0.061			11.1		75.7		64.3
STDEV				0.001			0.2		1.8		1.1
LONG	I	0.248	0.253	0.063	1.000	1.115	11.5	4725	75.0	3975	63.1
TRANSVERSE	II	0.248	0.245	0.061	1.000	1.113	11.3	4625	75.8	3940	64.6
	III	0.248	0.250	0.062	1.000	1.111	11.1	4695	75.7	3975	64.1
	IV	0.248	0.247	0.061	1.000	1.120	12.0	4630	75.9	3880	63.6
	V	0.247	0.250	0.062	1.000	1.122	12.2	4675	75.4	3875	62.5
AVERAGE				0.062			11.6		75.6		63.6
STDEV				0.001			0.5		0.4		0.8

ROUND TENSILE SPECIMENS 7075-T7351

DATE: 3/OCT/86

Sample number	Thickness (inches) (Dia)	Area (sq. inch) (d/2)^2*PI	Gage Initial (inches)	Length: Final (inches)	Percent Elong-ation	Ultimate Force (pounds)	Ultimate Strength (ksi)	Yield Force (pounds)	Yield Strength (ksi)
1	0.253	0.050	0.982	1.143	16.4	3680	73.2	3100	61.7
2	0.253	0.050	0.968	1.138	17.6	3685	73.3	2960	58.9
3	0.253	0.050	0.980	1.138	16.1	3665	72.9	2950	58.7
4	0.252	0.050	1.005	1.142	13.6	3670	73.6	3130	62.8
7	0.253	0.050	1.000	1.154	15.4	3595	71.5	3036	60.4
8	0.252	0.050	0.999	1.151	15.2	3650	73.2	3075	61.7
9	0.252	0.050	1.000	1.179	17.9	3640	73.0	3080	61.8
10	0.252	0.050	1.000	1.143	14.3	3580	71.8	2875	57.6
average		0.050			15.8		72.8		60.4
std. dev		0.000			1.5		0.7		1.8

APPENDIX C
TEST RESULTS — STATISTICAL AND GRAPH DATA

Contents

BASELINE TESTS

TEST CYCLE

SALT SPRAY	8 Hours	(MONDAY-FRIDAY)
PURGE AIR	16 Hours	(MONDAY-THURSDAY)
HOT SOAK (35 °C/95 °F)	28 Hours	(FRIDAY-SATURDAY)
CONDENSING SOAK (20 °C/68 °F)	35 Hours	(SATURDAY-MONDAY)

SALT FOG SOLUTION COMPOSITION

> 0.100 N Sodium Chloride (NaCl)
> 0.229 N Sodium Nitrate ($NaNO_3$)
> 0.089 N Sodium Sulfate (Na_2SO_4)
> chloride/nitrate ratio = 0.44
> chloride/sulfate ratio = 1.12
> pH 4.2-4.5

ACIDIFICATION STOCK SOLUTION

ACID*	NORMALITY
Sulfuric	0.333
Nitric	0.333
Hydrochloric	0.333

EXPOSURE SPECIMENS

8/85-10/85 TEST

PLATES 4″ × 6″ × 1/4″

3	Salt Fog-As Received
1	Immersed-As Received

C-RINGS 1.0″d × 0.75″w × 0.028″t

3	Salt Fog @ 31 ksi
1	Immersed @ 31 ksi

11/85-01/86 TEST

PLATES 4″ × 6″ × 1/4″

3	Salt Fog-As Received
3	Salt Fog-Polished
2	Immersed-Pol/As Received

C-RINGS 1.0″d × 0.75″w × 0.028″t

3	Salt Fog @ 3.1 ksi
3	Salt Fog @ 0 ksi
3	Immersed @ 3.1 ksi
3	Immersed @ 0 ksi

DURATION OF EXPOSURE 45 days/256 hours salt fog

*11/85 test used acetic acid for 10 days

BASELINE: AUG 1985 — NOV 1985

INTERGRANULAR CORROSION TEST 45 DAYS

REMARKS	Sample number	Thickness (inches)	Width (inches)	Area (sq. inch)	Gage Length: Initial (inches)	Gage Length: Final (inches)	Percent Elong-ation	Ultimate Force (pounds)	Ultimate Strength (ksi)	Yield Force (pounds)	Yield Strength (ksi)
7075-T73	LT 1	0.249	0.245	0.061	1.000	1.195	19.5	4280	70.2	3265	53.5
7075-T73	LT 2	0.253	0.245	0.062	1.000	1.174	17.4	4325	69.8	3610	58.2
7075-T73	LT 3	0.246	0.243	0.060	1.000	1.777	17.7	4130	68.8	3380	56.3
average				0.061			18.2		69.6		56.0
std. dev				0.001			1.1		0.7		2.4
7073-T73	LU 1	0.249	0.243	0.061	1.000	1.160	16.0	4150	68.0	3300	54.1
7073-T73	LU 2	0.249	0.248	0.062	1.000	1.157	15.7	4250	68.5	3520	56.8
7073-T73	LU 3	0.249	0.248	0.062	1.000	1.152	15.2	4245	68.5	3550	57.3
average				0.062			15.6		68.3		56.0
std. dev				0.001			0.4		0.3		1.7
7073-T73	LB 1	0.258	0.243	0.063	1.000	1.162	16.2	4195	66.6	3350	53.2
7073-T73	LB 2	0.251	0.243	0.061	1.000	1.159	15.9	4210	69.0	3530	57.9
7073-T73	LB 3	0.248	0.243	0.060	1.000	1.154	15.4	4170	69.5	3400	56.7
average				0.061			15.8		68.4		55.9
std. dev				0.002			0.4		1.6		2.4

BASELINE 7075-T73
TENSILE DATA 8/2/85

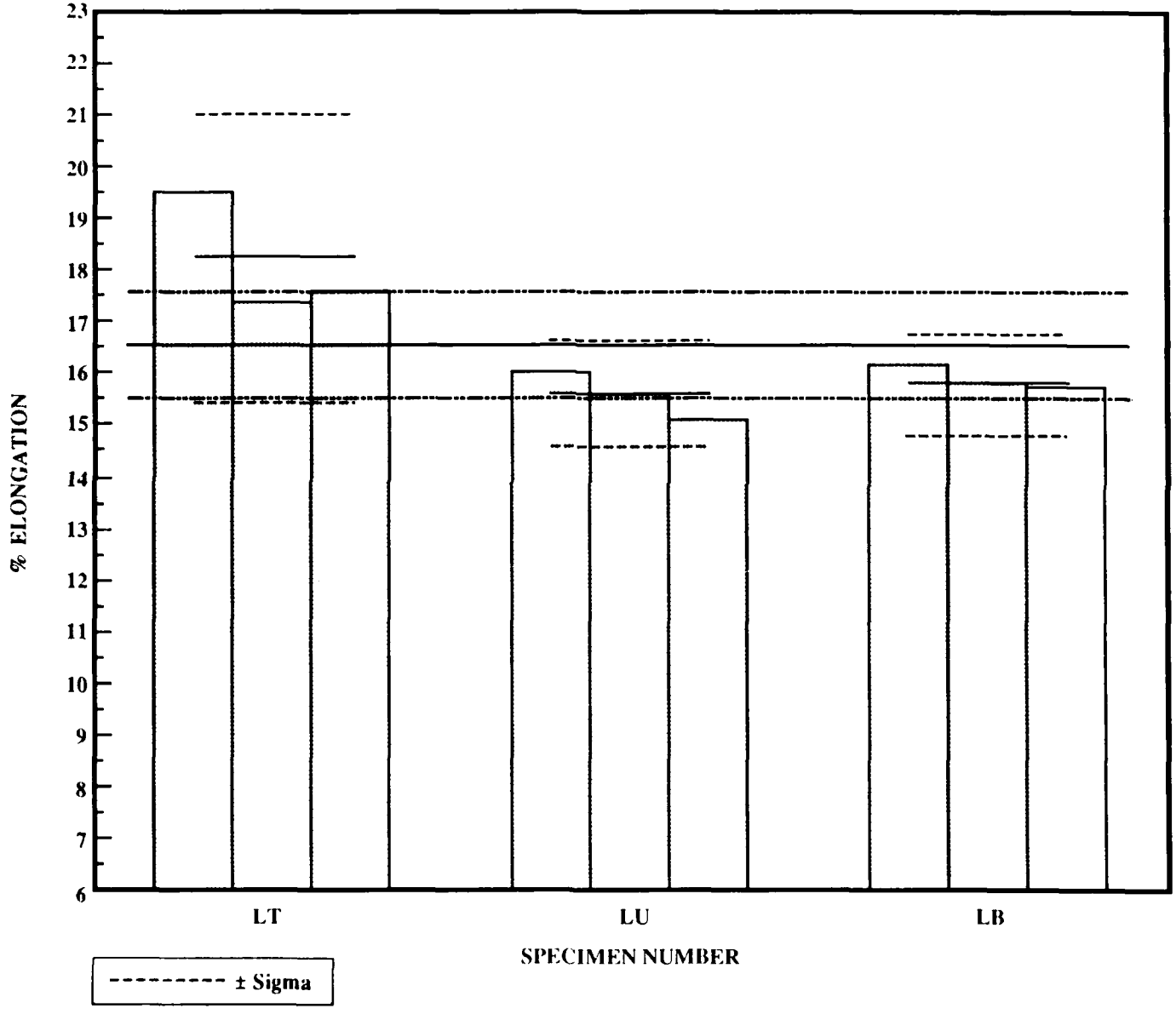

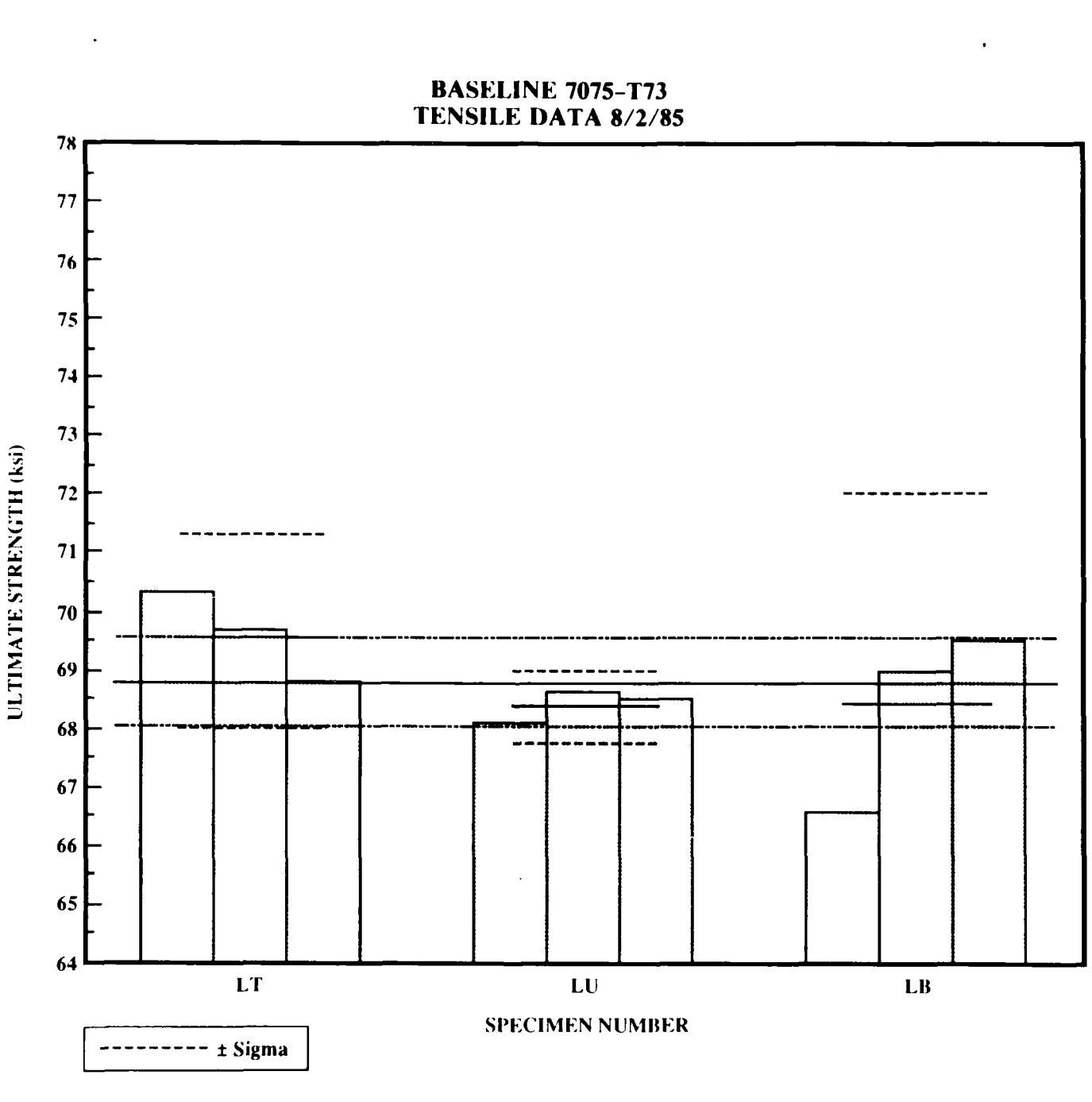
BASELINE 7075-T73
TENSILE DATA 8/2/85
ULTIMATE STRENGTH (ksi)
78
77
76
75
74
73
72
71
70
69
68
67
66
65
64
LT
LU
LB
SPECIMEN NUMBER
± Sigma

BASELINE 7075-T73
TENSILE DATA 8/2/85

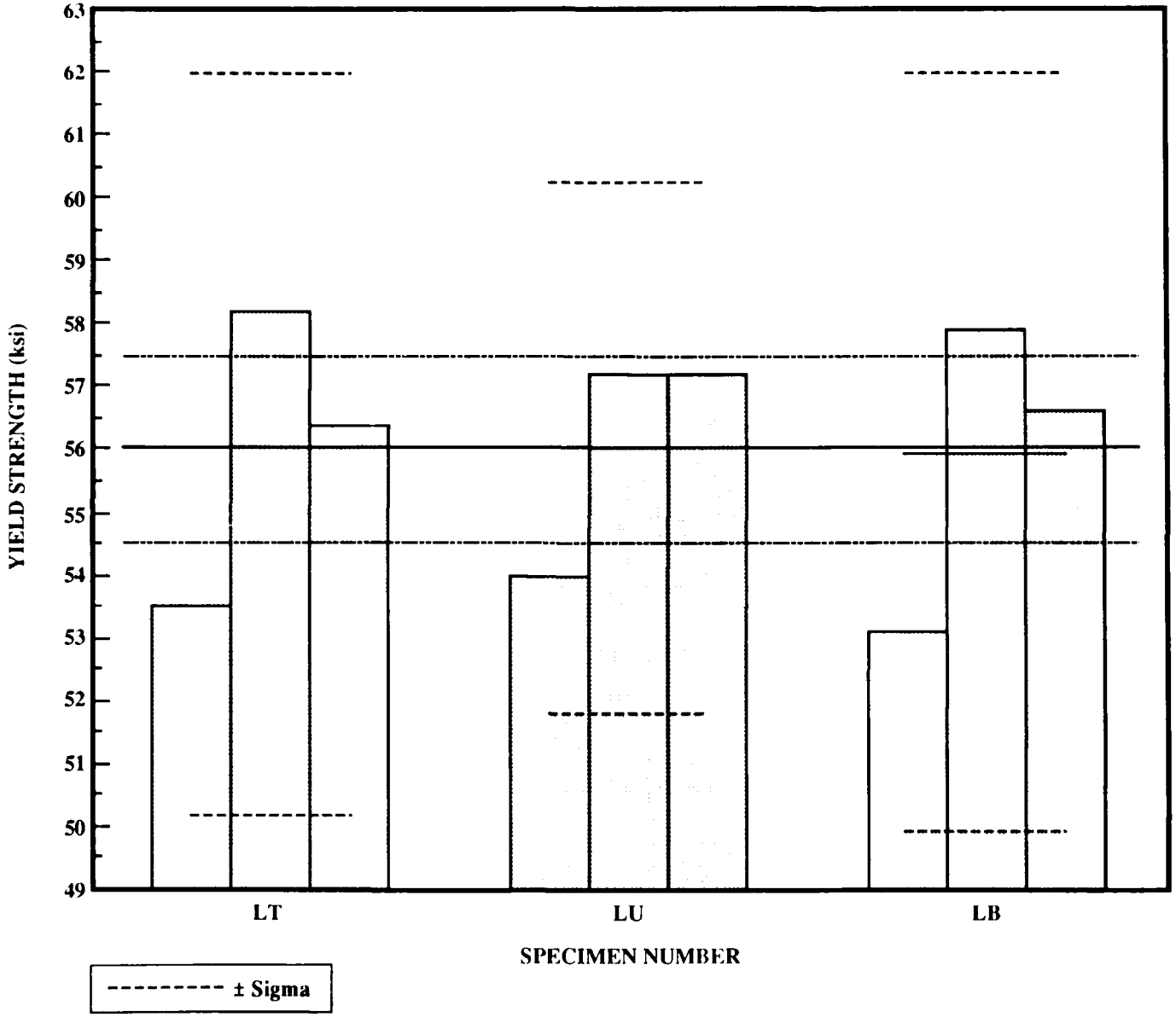

BASELINE: 27 NOV 1985 TO 17 JAN 1986

INTERGRANULAR CORROSION TEST 45 DAYS

REMARKS	Sample number	Thickness (inches)	Width (inches)	Area (sq. inch)	Gage Length: Initial (inches)	Gage Length: Final (inches)	Percent Elong-ation	Ultimate Force (pounds)	Ultimate Strength (ksi)	Yield Force (pounds)	Yield Strength (ksi)
IMMERSED	LM1	0.249	0.250	0.062	1.000	1.156	15.6	4310	69.5	3600	58.1
IMMERSED	LM2	0.249	0.249	0.062	1.000	1.167	16.7	4300	69.4	3595	58.0
IMMERSED	LM3	0.249	0.252	0.063	1.000	1.154	15.4	4375	69.4	3570	56.7
average				0.062			15.9		69.4		57.6
std. dev				0.001			0.7		0.1		0.8
IMMERSED	LP1	0.251	0.249	0.062	1.000	1.149	14.9	4480	72.3	3775	60.9
IMMERSED	LP2	0.251	0.249	0.062	1.000	1.163	16.3	4390	70.8	3725	60.1
IMMERSED	LP3	0.252	0.250	0.063	1.000	1.137	13.7	4450	70.6	3780	60.0
average				0.062			15.0		71.2		60.3
std. dev				0.001			1.3		0.9		0.5

BASELINE: IMMERSED
TENSILE DATA 11/27/85

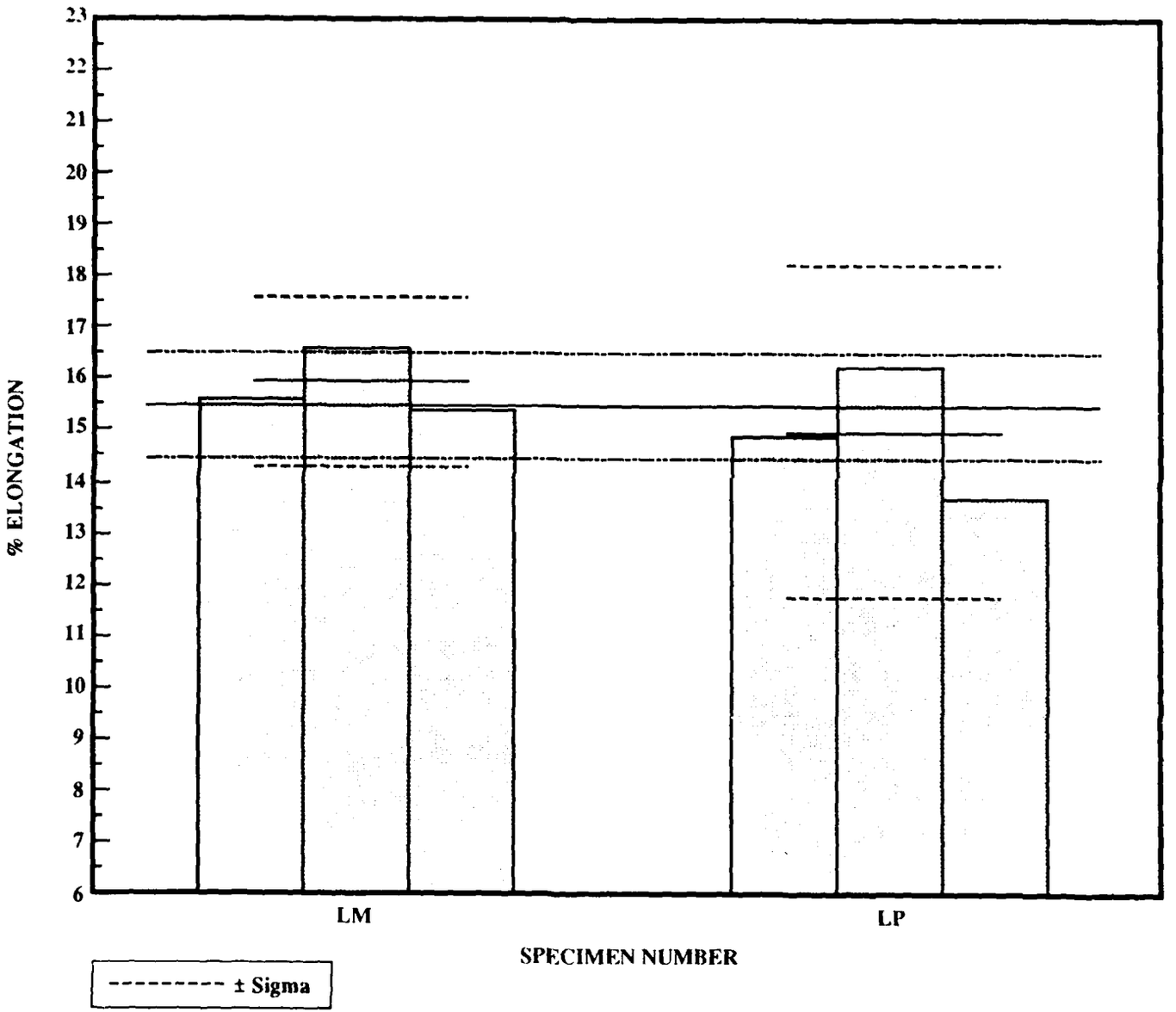

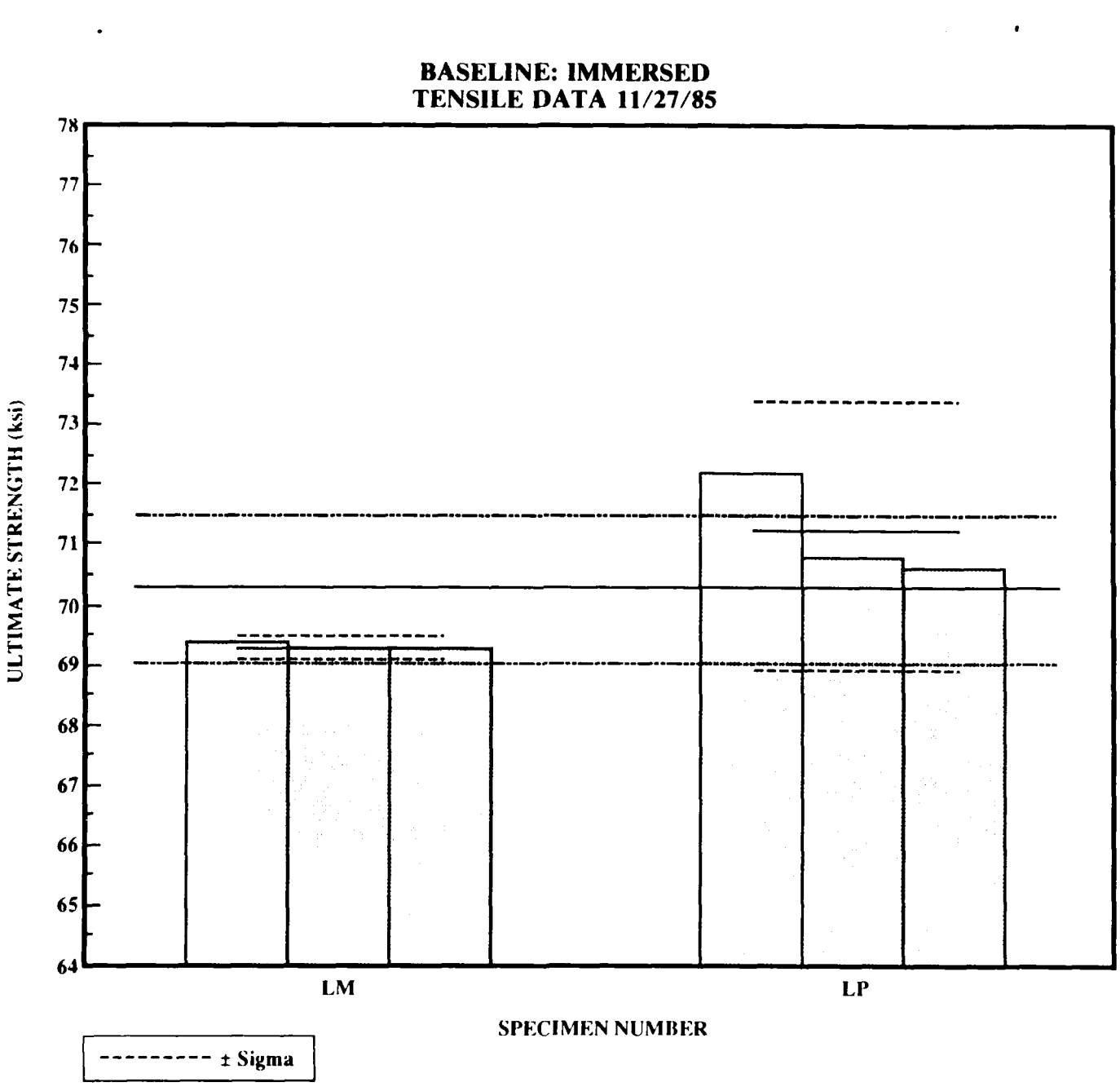
BASELINE: IMMERSED
TENSILE DATA 11/27/85
ULTIMATE STRENGTH (ksi)
78
77
76
75
74
73
72
71
70
69
68
67
66
65
64
LM
LP
SPECIMEN NUMBER
± Sigma

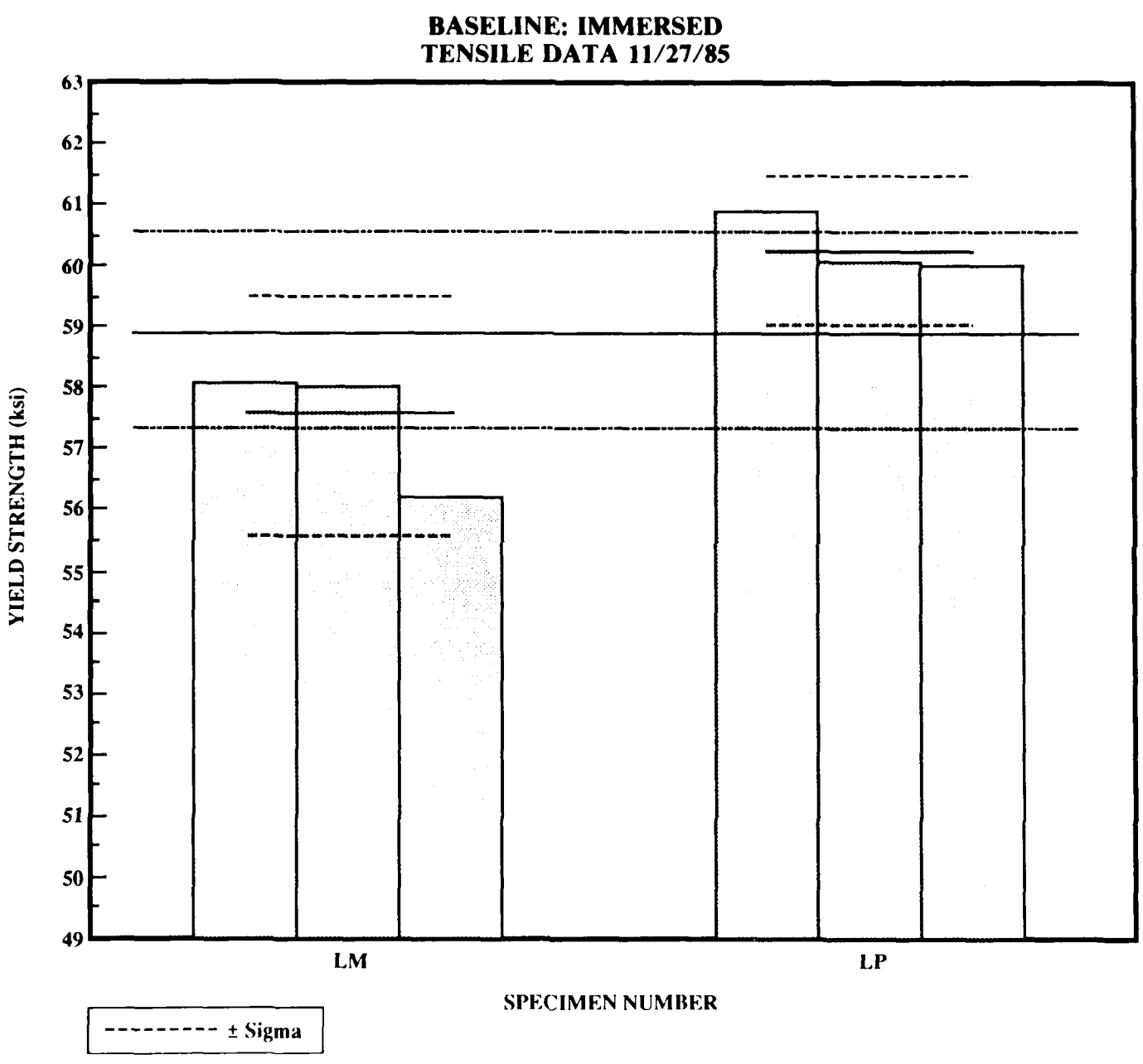
BASELINE: IMMERSED
TENSILE DATA 11/27/85
YIELD STRENGTH (ksi)
63
62
61
60
59
58
57
56
55
54
53
52
51
50
49
LM
LP
SPECIMEN NUMBER
± Sigma

BASELINE: 27 NOV 1985 — 17 JAN 1986

INTERGRANULAR CORROSION TEST 45 DAYS

REMARKS	Sample number	Thickness (inches)	Width (inches)	Area (sq. inch)	Gage Length: Initial (inches)	Final (inches)	Percent Elong-ation	Ultimate Force (pounds)	Ultimate Strength (ksi)	Yield Force (pounds)	Yield Strength (ksi)
POLISHED	LN1	0.250	0.249	0.062	1.000	1.167	16.7	4230	68.2	3500	56.5
POLISHED	LN2	0.250	0.249	0.062	1.000	1.170	17.0	4255	68.6	3475	56.0
POLISHED	LN3	0.251	0.246	0.062	1.000	1.171	17.1	4220	68.1	3425	55.2
average				0.062			16.9		68.3		55.9
std. dev				0.000			0.2		0.3		0.6
POLISHED	L01	0.251	0.248	0.062	1.000	1.176	17.6	4360	70.3	3525	56.9
POLISHED	L02	0.251	0.251	0.063	1.000	1.192	19.2	4400	69.8	3625	57.5
POLISHED	L03	0.252	0.251	0.063	1.000	1.191	19.1	4415	70.1	3540	56.2
average				0.063			18.6		70.1		56.9
std. dev				0.001			0.9		0.2		0.7
POLISHED	LQ1	0.251	0.248	0.062	1.000	1.175	17.5	4430	71.5	3640	58.7
POLISHED	LQ2	0.250	0.251	0.063	1.000	1.149	14.9	4450	70.6	3700	58.7
POLISHED	LQ3	0.251	0.251	0.063	1.000	1.156	15.6	4460	70.8	3660	58.1
average				0.063			16.0		71.0		58.5
std. dev				0.001			1.3		0.4		0.4

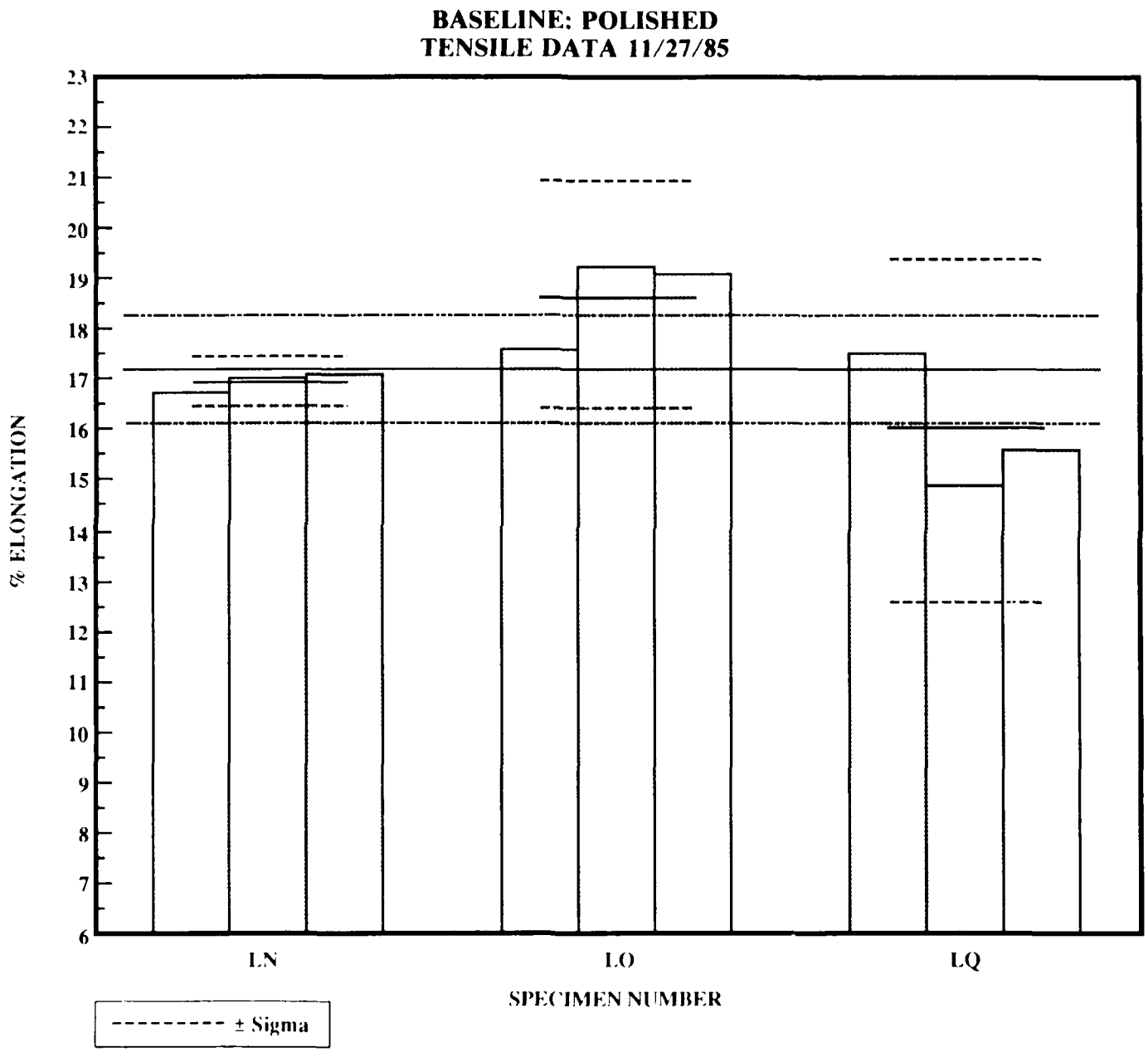
BASELINE: POLISHED
TENSILE DATA 11/27/85
% ELONGATION
23
22
21
20
19
18
17
16
15
14
13
12
11
10
9
8
7
6
LN
LO
LQ
SPECIMEN NUMBER
± Sigma

BASELINE: POLISHED
TENSILE DATA 11/27/85

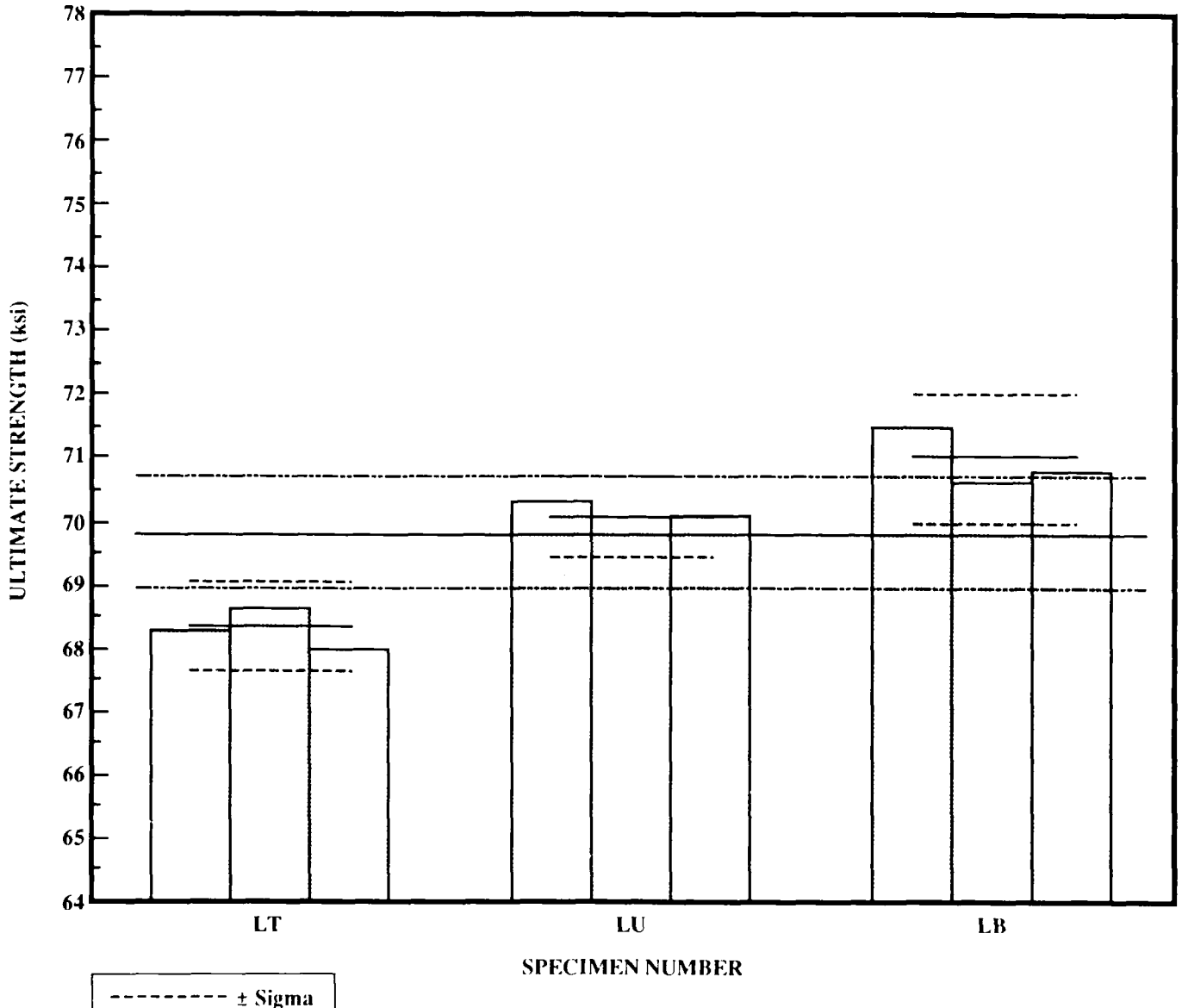

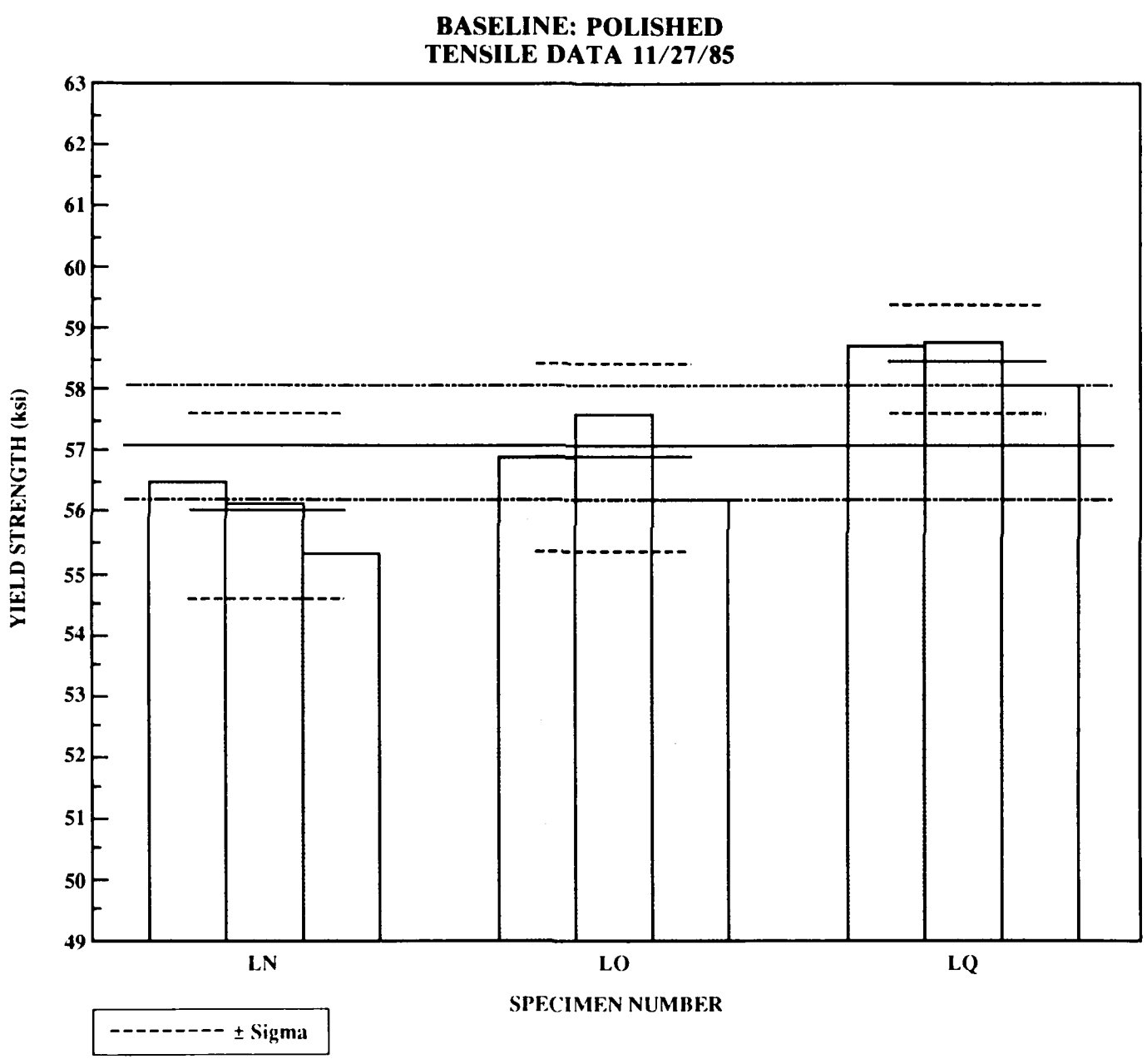
BASELINE: POLISHED
TENSILE DATA 11/27/85
YIELD STRENGTH (ksi)
63
62
61
60
59
58
57
56
55
54
53
52
51
50
49
LN
LO
LQ
SPECIMEN NUMBER
± Sigma

BASELINE: 27 NOV 1985 TO 17 JAN 1986

INTERGRANULAR CORROSION TEST 45 DAYS

REMARKS	Sample number	Thickness (inches)	Width (inches)	Area (sq. inch)	Gage Length: Initial (inches)	Gage Length: Final (inches)	Percent Elong-ation	Ultimate Force (pounds)	Ultimate Strength (ksi)	Yield Force (pounds)	Yield Strength (ksi)
AS REC'D	LV1	0.250	0.250	0.063	1.000	1.135	13.5	4330	68.7	3615	57.4
AS REC'D	LV2	0.250	0.251	0.063	1.000	1.132	13.2	4410	70.0	3700	58.7
AS REC'D	LV3	0.250	0.250	0.063	1.000	1.123	12.3	4450	70.6	3710	58.9
average				0.063			13.0		69.8		58.3
std. dev				0.000			0.6		1.0		0.8
AS REC'D	LX1	0.250	0.248	0.062	1.000	1.163	16.3	4440	71.6	3820	61.6
AS REC'D	LX2	0.251	0.251	0.063	1.000	1.165	16.5	4460	70.8	3735	59.3
AS REC'D	LX3	0.250	0.252	0.063	1.000	1.178	17.8	4480	71.1	3800	60.3
average				0.063			16.9		71.2		60.4
std. dev				0.001			0.8		0.4		1.2
AS REC'D	LW1	0.250	0.251	0.063	1.000	1.156	15.6	4410	70.0	3730	59.2
AS REC'D	LW2	0.250	0.251	0.063	1.000	1.163	16.3	4380	69.5	3700	58.7
AS REC'D	LW3	0.251	0.250	0.063	1.000	1.146	14.6	4420	70.2	3700	58.7
AS REC'D	LW4	0.250	0.250	0.063	1.000	1.161	16.1	4430	70.3	3700	58.7
AS REC'D	LW5	0.250	0.251	0.063	1.000	1.149	14.9	4400	69.8	3695	58.7
average				0.063			15.5		70.0		58.8
std. dev				0.000			0.7		0.3		0.2

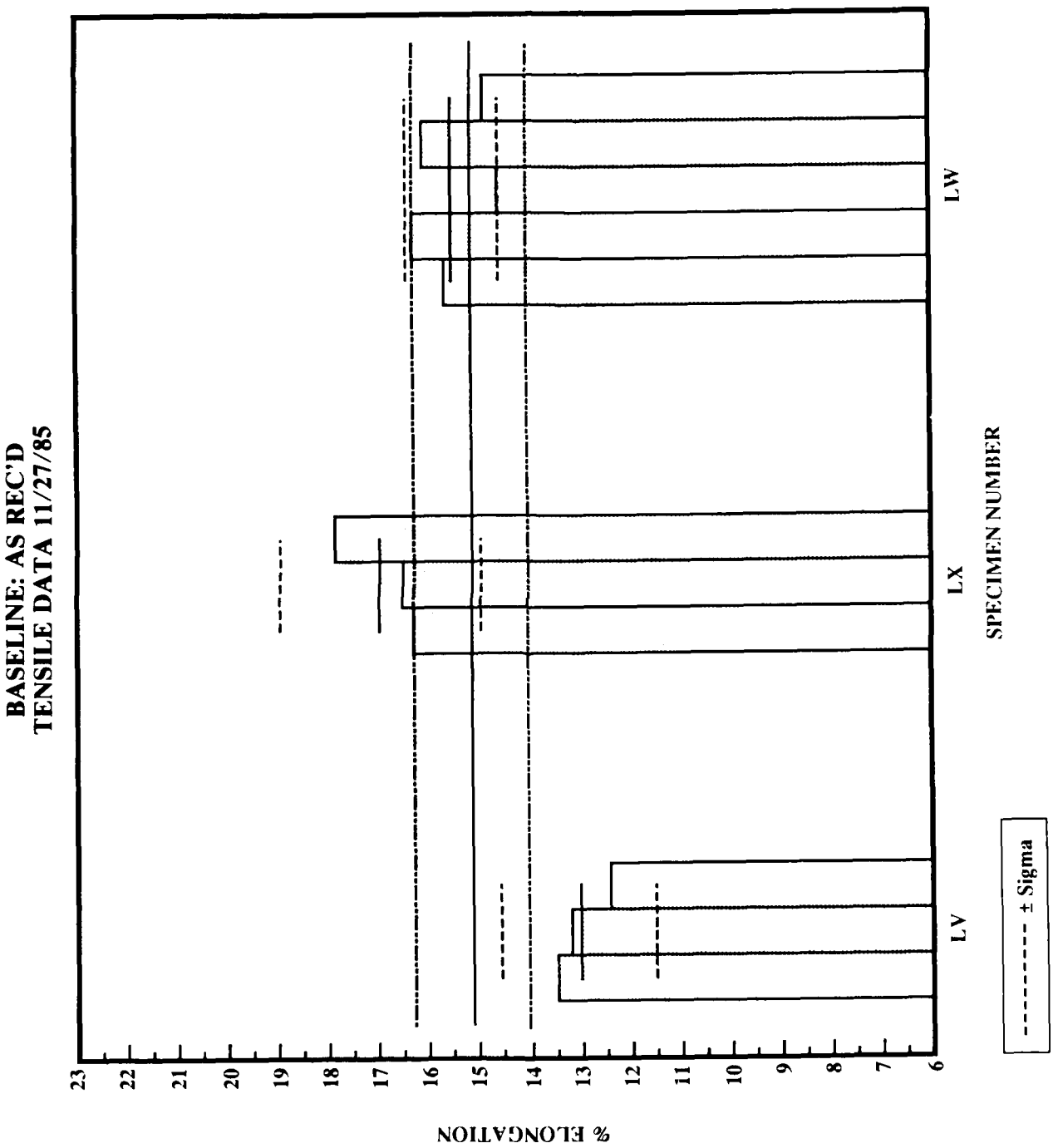
BASELINE: AS REC'D
TENSILE DATA 11/27/85
% ELONGATION
23
22
21
20
19
18
17
16
15
14
13
12
11
10
9
8
7
6
LV
LX
LW
SPECIMEN NUMBER
± Sigma

BASELINE: AS REC'D
TENSILE DATA 11/27/85

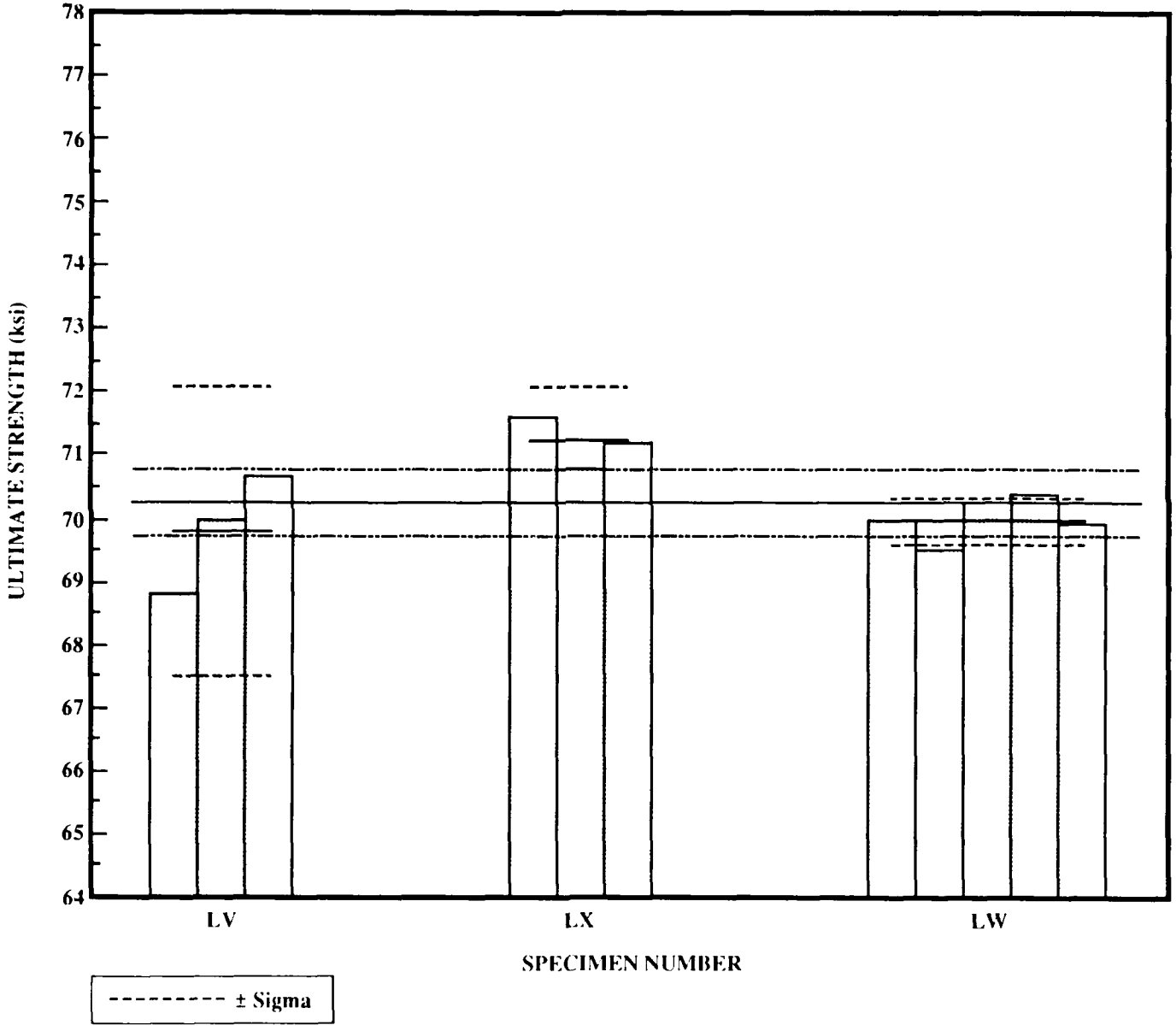

BASELINE: AS REC'D
TENSILE DATA 11/27/85

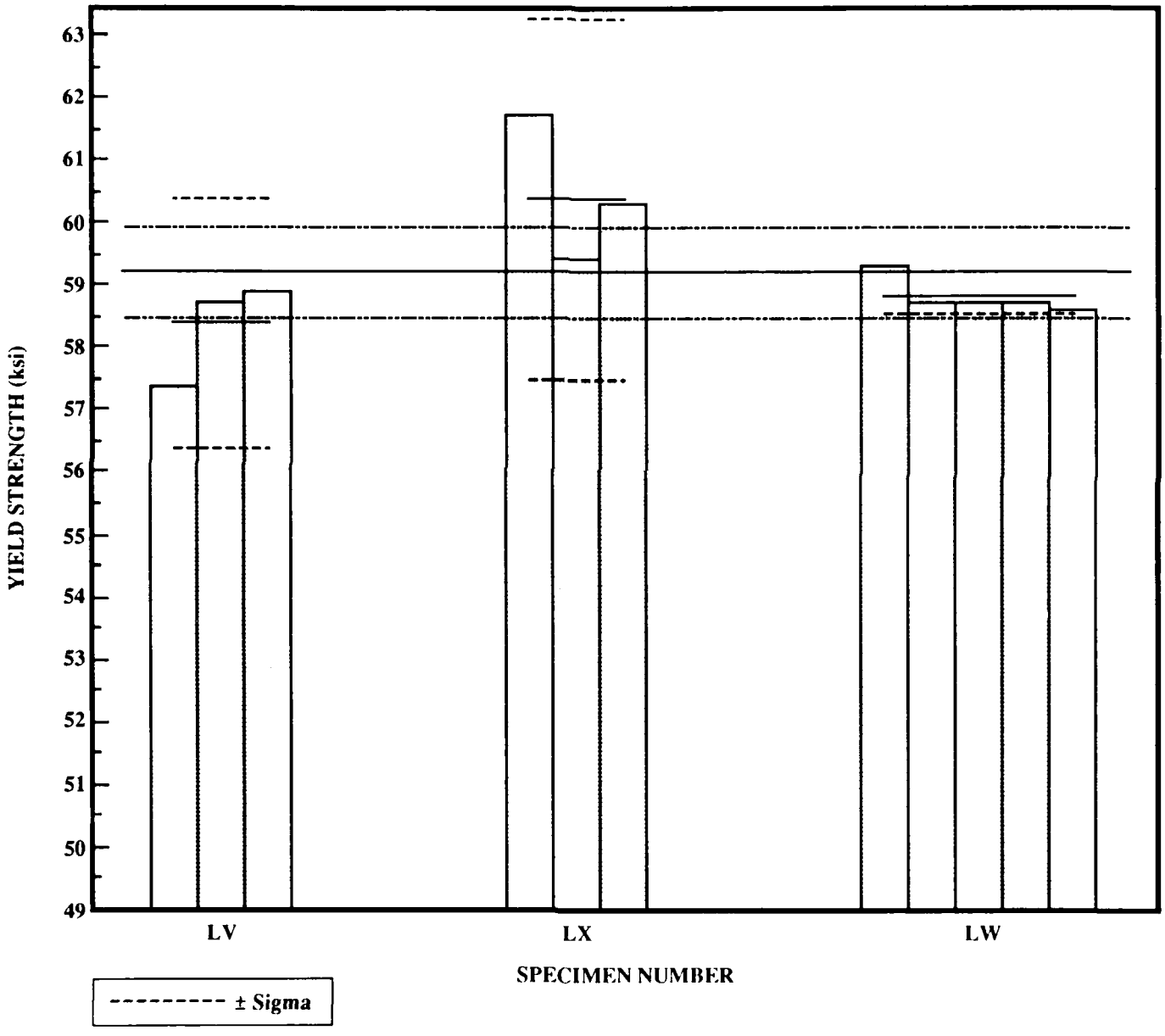

TEST II

TEST CYCLE

SALT SPRAY	8 Hours	(MONDAY-FRIDAY)
PURGE AIR	16 Hours	(MONDAY-THURSDAY)
HOT SOAK (35 °C/95 °F)	28 Hours	(FRIDAY-SATURDAY)
CONDENSING SOAK (20 °C/68 °F)	35 Hours	(SATURDAY-MONDAY)

SALT FOG SOLUTION COMPOSITION

> 0.100 N Sodium Chloride (NaCl)
> 0.344 N Sodium Nitrate ($NaNO_3$)
> 0.089 N Sodium Sulfate (Na_2SO_4)
> chloride/nitrate ratio = 0.29
> chloride/sulfate ratio = 1.12
> pH 4.2-4.5

ACIDIFICATION STOCK SOLUTION

ACID	NORMALITY
Sulfuric	0.333
Nitric	0.333
Hydrochloric	0.333

EXPOSURE SPECIMENS

PLATES	4" × 1/2" × 1/4"		
		12	Salt Fog-As Received
C-RINGS	1.0"d × 0.75"w × 0.028"t		
		3	Salt Fog @ 31 ksi
		1	Salt Fog @ 0 ksi

DURATION OF EXPOSURE 45 days/256 hours salt fog

TEST II

INTERGRANULAR CORROSION TEST 45 DAYS

REMARKS	Sample number	Thickness (inches)	Width (inches)	Area (sq. inch)	Gage Length: Initial (inches)	Gage Length: Final (inches)	Percent Elong-ation	Ultimate Force (pounds)	Ultimate Strength (ksi)	Yield Force (pounds)	Yield Strength (ksi)
.3 M NITRATE	II B	0.250	0.231	0.058	1.000	1.126	12.6	4260	73.4	3440	59.3
.3 M NITRATE	II C	0.250	0.252	0.063	1.000	1.136	13.6	4200	66.7	3590	57.0
.3 M NITRATE	II D	0.250	0.251	0.063	1.000	1.145	14.5	4435	70.4	3625	57.5
.3 M NITRATE	II E	0.251	0.251	0.063	1.000	1.148	14.8	4410	70.0	3715	59.0
.3 M NITRATE	II G	0.252	0.249	0.063	1.000	1.170	17.0	4430	70.3	3665	58.2
.3 M NITRATE	II H	0.250	0.235	0.059	1.000	1.106	10.6	4170	70.7	3470	58.8
.3 M NITRATE	II J	0.250	0.246	0.062	1.000	1.144	14.4	4375	70.6	3600	58.1
.3 M NITRATE	II K	0.250	0.236	0.059	1.000	1.134	13.4	4240	71.9	3605	61.1
.3 M NITRATE	II L	0.250	0.255	0.064	1.000	1.150	15.0	4515	70.5	3850	60.2
average				0.062			14.0		70.5		58.8
std. dev				0.003			1.8		1.8		1.3

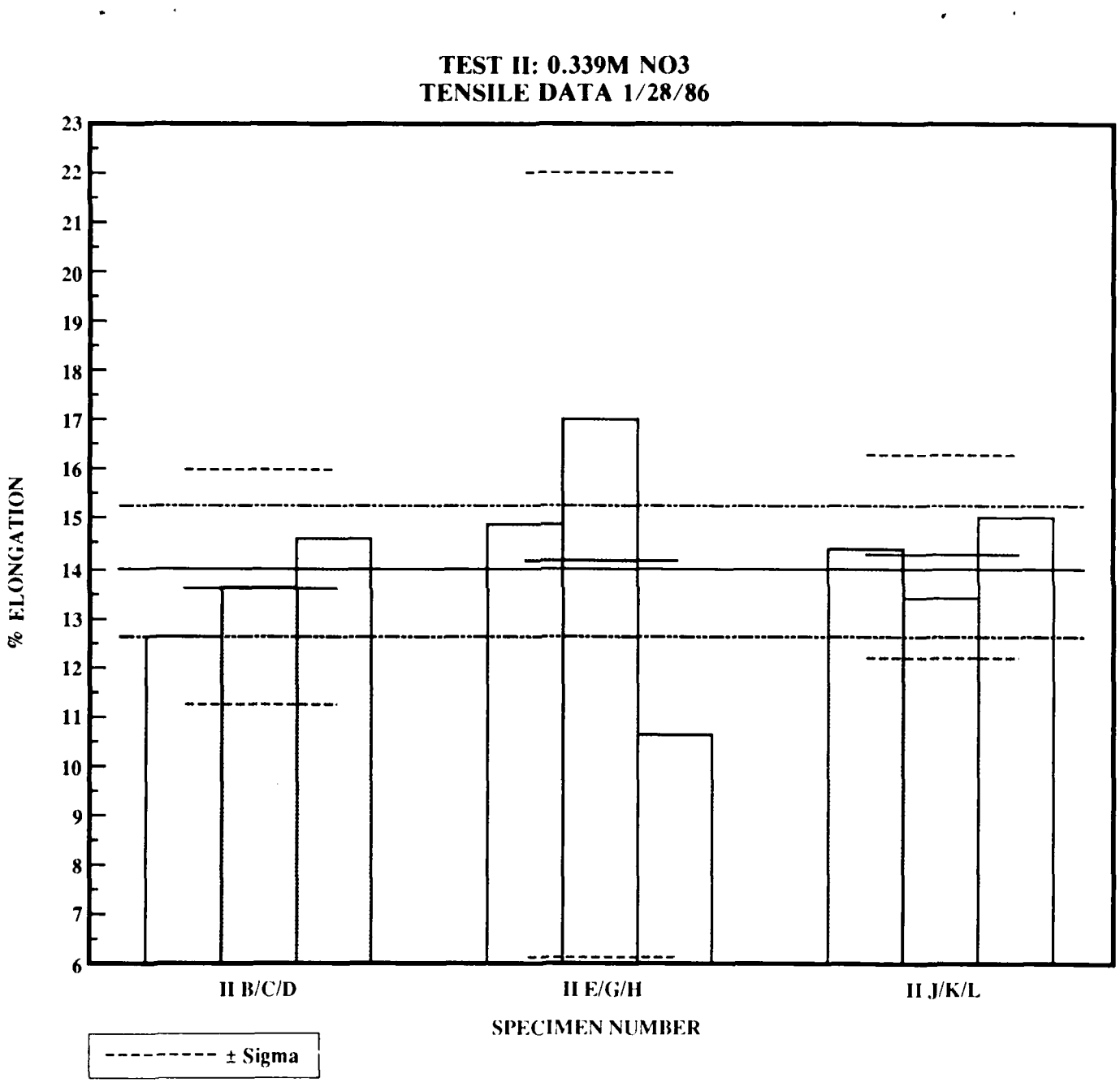
TEST II: 0.339M NO3
TENSILE DATA 1/28/86
% ELONGATION
23
22
21
20
19
18
17
16
15
14
13
12
11
10
9
8
7
6
II B/C/D
II E/G/H
II J/K/L
SPECIMEN NUMBER
± Sigma

TEST II: 0.339M NO3
TENSILE DATA 1/28/86

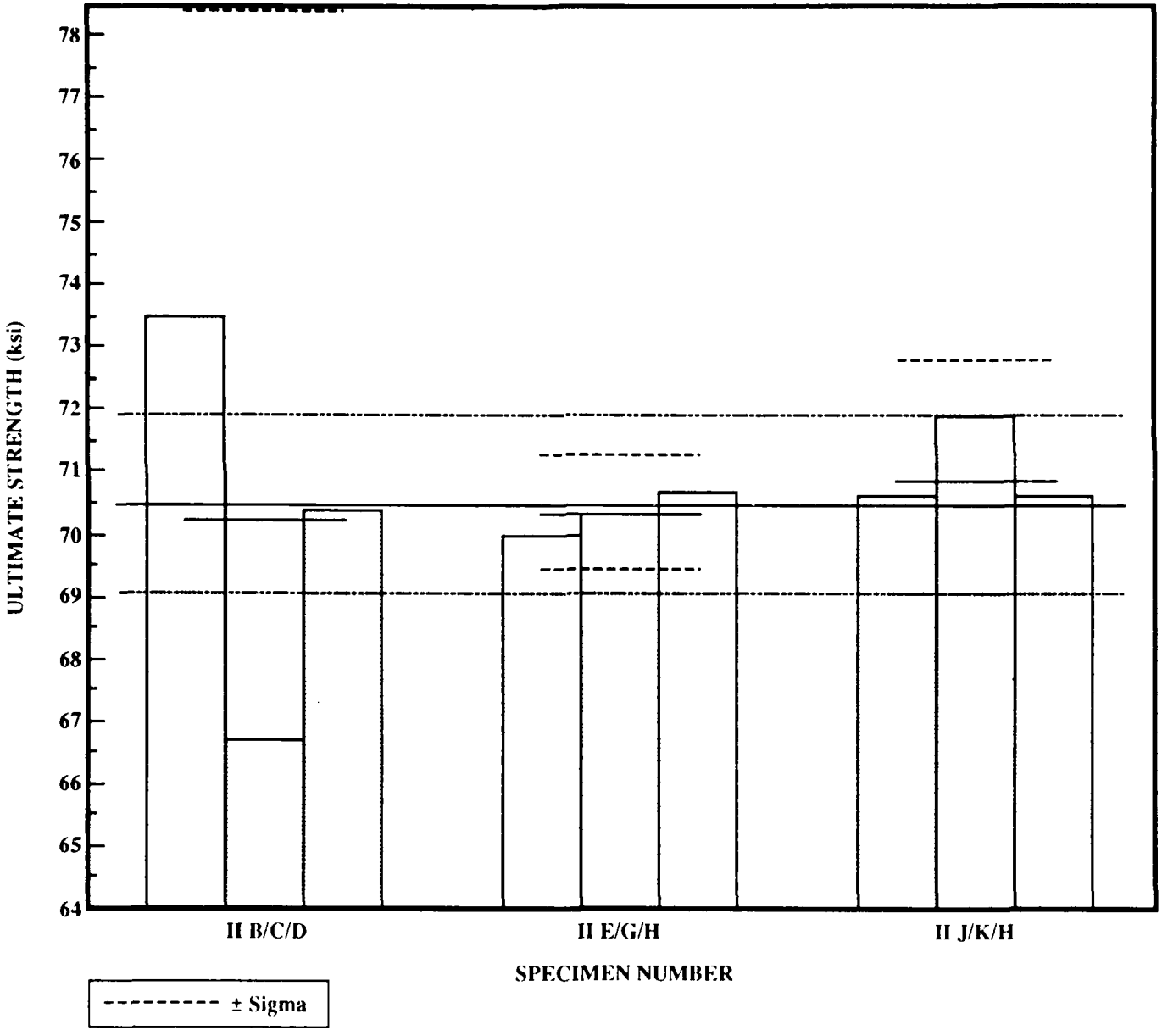

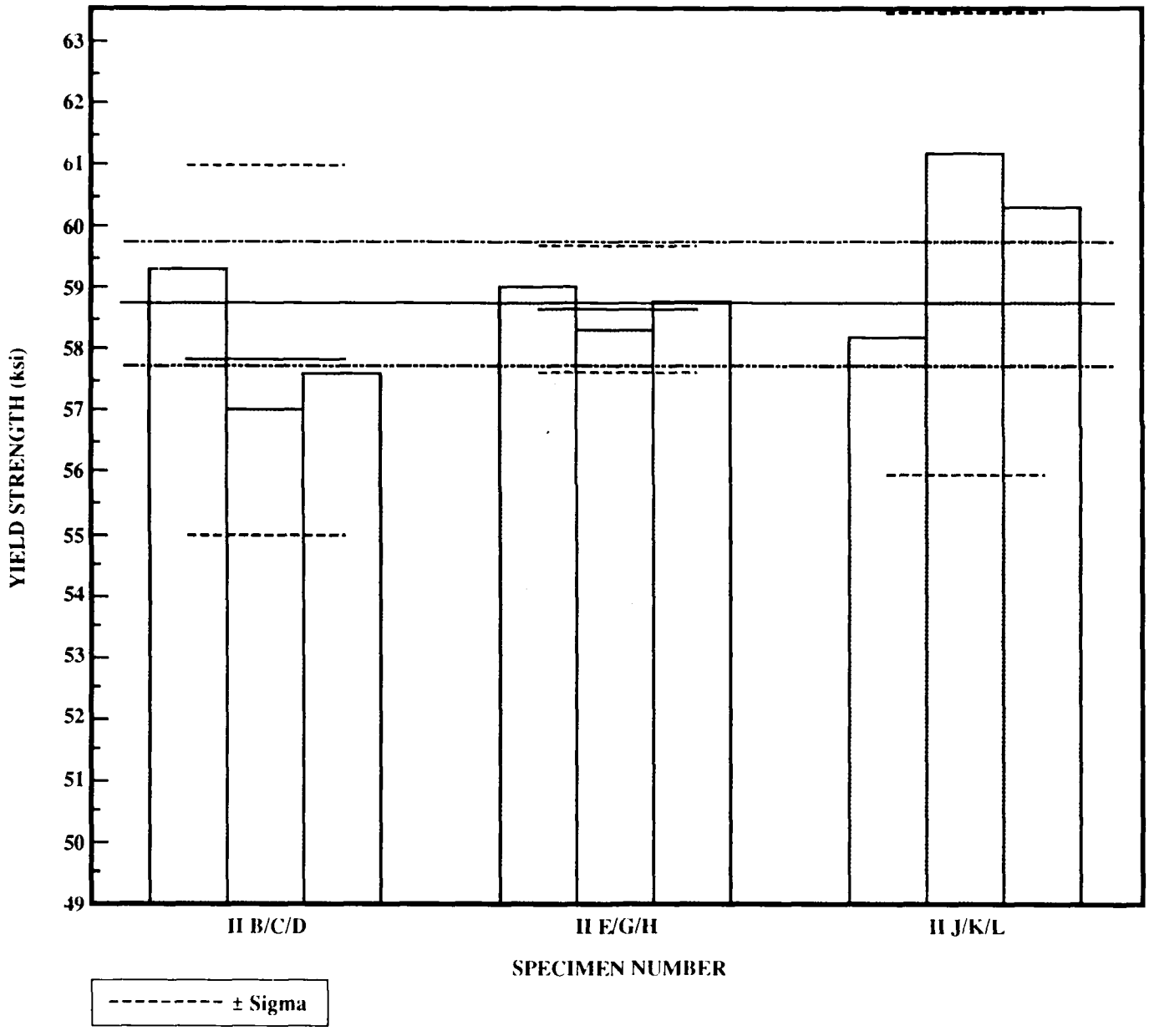
TEST II: 0.339M NO3
TENSILE DATA 1/28/86
YIELD STRENGTH (ksi)
63
62
61
60
59
58
57
56
55
54
53
52
51
50
49
II B/C/D
II E/G/H
II J/K/L
SPECIMEN NUMBER
± Sigma

TEST III

TEST CYCLE

SALT SPRAY	8 Hours	(MONDAY-FRIDAY)
PURGE AIR	16 Hours	(MONDAY-THURSDAY)
HOT SOAK (35 °C/95 °F)	28 Hours	(FRIDAY-SATURDAY)
CONDENSING SOAK (20 °C/68 °F)	35 Hours	(SATURDAY-MONDAY)

SALT FOG SOLUTION COMPOSITION

> 0.010 N Sodium Chloride (NaCl)
> 0.023 N Sodium Nitrate ($NaNO_3$)
> 0.009 N Sodium Sulfate (Na_2SO_4)
> chloride/nitrate ratio = 0.29
> chloride/sulfate ratio = 1.12
> pH 4.2-4.5

ACIDIFICATION STOCK SOLUTION

ACID	NORMALITY
Sulfuric	0.333
Nitric	0.333
Hydrochloric	0.333

EXPOSURE SPECIMENS

PLATES	4" × 1/2" × 1/4"		
		12	Salt Fog-As Received
C-RINGS	1.0"d × 0.75"w × 0.028"t		
		3	Salt Fog @ 31 ksi
		1	Salt Fog @ 0 ksi
DURATION OF EXPOSURE		45 days/256 hours salt fog	

TEST III

INTERGRANULAR CORROSION TEST 45 DAYS

REMARKS	Sample number	Thickness (inches)	Width (inches)	Area (sq. inch)	Gage Length: Initial (inches)	Gage Length: Final (inches)	Percent Elong-ation	Ultimate Force (pounds)	Ultimate Strength (ksi)	Yield Force (pounds)	Yield Strength (ksi)
.010 M Cl	III B	0.251	0.246	0.062	1.000	1.158	15.8	4455	71.9	3755	60.6
.010 M Cl	III C	0.250	0.244	0.061	1.000	1.157	15.7	4350	71.3	3650	59.8
.010 M Cl	III D	0.250	0.245	0.061	1.000	1.150	15.0	4310	70.7	3625	59.4
.010 M Cl	III E	0.250	0.240	0.060	1.000	1.402	40.2	4270	71.2	3540	59.0
.010 M Cl	III G	0.250	0.254	0.064	1.000	1.167	16.7	4545	71.0	3855	60.2
.010 M Cl	III H	0.251	0.245	0.061	1.000	1.155	15.5	4305	70.6	3675	60.2
.010 M Cl	III J	0.250	0.250	0.063	1.000	1.135	13.5	4410	70.0	3640	57.8
.010 M Cl	III K	0.250	0.244	0.061	1.000	1.141	14.1	4305	70.6	3675	60.2
.010 M Cl	III L	0.250	0.252	0.063	1.000	1.153	15.3	4435	70.4	3670	58.3
average				0.062			18.0		70.8		59.5
std. dev				0.001			8.4		0.6		1.0

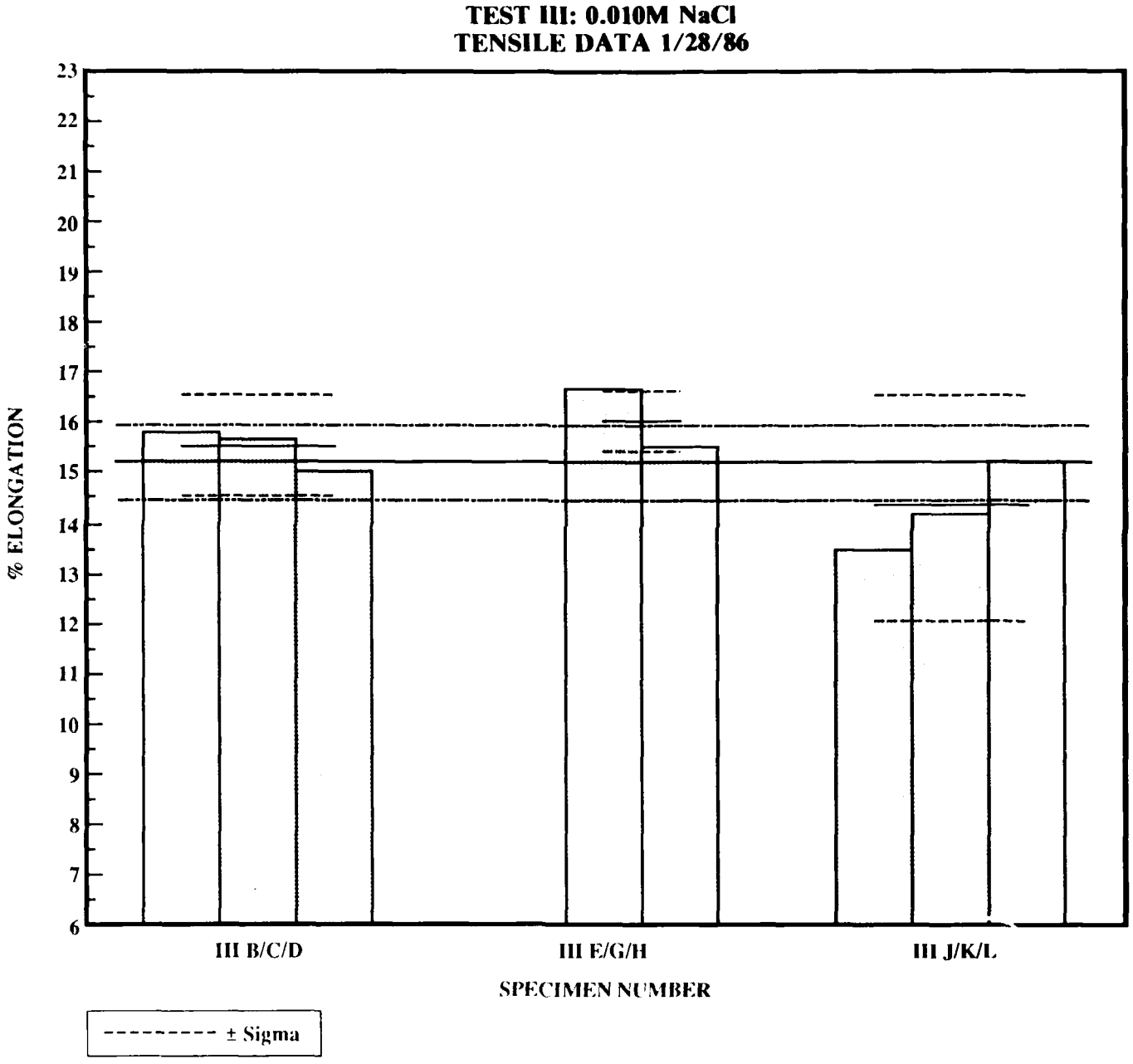
TEST III: 0.010M NaCl
TENSILE DATA 1/28/86
% ELONGATION
23
22
21
20
19
18
17
16
15
14
13
12
11
10
9
8
7
6
III B/C/D
III E/G/H
III J/K/L
SPECIMEN NUMBER
± Sigma

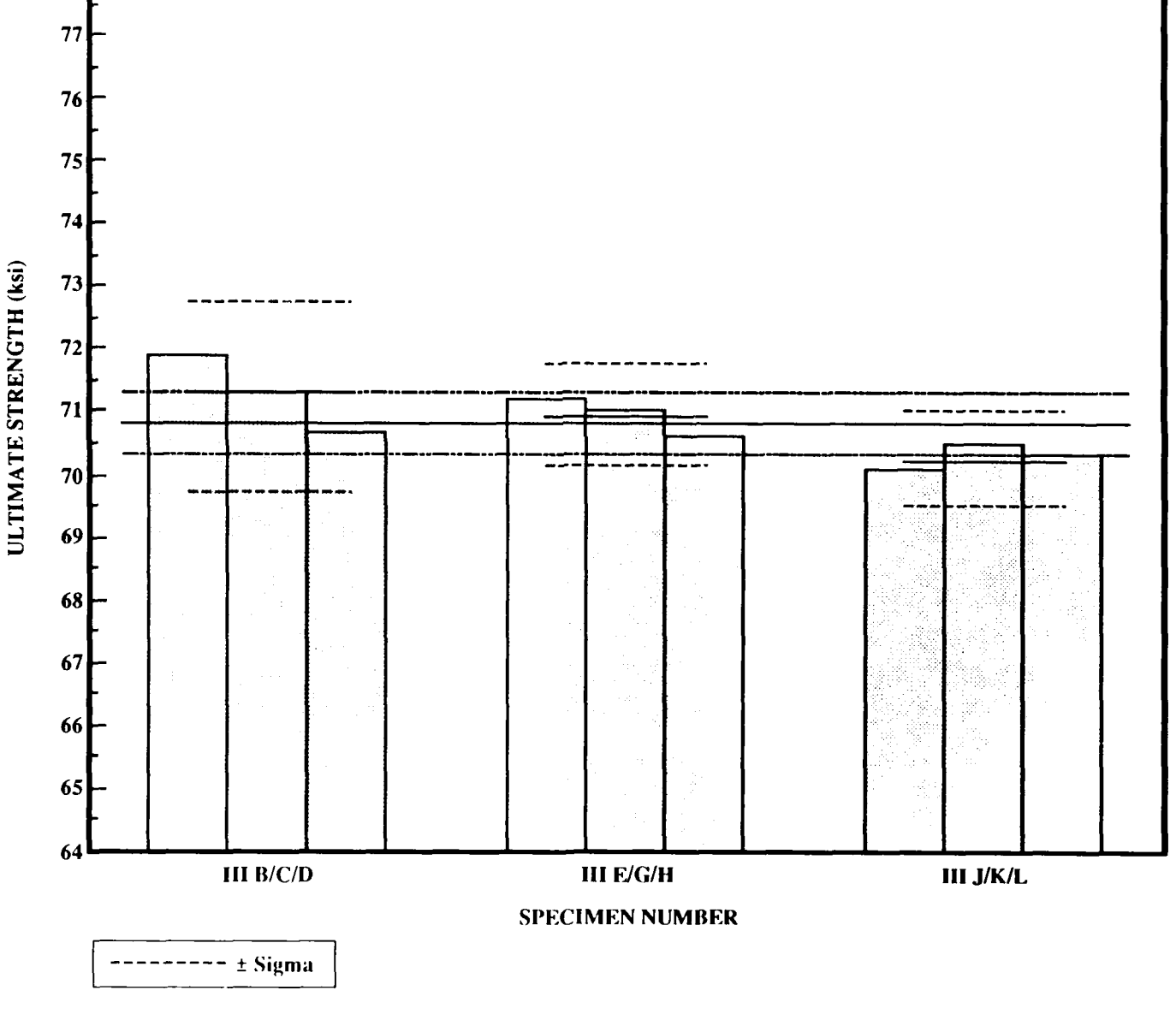
TEST III: 0.010M NaCl
TENSILE DATA 1/28/86
ULTIMATE STRENGTH (ksi)
78
77
76
75
74
73
72
71
70
69
68
67
66
65
64
III B/C/D
III E/G/H
III J/K/L
SPECIMEN NUMBER
± Sigma

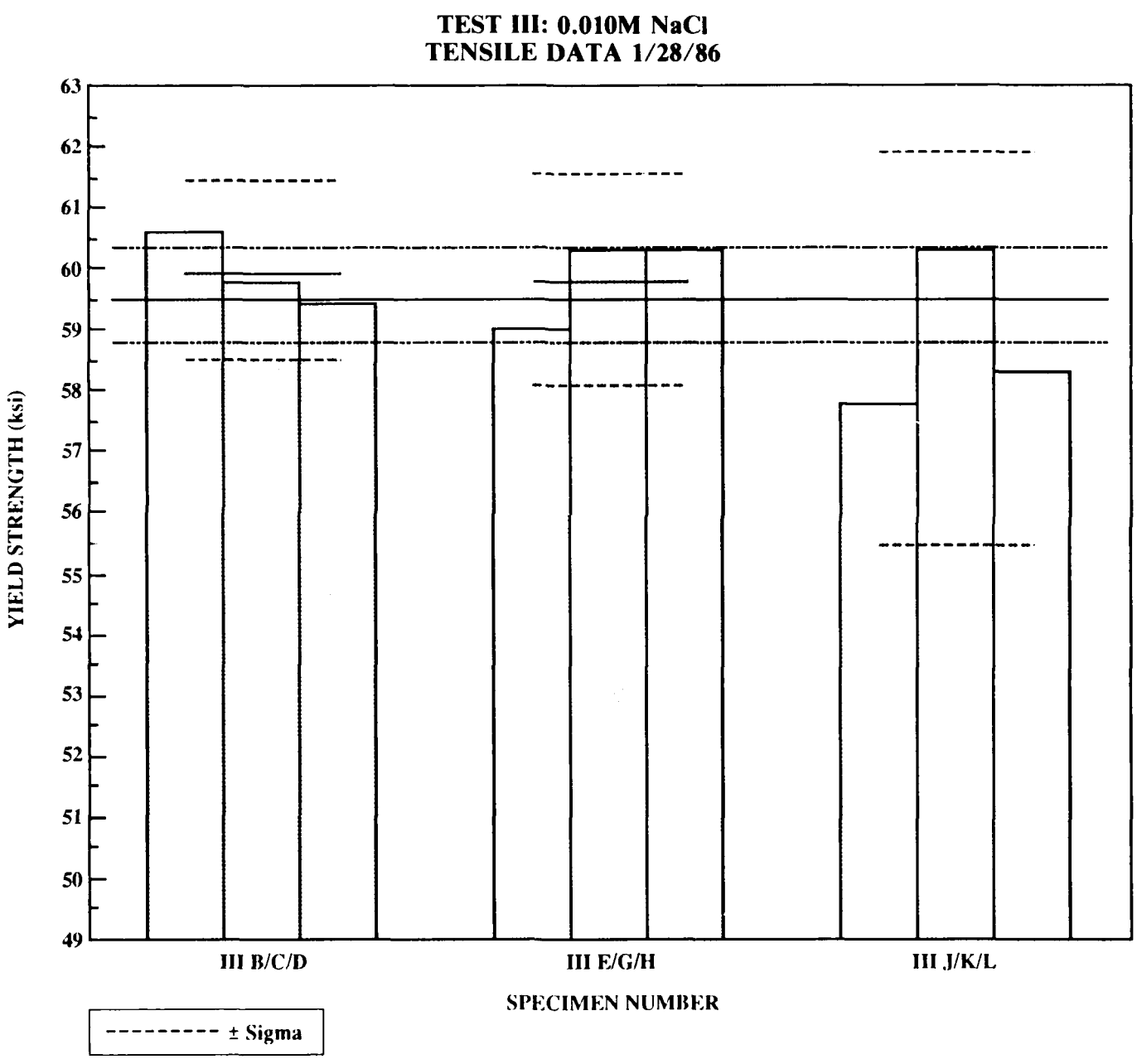
TEST III: 0.010M NaCl
TENSILE DATA 1/28/86
YIELD STRENGTH (ksi)
63
62
61
60
59
58
57
56
55
54
53
52
51
50
49
III B/C/D
III E/G/H
III J/K/L
SPECIMEN NUMBER
± Sigma

TEST IV

TEST CYCLE

SALT SPRAY	4 Hours	(MONDAY-FRIDAY)
HOT SOAK (35 °C/95 °F)	16 Hours	(FRIDAY-SATURDAY)
PURGE AIR	4 Hours	(MONDAY-THURSDAY)
HOT SOAK (35 °C/95 °F)	28 Hours	(FRIDAY-SATURDAY)
CONDENSING SOAK (20 °C/68 °F)	35 Hours	(SATURDAY-MONDAY)

TEST ENVIRONMENT

ACID GAS	CONCENTRATION
Sulfur Dioxide	0.30 ppm(c)
Nitric Oxide	0.49 ppm(c)
Nitrogen Dioxide	0.20 ppm(c)
Ozone	0.05 ppm(m)

(c) cabinet concentration calculated
(m) cabinet concentration measured

SALT FOG SOLUTION COMPOSITION

STOCK	SPRAY
> 0.100 N Hydrochloric Acid (HCl)	4.0×10^{-5} N
> 0.229 N Nitric Acid (HNO_3)	9.2×10^{-5} N
> 0.089 N Sulfuric Acid (H_2SO_4)	3.6×10^{-5} N
> chloride/nitrate ratio = 0.44	
> chloride/sulfate ratio = 1.12	
> pH 4.2-4.5	

EXPOSURE SPECIMENS

PLATES 4″ × 1/2″ × 1/4″ (solid bars)

4	As Received	45 days
7	As Received	67 days
7	As Received	90 days

4″ × 1/4″ × 1/4″ (tensile bars)

4	As Received	45 days
7	As Received	67 days
7	As Received	90 days

C-RINGS 1.0″d × 0.75″w × 0.028″t

3	@ 31 ksi-45 days
1	@ 0 ksi-45 days
3	@ 31 ksi-67 days
1	@ 0 ksi-67 days
3	@ 31 ksi-90 days
1	@ 0 ksi-90 days

1.0″d × 0.75″w × 0.058″t

3	@ 31 ksi-45 days
1	@ 0 ksi-45 days
3	@ 31 ksi-67 days
1	@ 0 ksi-67 days
3	@ 31 ksi-90 days
1	@ 0 ksi-90 days

DURATION OF EXPOSURES 45 days/128 hours salt fog
67 days/190 hours salt fog
90 days/256 hours salt fog

TEST IV: SOLID BARS

INTERGRANULAR CORROSION TEST 45 DAYS

REMARKS	Sample number	Thickness (inches)	Width (inches)	Area (sq. inch)	Gage Length: Initial (inches)	Gage Length: Final (inches)	Percent Elong-ation	Ultimate Force (pounds)	Ultimate Strength (ksi)	Yield Force (pounds)	Yield Strength (ksi)
CONTROLS	IVD	0.251	0.251	0.063	1.000	1.163	16.3	4450	70.6	3700	58.7
	IVE	0.250	0.240	0.060	1.000	1.160	16.0	4195	69.9	3460	57.7
below tolerance	IVG	0.250	0.249	0.062	1.000	1.150	(15.0)	4415	(71.2)	3460	(55.8)
average				0.062			16.2		70.3		58.2
std. dev				0.002			0.2		0.5		0.8
EXPOSED	IVS	0.250	0.253	0.063	1.000	1.182	18.2	4450	70.6	3625	57.5
	IVT	0.250	0.251	0.063	1.000	1.170	17.0	4395	69.8	3570	56.7
	IVW	0.245	0.245	0.060	1.000	1.129	12.9	4275	71.3	3500	58.3
average				0.062			16.0		70.5		57.5
std. dev				0.002			2.8		0.7		0.8

TEST IV: SOLID BARS

INTERGRANULAR CORROSION TEST 67 DAYS

REMARKS	Sample number	Thickness (inches)	Width (inches)	Area (sq. inch)	Gage Length: Initial (inches)	Gage Length: Final (inches)	Percent Elong-ation	Ultimate Force (pounds)	Ultimate Strength (ksi)	Yield Force (pounds)	Yield Strength (ksi)
CONTROLS	IVA	0.252	0.243	0.061	1.000	1.118	11.8	4350	71.3	3580	58.7
	IVB	0.251	0.253	0.064	1.000	1.153	15.3	4375	68.4	3740	58.4
	IVC	0.250	0.235	0.059	1.000	1.134	13.4	4075	69.1	3525	59.7
average				0.061			13.5		69.6		58.9
std. dev				0.003			1.8		1.5		0.7
EXPOSED	IVN	0.254	0.247	0.063	1.000	1.163	16.3	4270	67.8	3605	57.2
	IVO	0.252	0.250	0.063	1.000	1.160	16.0	4380	69.5	3775	59.9
	IVR	0.251	0.250	0.063	1.000	1.147	14.7	4345	69.0	3780	60.0
	IVU	0.250	0.252	0.063	1.000	1.153	15.3	4385	69.6	3575	56.7
	IVBB	0.251	0.245	0.061	1.000	1.156	15.6	4265	69.9	3655	59.9
	IVEE	0.253	0.246	0.062	1.000	1.147	14.7	4270	68.9	3675	59.3
average				0.063			15.4		69.1		58.8
std. dev				0.001			0.7		0.8		1.5

TEST IV: SOLID BARS

INTERGRANULAR CORROSION TEST 90 DAYS

REMARKS	Sample number	Thickness (inches)	Width (inches)	Area (sq. inch)	Gage Length: Initial (inches)	Gage Length: Final (inches)	Percent Elong-ation	Ultimate Force (pounds)	Ultimate Strength (ksi)	Yield Force (pounds)	Yield Strength (ksi)
CONTROLS	IVF	0.253	0.251	0.064	1.000	1.162	16.2	4405	68.8	3830	59.8
	IVF	0.253	0.253	0.064	1.000	1.157	15.7	4440	69.4	3730	58.3
	IVJ	0.250	0.252	0.063	1.000	1.189	18.9	4390	69.7	3740	59.4
average				0.064			16.9		69.3		59.1
std. dev				0.001			1.7		0.4		0.8
EXPOSED	IVL	0.253	0.251	0.064	1.000	1.174	17.4	4320	67.5	3680	57.5
	IVP	0.253	0.249	0.063	1.000	1.164	16.4	4330	68.7	3745	59.4
	IVQ	0.252	0.250	0.063	1.000	1.177	17.7	4300	68.3	3620	57.5
	IVX	0.255	0.253	0.065	1.000	1.161	16.1	4455	68.5	3795	58.4
	IVAA	0.252	0.253	0.064	1.000	1.146	14.6	4405	68.8	3750	58.6
	IVCC	0.252	0.252	0.064	1.000	1.162	16.2	4345	67.9	3665	57.3
average				0.064			16.4		68.3		58.1
std. dev				0.001			1.1		0.5		0.8

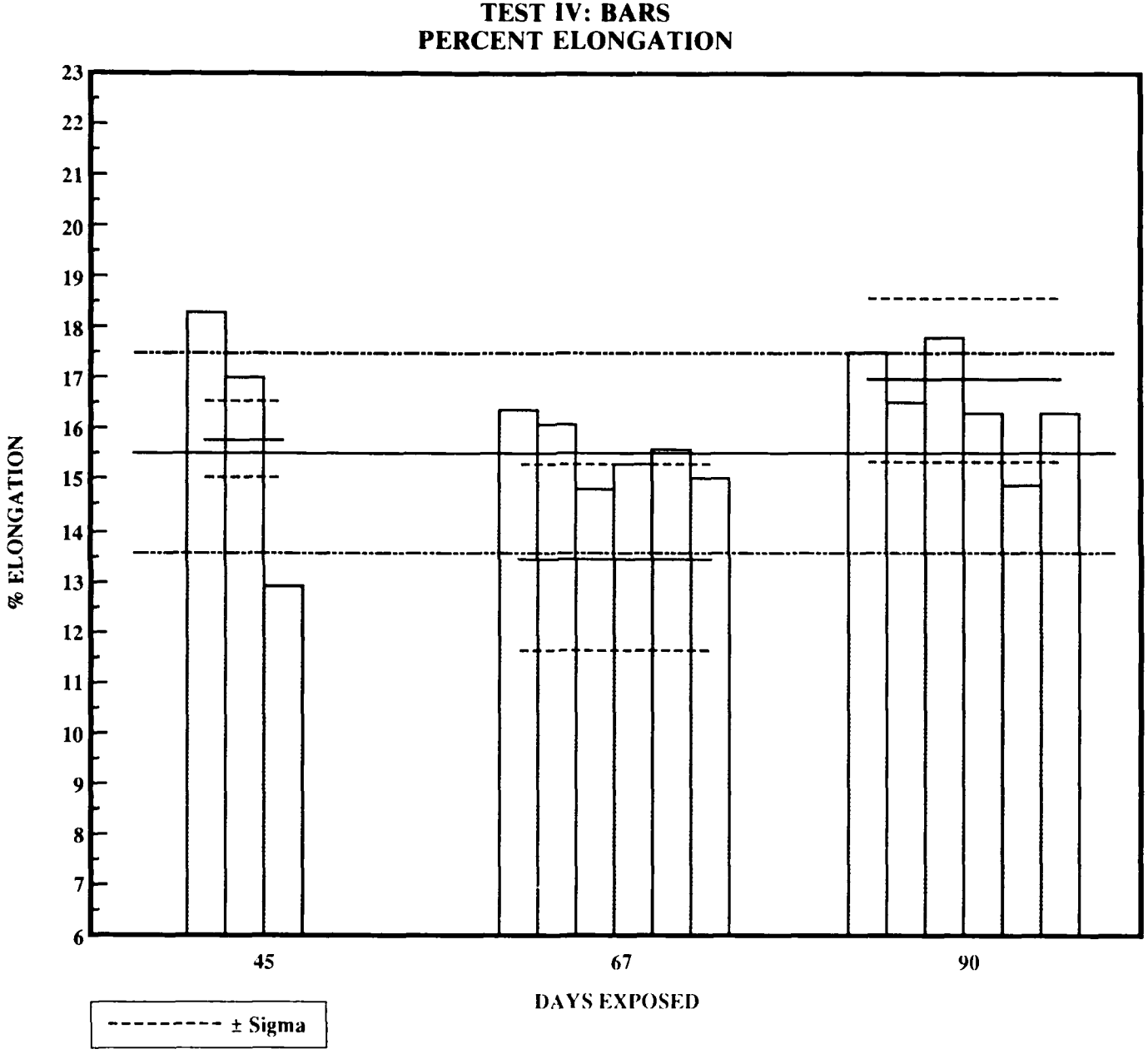
TEST IV: BARS
PERCENT ELONGATION
% ELONGATION
23
22
21
20
19
18
17
16
15
14
13
12
11
10
9
8
7
6
45
67
90
DAYS EXPOSED
± Sigma

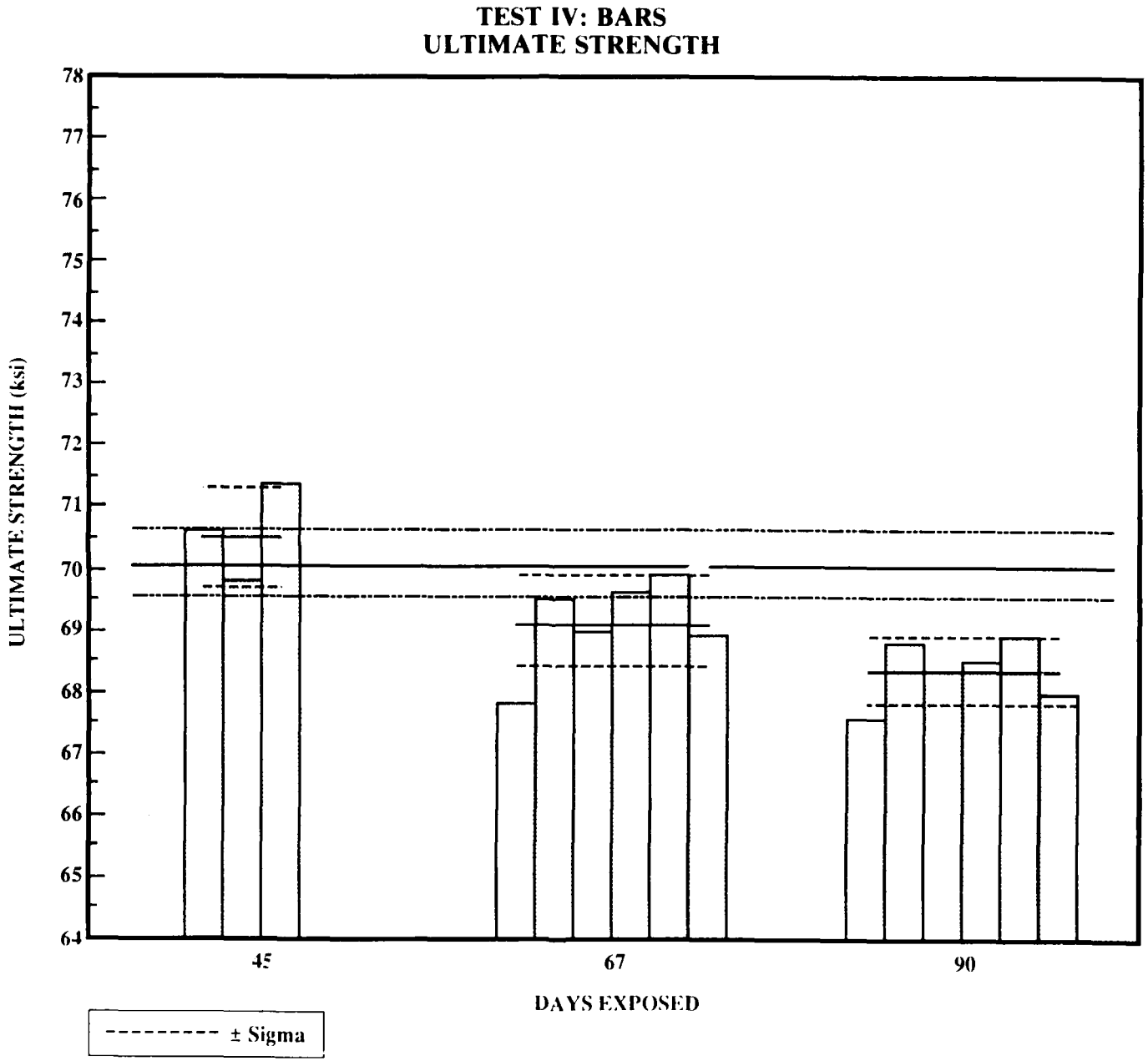
TEST IV: BARS
ULTIMATE STRENGTH
ULTIMATE STRENGTH (ksi)
78
77
76
75
74
73
72
71
70
69
68
67
66
65
64
45
67
90
DAYS EXPOSED
± Sigma

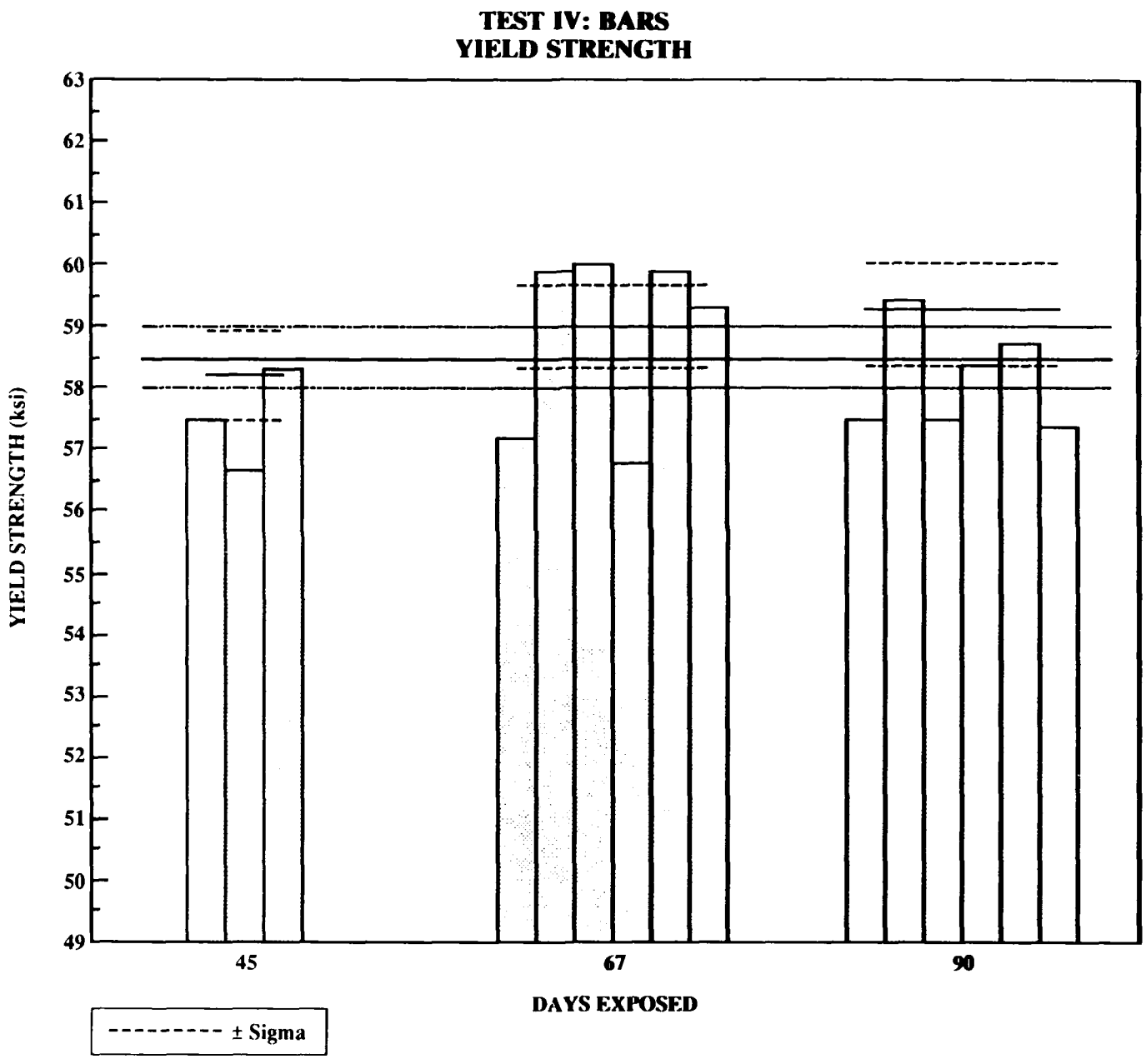
TEST IV: BARS
YIELD STRENGTH
YIELD STRENGTH (ksi)
63
62
61
60
59
58
57
56
55
54
53
52
51
50
49
45
67
90
DAYS EXPOSED
± Sigma

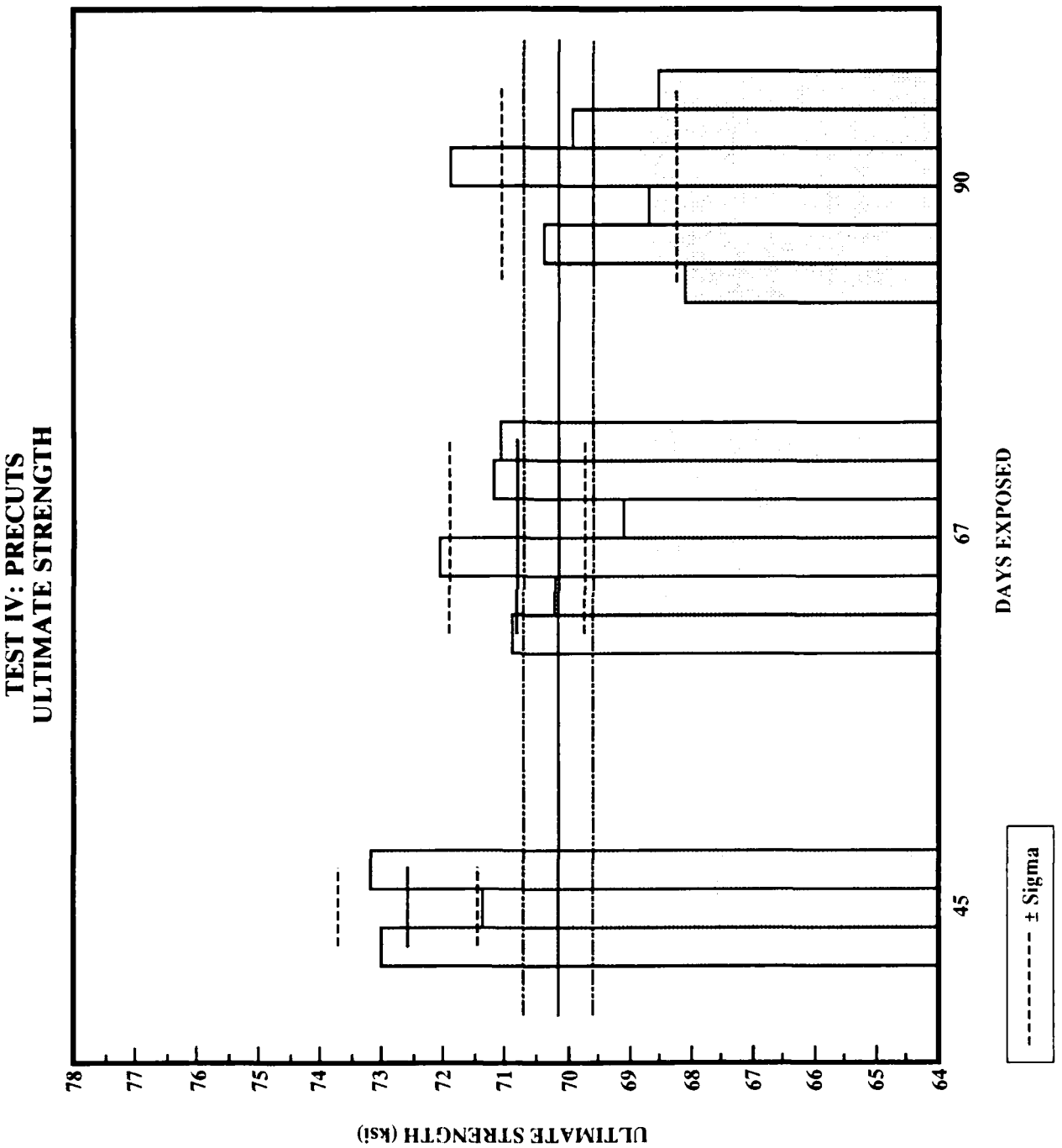
TEST IV: PRECUTS
ULTIMATE STRENGTH
ULTIMATE STRENGTH (ksi)
78
77
76
75
74
73
72
71
70
69
68
67
66
65
64
45
67
90
DAYS EXPOSED
± Sigma

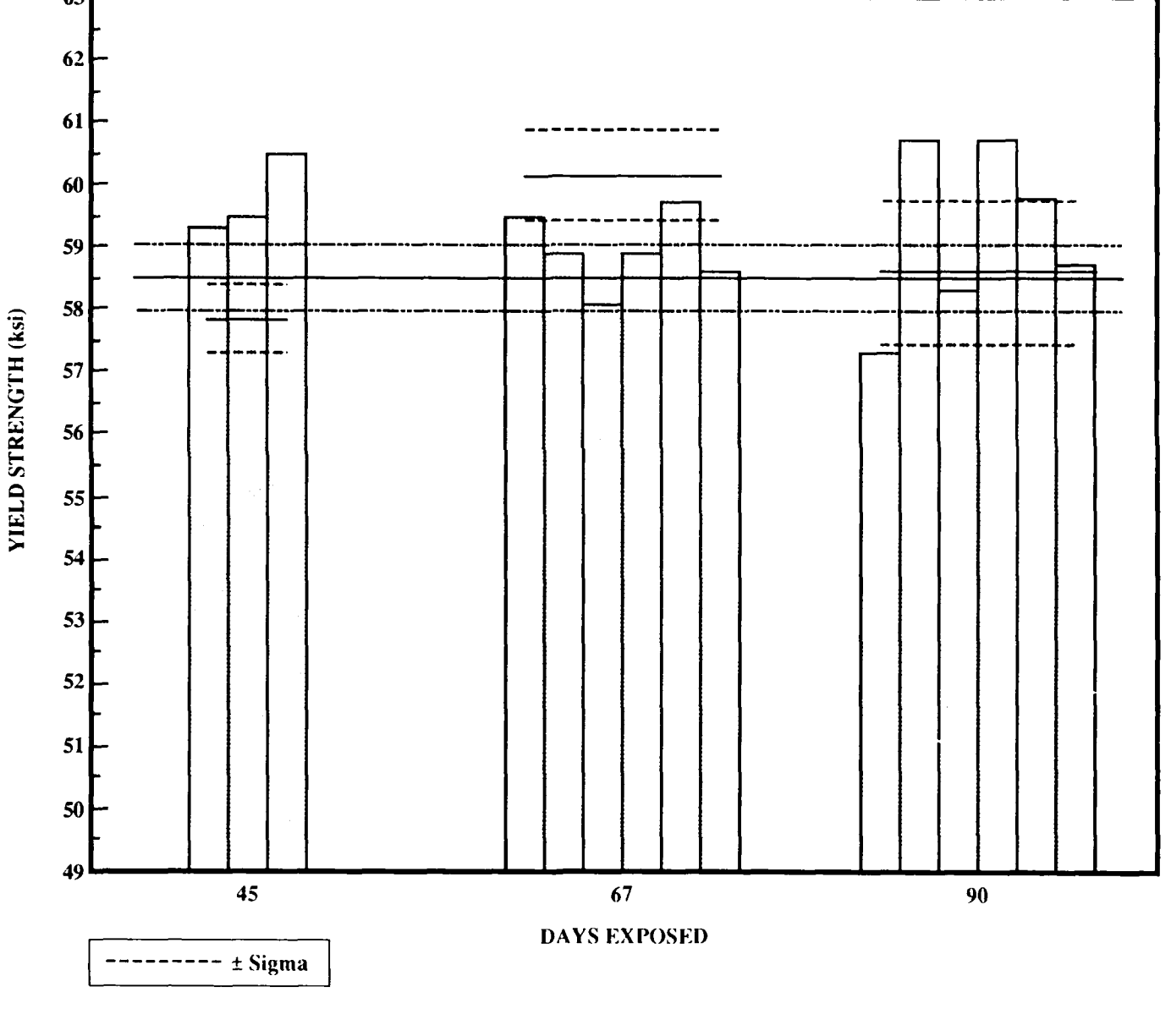
TEST IV: PRECUTS
YIELD STRENGTH
YIELD STRENGTH (ksi)
63
62
61
60
59
58
57
56
55
54
53
52
51
50
49
45
67
90
DAYS EXPOSED
± Sigma

TEST IV: TENSILE BARS

INTERGRANULAR CORROSION TEST 45 DAYS

REMARKS	Sample number	Thickness (inches)	Width (inches)	Area (sq. inch)	Gage Length: Initial (inches)	Gage Length: Final (inches)	Percent Elong-ation	Ultimate Force (pounds)	Ultimate Strength (ksi)	Yield Force (pounds)	Yield Strength (ksi)
CONTROLS	TIVA	0.249	0.250	0.062	1.000	1.163	16.3	4420	71.3	3620	58.4
	TIVB	0.249	0.250	0.062	1.000	1.157	15.7	4370	70.5	3555	57.3
	TIVD	0.250	0.245	0.061	1.000	1.150	15.0	4295	70.4	3525	57.8
average				0.062			15.7		70.7		57.8
std. dev				0.001			0.7		0.5		0.5
EXPOSED	TIVS	0.250	0.249	0.062	1.000	1.138	13.8	4535	73.1	3675	59.3
	TIVT	0.250	0.248	0.062	1.000	1.164	16.4	4425	71.4	3690	59.5
	TIVW	0.250	0.249	0.062	1.000	1.125	12.5	4540	73.2	3750	60.5
average				0.062			14.2		72.6		59.8
std. dev				0.000			2.0		1.0		0.6

TEST IV: TENSILE BARS

INTERGRANULAR CORROSION TEST 67 DAYS

REMARKS	Sample number	Thickness (inches)	Width (inches)	Area (sq. inch)	Gage Length: Initial (inches)	Gage Length: Final (inches)	Percent Elong-ation	Ultimate Force (pounds)	Ultimate Strength (ksi)	Yield Force (pounds)	Yield Strength (ksi)
CONTROLS	TIVC	0.252	0.250	0.063	1.000	1.155	15.5	4375	69.4	3830	60.8
	TIVE	0.250	0.253	0.063	1.000	1.170	17.0	4320	68.6	3745	59.4
	TIVG	0.252	0.255	0.064	1.000	1.170	17.0	4470	69.8	3840	60.0
average				0.063			16.5		69.3		60.1
std. dev				0.001			0.9		0.6		0.7
EXPOSED	TIVN	0.251	0.254	0.064	1.000	1.163	16.3	4535	70.9	3805	59.5
	TIVO	0.251	0.245	0.061	1.000	1.166	16.6	4285	70.2	3595	58.9
	TIVR	0.251	0.251	0.063	1.000	1.140	14.0	4540	72.1	3660	58.1
	TIVU	0.250	0.246	0.062	1.000	1.168	16.8	4285	69.1	3650	58.9
	TIVBB	0.251	0.249	0.062	1.000	1.158	15.8	4415	71.2	3700	59.7
	TIVEE	0.251	0.235	0.059	1.000	1.165	16.5	4195	71.1	3460	58.6
average				0.062			16.0		70.8		58.9
std. dev				0.002			1.0		1.0		0.6

TEST IV: TENSILE BARS

INTERGRANULAR CORROSION TEST 90 DAYS

REMARKS	Sample number	Thickness (inches)	Width (inches)	Area (sq. inch)	Gage Length: Initial (inches)	Gage Length: Final (inches)	Percent Elong-ation	Ultimate Force (pounds)	Ultimate Strength (ksi)	Yield Force (pounds)	Yield Strength (ksi)
CONTROLS	TIVG	0.251	0.252	0.063	1.000	1.139	13.9	4390	69.7	3775	59.9
	TIVH	0.251	0.250	0.063	1.000	1.185	18.5	4440	70.5	3650	57.9
	TIVJ	0.252	0.246	0.062	1.000	1.185	18.5	4510	72.7	3590	57.9
average				0.063			17.0		71.0		58.6
std. dev				0.001			2.7		1.6		1.2
EXPOSED	TIVL	0.251	0.250	0.063	1.000	1.170	17.0	4290	68.1	3610	57.3
	TIVP	0.252	0.251	0.063	1.000	1.150	15.0	4435	70.4	3800	60.3
	TIVQ	0.250	0.247	0.062	1.000	1.182	18.2	4265	68.8	3615	58.3
	TIVX	0.251	0.254	0.064	1.000	1.164	16.4	4600	71.9	3860	60.3
	TIVAA	0.249	0.248	0.062	1.000	1.167	16.7	4335	69.9	3705	59.8
	TIVCC	0.252	0.245	0.062	1.000	1.187	18.7	4255	68.6	3640	58.7
average				0.063			17.0		69.6		59.1
std. dev				0.001			1.3		1.4		1.2

AD-A195 118 SOME EFFECTS OF NITRATES ON THE TENSILE PROPERTIES OF AL 7075-T7351(U) ARMY BELVOIR RESEARCH DEVELOPMENT AND ENGINEERING CENTER FORT BELVOIR VA D HARRIS ET AL 2/2

UNCLASSIFIED MAR 88 BRDEC-2461 F/G 11/6.1 NL

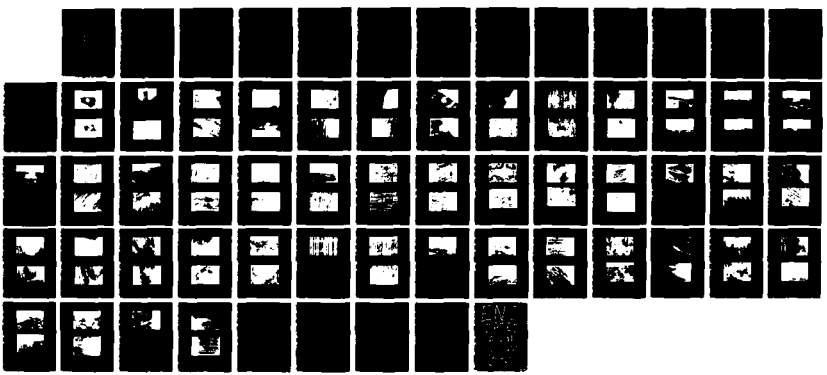

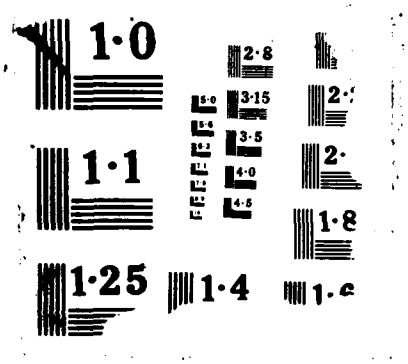
1·0
1·1
1·25
1·4
2·8
3·15
3·5
4·0
4·5
2·
1·8

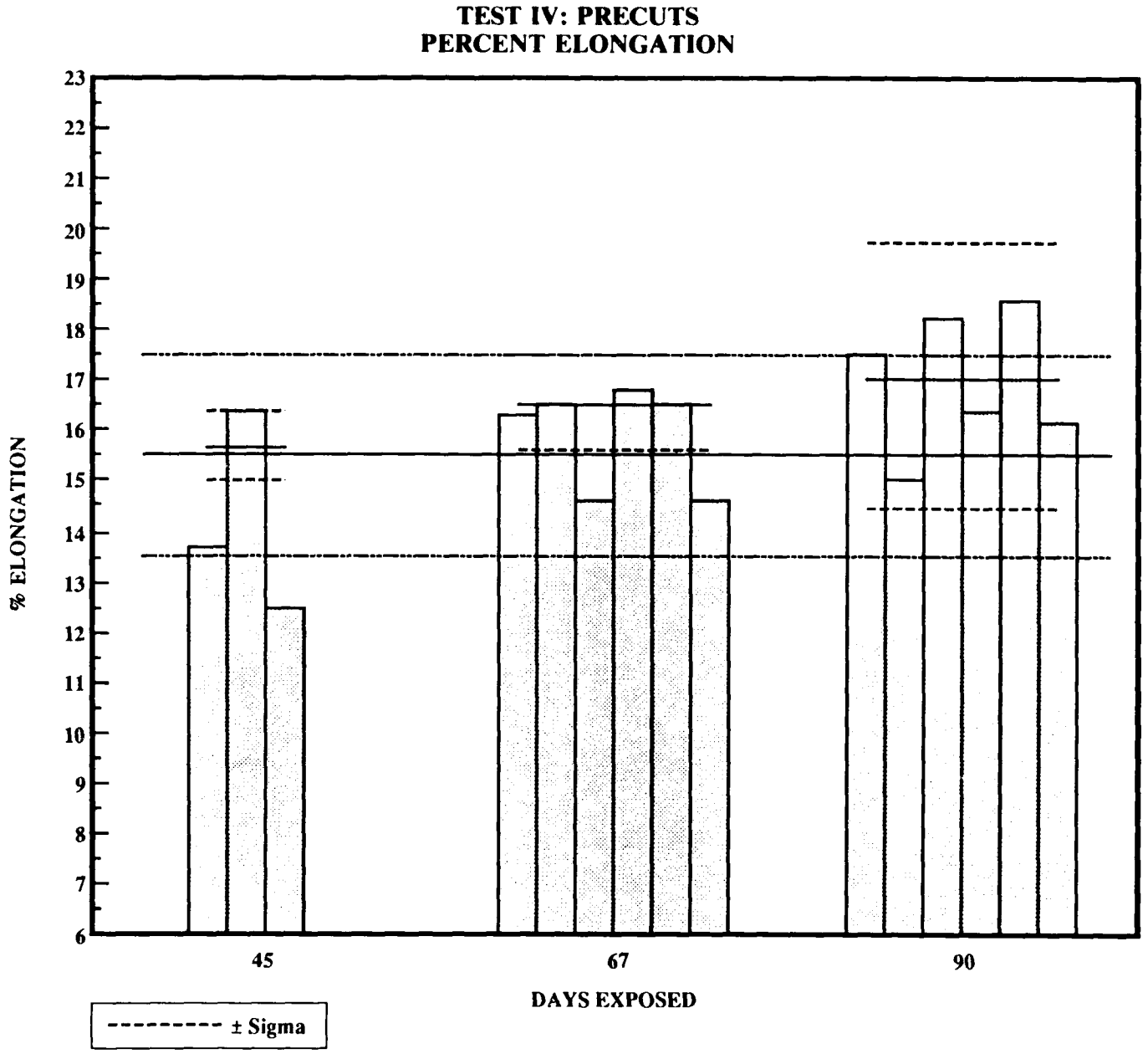
TEST IV: PRECUTS
PERCENT ELONGATION
% ELONGATION
23
22
21
20
19
18
17
16
15
14
13
12
11
10
9
8
7
6
45
67
90
DAYS EXPOSED
± Sigma

TEST V

TEST CYCLE

SALT SPRAY	4 Hours	(MONDAY-FRIDAY)
HOT SOAK (35 °C/95 °F)	16 Hours	(FRIDAY-SATURDAY)
PURGE AIR	4 Hours	(MONDAY-THURSDAY)
HOT SOAK (35 °C/95 °F)	28 Hours	(FRIDAY-SATURDAY)
CONDENSING SOAK (20 °C/68 °F)	35 Hours	(SATURDAY-MONDAY)

TEST ENVIRONMENT

ACID GAS	CONCENTRATION
Sulfur Dioxide	71 ppm
Nitric Oxide	258 ppm
Nitrogen Dioxide	260 ppm
Air Force Inhibitor 7	

AIR FORCE INHIBITOR #7

COMPOUND	NOMINAL GM-WT/L
Sodium Borate	3.5
Sodium Nitrate	2.0
Sodium Nitrite	2.0
Sodium Meta-Silicate	0.1
Sodium Hexa-Meta-Phosphate	0.5
Triton X-114	0.075
Zinc Sulfate	0.5

EXPOSURE SPECIMENS

PLATES	4″ × 1/2″ × 1/4″	12 As Received
C-RINGS	1.0″d × 0.75″w × 0.028″t	1 @ 31 ksi
	1.0″d × 0.75″w × 0.058″t	3 @ 31 ksi

DURATION OF EXPOSURE 45 days/256 hours salt fog

TEST V

INTERGRANULAR

Specimen	Thickness (inches)	Width (inches)	Area (sq. inch)	Gage Length: Initial (inches)	Gage Length: Final (inches)	Percent Elongation	Ultimate Force (pounds)	Ultimate Strength (ksi)	Yield Force (pounds)	Yield Strength (ksi)
V B	0 250	0.244	0.061	1.000	1.160	16.0	4255	69.8	3525	57.8
V C	0.251	0.250	0.063	1.000	1.150	15.0	4455	71.0	3760	59.9
V D	0.250	0.253	0.063	1.000	1.149	14.9	4460	70.5	3750	59.3
average						15.3		70.4		59.0
std. dev						0.6		0.6		1.1
V E	0.251	0.253	0.064	1.000	1.159	15.9	4523	71.2	3810	60.0
V G	0.250	0.240	0.060	1.000	1.147	14.7	4145	69.1	3525	58.8
V H	0.251	0.239	0.060	1.000	1.157	15.7	4215	70.3	3590	59.8
average						15.4		70.2		59.5
std. dev						0.6		1.1		0.6
V J	0.251	0.256	0.064	1.000	1.148	14.8	4495	70.0	3840	59.8
V K	0.251	0.250	0.063	1.000	1.158	15.8	4410	70.3	3740	59.6
V L	0.251	0.231	0.058	1.000	1.133	13.3	4025	69.4	3350	57.8
average						14.6		69.9		59.1
std. dev						1.3		0.5		1.1
combined average						15.1		70.2		59.2
combined std. dev						0.9		0.7		0.9

TEST VI

TEST CYCLE

SALT SPRAY	4 Hours	(MONDAY-FRIDAY)
HOT SOAK (35 °C/95 °F)	16 Hours	(FRIDAY-SATURDAY)
PURGE AIR	4 Hours	(MONDAY-THURSDAY)
HOT SOAK (35 °C/95 °F)	28 Hours	(FRIDAY-SATURDAY)
CONDENSING SOAK (20 °C/68 °F)	35 Hours	(SATURDAY-MONDAY)

TEST ENVIRONMENT

ACID GAS	CONCENTRATION
Sulfur Dioxide	71 ppm
Nitric Oxide	258 ppm
Nitrogen Dioxide	260 ppm

SALT FOG SOLUTION COMPOSITION

STOCK		FOG
> 0.100 N	Sodium Chloride (NaCl)	100 ppm
> 0.229 N	Sodium Nitrate ($NaNO_3$)	333 ppm
> 0.089 N	Sodium Sulfate (Na_2SO_4)	107 ppm
>	chloride/nitrate ratio = 0.44	
>	chloride/sulfate ratio = 1.12	
>	pH 4.2-4.5	

ACIDIFICATION STOCK SOLUTION

ACID	NORMALITY
Sulfuric	0.089
Nitric	0.229
Hydrochloric	0.100

EXPOSURE SPECIMENS

PLATES	4" × 1/2" × 1/4"	12 As Received
C-RINGS	1.0"d × 0.75"w × 0.028"t	1 @ 31 ksi
	1.0"d × 0.75"w × 0.058"t	3 @ 31 ksi

DURATION OF EXPOSURE 45 days/256 hours salt fog

TEST VI

INTERGRANULAR

Specimen	Thickness (inches)	Width (inches)	Area (sq. inch)	Gage Length: Initial (inches)	Gage Length: Final (inches)	Percent Elong-ation	Ultimate Force (pounds)	Ultimate Strength (ksi)	Yield Force (pounds)	Yield Strength (ksi)
VI B	0.251	0.253	0.064	1.000	1.175	17.5	4370	68.8	3675	57.9
VI C	0.250	0.250	0.063	1.000	1.156	15.6	4285	68.6	3610	57.8
VI D	0.250	0.242	0.061	1.000	1.132	13.2	4200	69.4	3450	57.0
average						15.4		68.9		57.6
std. dev						2.2		0.4		0.5
VI E	0.250	0.251	0.063	1.000	1.170	17.0	4390	70.0	3625	57.8
VI G	0.248	0.245	0.061	1.000	1.159	15.9	4270	70.3	3575	58.9
VI H	0.248	0.258	0.064	1.000	1.155	15.5	4508	70.5	3725	58.2
average						16.1		70.2		58.3
std. dev						0.8		0.3		0.6
VI J	0.250	0.239	0.060	1.000	1.119	11.9	4080	68.3	3460	57.9
VI K	0.250	0.250	0.063	1.000	1.168	16.8	4400	70.4	3700	59.2
VI L	0.251	0.247	0.062	1.000	1.167	16.7	4230	68.2	3420	55.2
average						15.1		69.0		57.4
std. dev						2.8		1.2		2.1
combined average						15.6		69.4		57.8
combined std. dev						1.9		0.9		1.2

TEST VII

TEST CYCLE

SALT SPRAY	4 Hours	(MONDAY-FRIDAY)
HOT SOAK (35 °C/95 °F)	16 Hours	(FRIDAY-SATURDAY)
PURGE AIR	4 Hours	(MONDAY-THURSDAY)
HOT SOAK (35 °C/95 °F)	28 Hours	(FRIDAY-SATURDAY)
CONDENSING SOAK (20 °C/68 °F)	35 Hours	(SATURDAY-MONDAY)

TEST ENVIRONMENT

ACID GAS	CONCENTRATION
Sulfur Dioxide	71 ppm
Nitric Oxide	258 ppm
Nitrogen Dioxide	260 ppm
Air Force Inhibitor 7	

AIR FORCE INHIBITOR #7

COMPOUND	NOMINAL GM-WT/L
Sodium Borate	3.5
Sodium Nitrate	2.0
Sodium Nitrite	2.0
Sodium Meta-Silicate	0.1
Sodium Hexa-Meta-Phosphate	0.5
Triton X-114	0.075
Zinc Sulfate	0.5

SALT FOG SOLUTION COMPOSITION

STOCK		FOG
> 0.100 N	Sodium Chloride (NaCl)	100 ppm
> 0.229 N	Sodium Nitrate ($NaNO_3$)	333 ppm
> 0.089 N	Sodium Sulfate (Na_2SO_4)	107 ppm
>	chloride/nitrate ratio = 0.44	
>	chloride/sulfate ratio = 1.12	
>	pH 4.2-4.5	

ACIDIFICATION STOCK SOLUTION

ACID	NORMALITY
Sulfuric	0.089
Nitric	0.229
Hydrochloric	0.100

EXPOSURE SPECIMENS

PLATES	4" × 1/2" × 1/4"	
	12	As Received
C-RINGS	1.0"d × 0.75"w × 0.028"t	
	1	@ 31 ksi
	1.0"d × 0.75"w × 0.058"t	
	3	@ 31 ksi

TEST VII

INTERGRANULAR

Specimen	Thickness (inches)	Width (inches)	Area (sq. inch)	Gage Length: Initial (inches)	Gage Length: Final (inches)	Percent Elong-ation	Ultimate Force (pounds)	Ultimate Strength (ksi)	Yield Force (pounds)	Yield Strength (ksi)
VII B	0.250	0.253	0.063	1.000	1.172	17.2	4450	70.4	3800	60.1
VII C	0.251	0.249	0.062	1.000	1.120	12.0	4220	68.5	3525	56.4
VII D	0.250	0.250	0.063	1.000	1.145	14.5	4315	69.0	3650	58.4
average						14.6		69.2		58.3
std. dev						2.6		0.9		1.8
VII E	0.251	0.249	0.062	1.000	1.137	13.7	4380	70.1	3720	59.5
VII G	0.251	0.253	0.064	1.000	1.146	14.6	4390	69.1	3600	56.7
VII H	0.250	0.253	0.063	1.000	1.158	15.8	4431	70.1	3765	59.5
average						14.7		69.8		58.6
std. dev						1.1		0.5		1.6
VII J	0.252	0.251	0.063	1.000	1.145	14.5	4475	70.7	3740	59.1
VII K	0.250	0.251	0.063	1.000	1.172	17.2	4450	70.9	3660	58.3
VII L	0.251	0.255	0.064	1.000	1.164	16.4	4365	68.2	3560	55.6
average						16.0		70.0		57.7
std. dev						1.4		1.5		1.8
combined average						15.1		69.7		58.2
combined std. dev						1.7		1.0		1.6

TEST VIII

TEST CYCLE

SALT SPRAY	4 Hours	(MONDAY-FRIDAY)
HOT SOAK (35 °C/95 °F)	16 Hours	(FRIDAY-SATURDAY)
PURGE AIR	4 Hours	(MONDAY-THURSDAY)
HOT SOAK (35 °C/95 °F)	28 Hours	(FRIDAY-SATURDAY)
CONDENSING SOAK (20 °C/68 °F)	35 Hours	(SATURDAY-MONDAY)

TEST ENVIRONMENT

ACID GAS	CONCENTRATION
Sulfur Dioxide	71 ppm
Nitric Oxide	258 ppm
Nitrogen Dioxide	260 ppm

EXPOSURE SPECIMENS

PLATES 4″ × 1/2″ × 1/4″
12 As Received

C-RINGS 1.0″d × 0.75″w × 0.028″t
1 @ 31 ksi
1.0″d × 0.75″w × 0.058″t
3 @ 31 ksi

DURATION OF EXPOSURE 45 days/256 hours salt fog

TEST VIII

INTERGRANULAR

Specimen	Thickness (inches)	Width (inches)	Area (sq. inch)	Gage Length: Initial (inches)	Gage Length: Final (inches)	Percent Elong-ation	Ultimate Force (pounds)	Ultimate Strength (ksi)	Yield Force (pounds)	Yield Strength (ksi)
VIII B	0.249	0.239	0.060	1.000	1.132	13.2	4195	70.5	3515	59.1
VIII C	0.249	0.253	0.063	1.000	1.146	14.6	4445	70.6	3725	59.1
VIII D	0.250	0.238	0.060	1.000	1.171	17.1	4175	70.2	3500	58.8
average						15.0		70.4		59.0
std. dev						2.0		0.2		0.2
VIII E	0.250	0.253	0.063	1.000	1.179	17.9	4400	69.6	3625	57.3
VIII G	0.252	0.256	0.065	1.000	1.163	16.3	4525	70.1	3725	57.7
VIII H	0.252	0.246	0.062	1.000	1.145	14.5	4335	69.9	3655	59.0
average						16.2		69.9		58.0
std. dev						1.7		0.3		0.9
VIII J	0.251	0.241	0.060	1.000	1.143	14.3	4200	69.4	3450	57.0
VIII K	0.250	0.244	0.061	1.000	1.151	15.1	4255	69.8	3650	59.8
VIII L	0.251	0.251	0.063	1.000	1.180	18.0	4345	69.0	3675	58.3
average						15.8		69.4		58.4
std. dev						1.9		0.4		1.4
combined average						15.7		69.9		58.5
combined std. dev						1.7		0.5		0.9

APPENDIX D
PHOTOGRAPHIC TEST RESULTS

Contents

APPENDIX D
PHOTOGRAPHIC TEST RESULTS

Contents (continued)

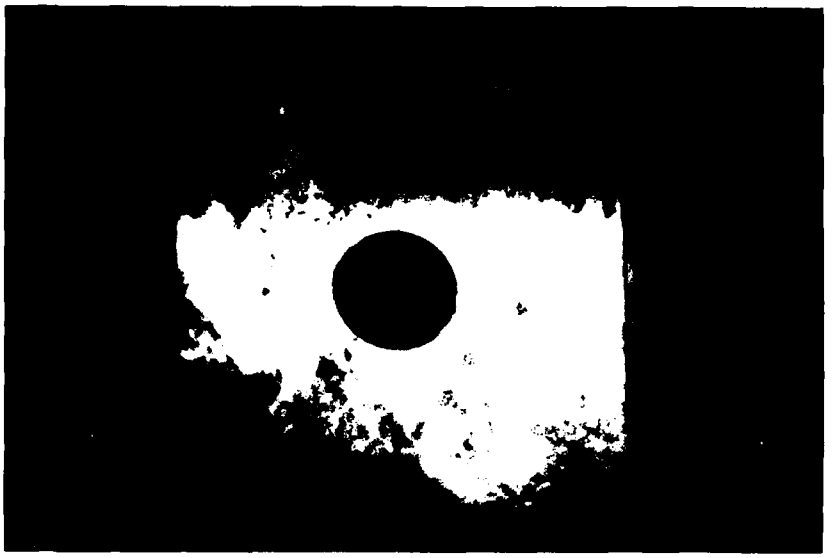

Figure 1. Control (unstressed) C-ring after exposure

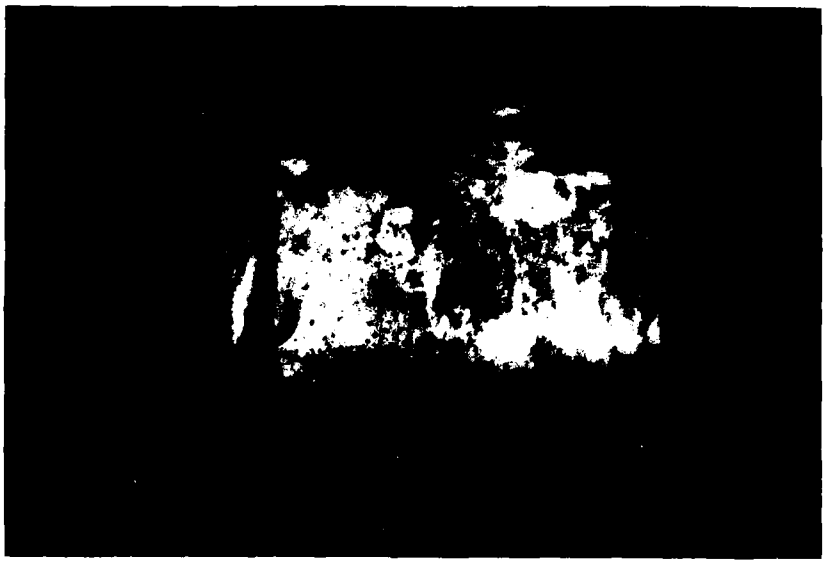

Figure 2. Stressed C-ring after exposure

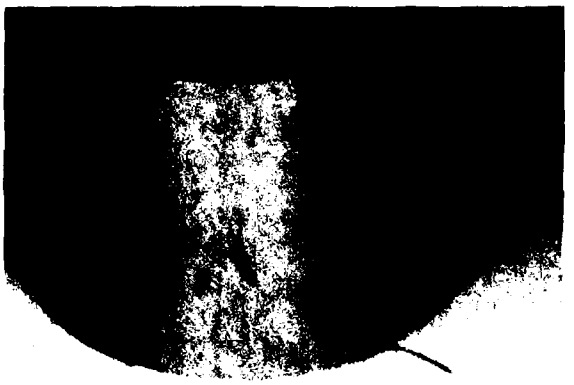

Figure 3. C-ring with extensive corrosion damage near bottom

Figure 4. Type A corrosion (equiaxed pits) on interior surface of C-ring. Light circular areas are due to water marks (50X)

Figure 5. Type B corrosion (deep elongated pit) on exterior surface of the C-ring (100X)

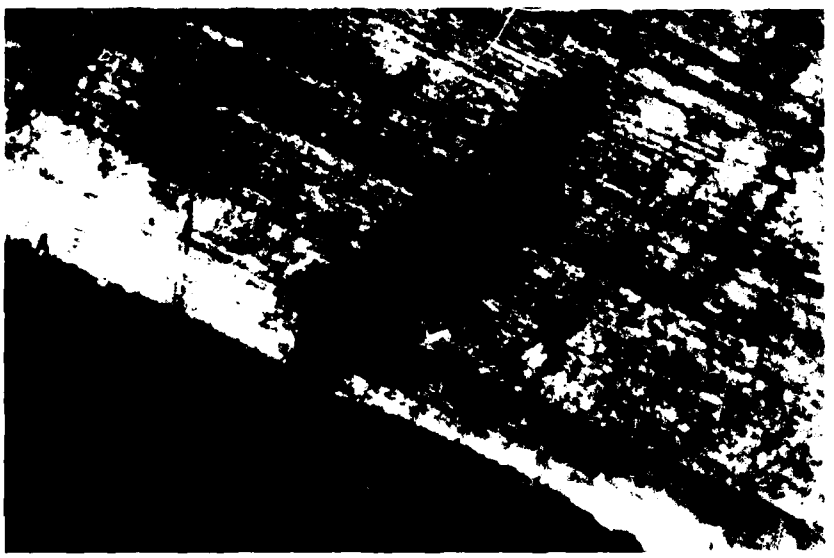

Figure 6. Type C corrosion (elongated shallow pits) on edge of the C-ring (200X)

Figure 7. Type E corrosion (crack) on edge of stressed C-ring (100X)

Figure 8. Pit in which grain removal was part of the cause of damage (200X)

Figure 9. Pit which had penetrated through C-ring specimen after exposure in baseline test (100X)

Figure 10. Small surface pit in unstressed C-ring after exposure in baseline environment (200X)

Figure 11. Large shallow surface pit in unstressed C-ring after exposure to baseline environment (100X)

Figure 12. Deep pit which follows the grain direction in C-ring after exposure to baseline environment (100X)

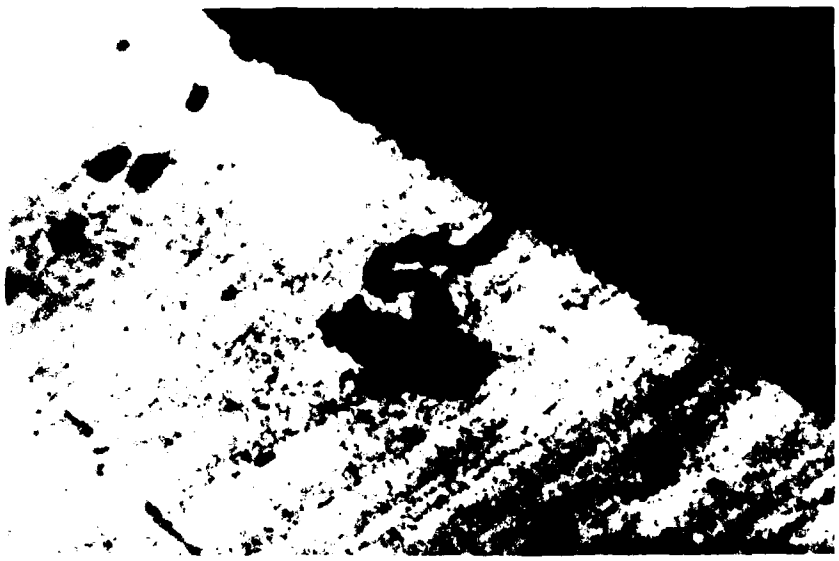

Figure 13. Pit with an unusual wormhole pipe in unstressed C-ring after exposure to baseline environment (500X)

Figure 14. Large pit in stressed C-ring after exposure to baseline environment (200X)

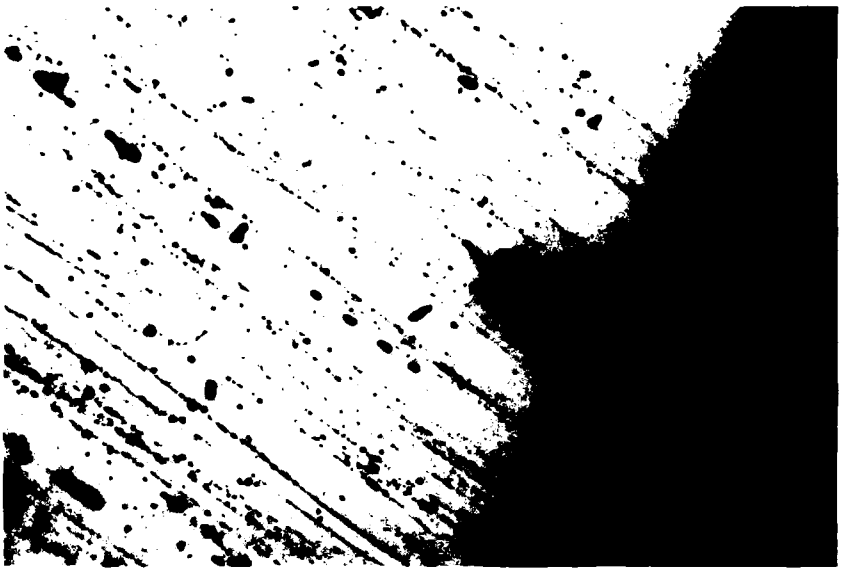

Figure 15. Narrow pit travelling in the grain direction in stressed C-ring after exposure to baseline environment (200X)

Figure 16. Corrosion streaks on rolled surface of flat specimen after exposure to baseline environment (100X)

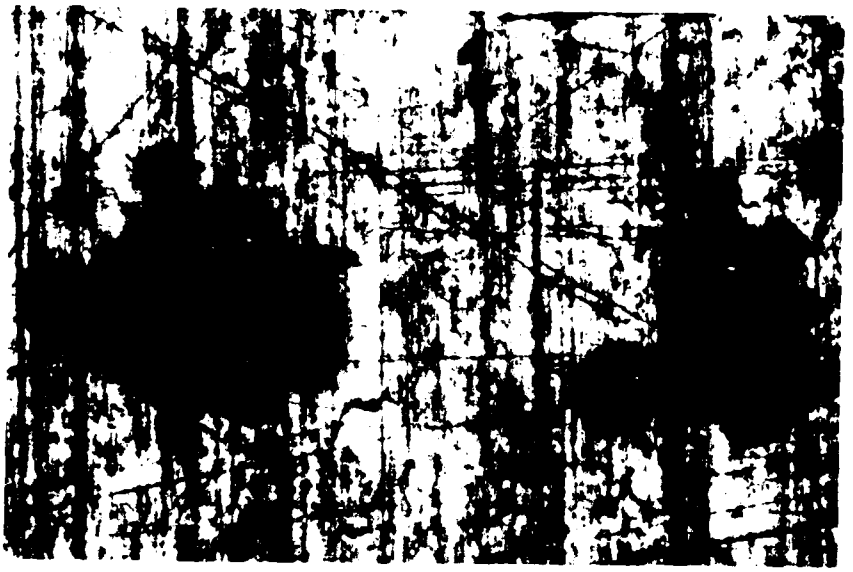

Figure 17. Two large inclusions of surface of flat specimen (100X)

Figure 18. Surface cracks from the rolling operation (100X)

A. 100X

B. 100X

Figure 19. Surface imperfections on a flat specimen acting as initiation site for corrosion. A. Surface cracks. B. Surface cracks and an inclusion

Figure 20. Under surface corrosion of a flat specimen after exposure to baseline environment (200X)

Figure 21. Superficial surface damage of a flat specimen after exposure to baseline environment (500X)

A. 500X

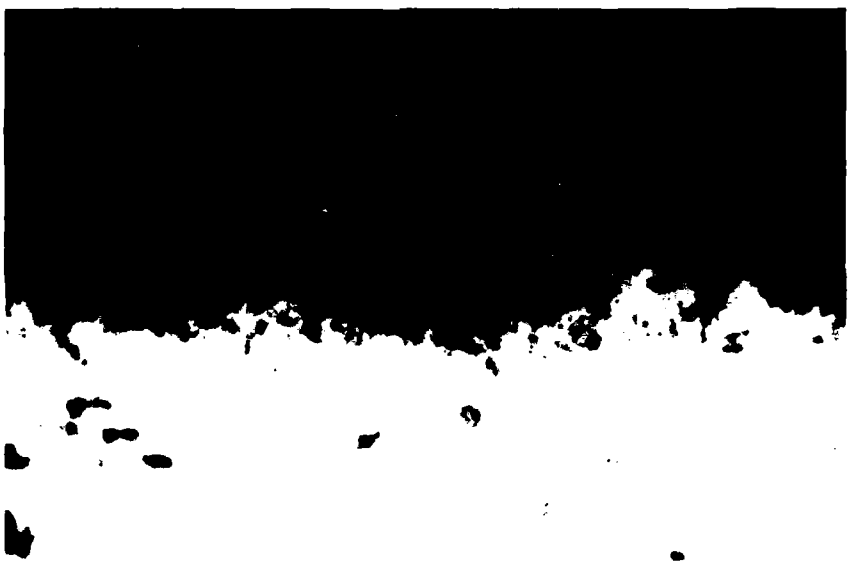

B. 500X

Figure 22. A. Incipient grain removal which results in B. Shallow surface corrosion (removal) after exposure to baseline environment

A. 500X

B. 500X

Figure 23. Pitting on the flat specimens. A. Pit with a crack. B. Normal pit. C. Pit which has a small orifice with respect to its volume after exposure to baseline environment
(continued)

C. 500X

Figure 23. Pitting on the flat specimens. A. Pit with a crack. B. Normal pit. C. Pit which has a small orifice with respect to its volume after exposure to baseline environment

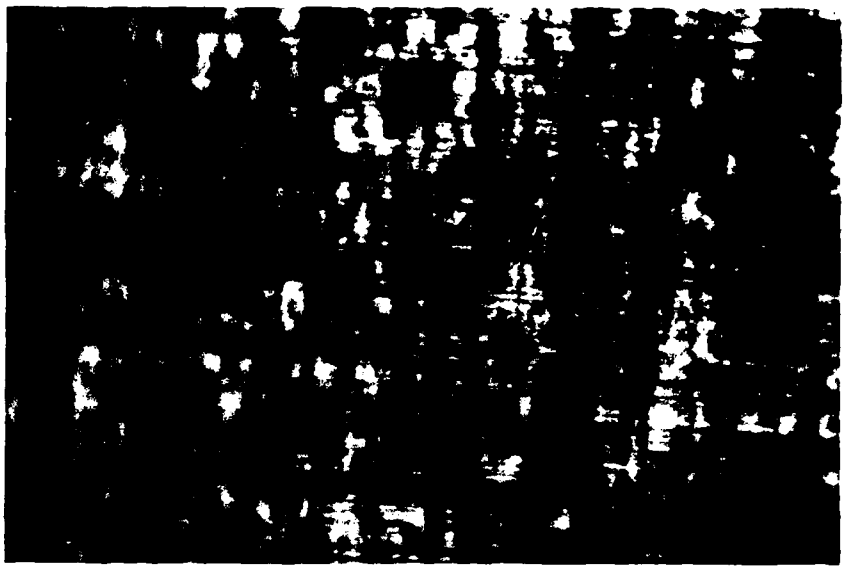

Figure 24. Shallow surface corrosion on C-ring after Test II exposure (100X)

Figure 25. Surface pits initiated at the grain boundary of the C-ring after exposure to Test II environment (200X)

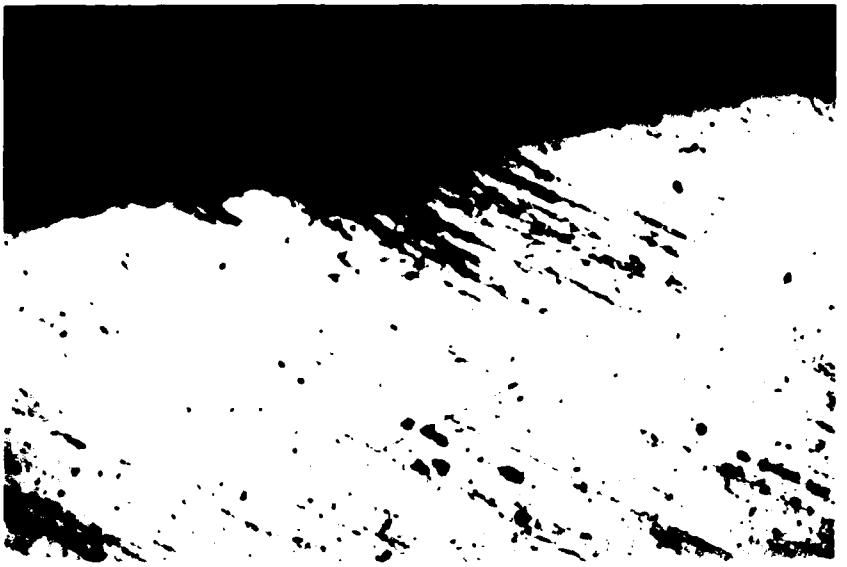

Figure 26. Intergranular corrosion on C-ring after Test II exposure (200X)

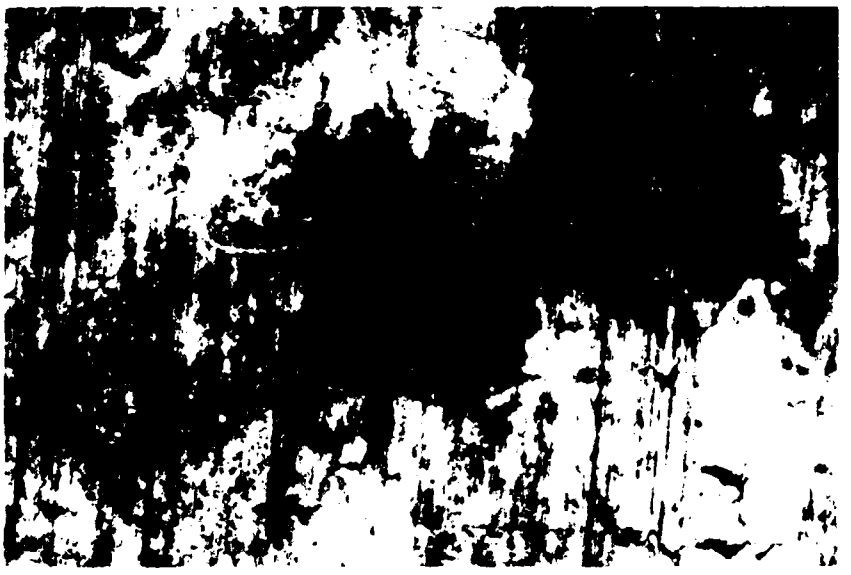

Figure 27. Shallow surface attack, dark area was under a microbiological colony, flat specimen after Test II exposure (100X)

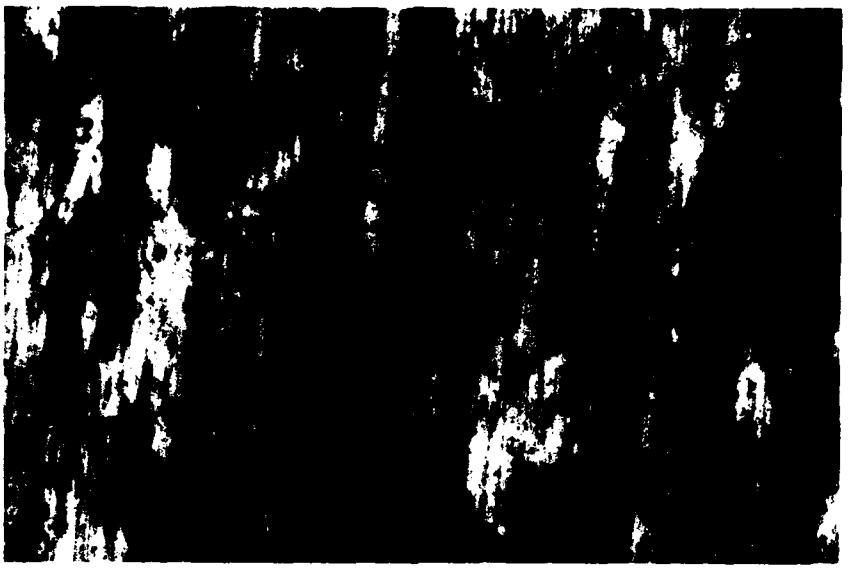

Figure 28. Normal surface attack on flat specimen after Test II exposure (100X)

Figure 29. Shallow under-surface corrosion with surface corrosion in flat specimen after Test II exposure (200X)

Figure 30. Localized corrosion attack on flat specimen after Test II exposure (200X)

Figure 31. Pit due to localized attack on flat specimen after Test II exposure (200X)

Figure 32. Small shallow pit on C-ring after exposure to Test III environment (200X)

Figure 33. Surface corrosion of flat specimen after Test III exposure (100X)

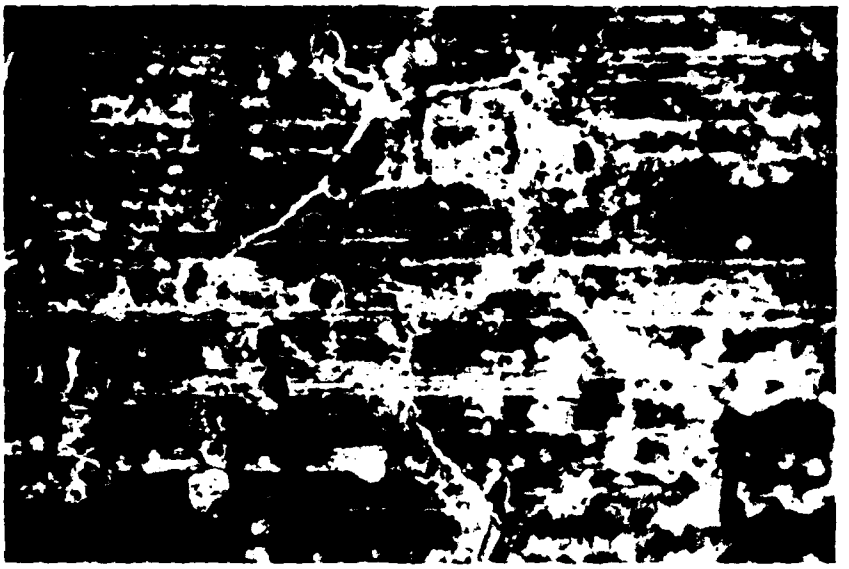

Figure 34. Small pits and water marks on C-ring after 45 day exposure to Test IV environment (100X)

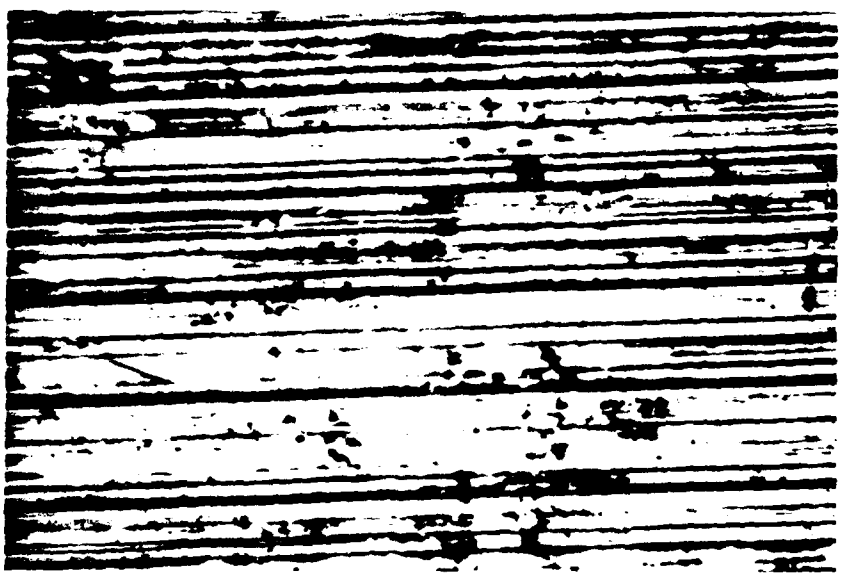

Figure 35. A typical machined surface of the C-rings kept in a desiccator, not exposed (100X)

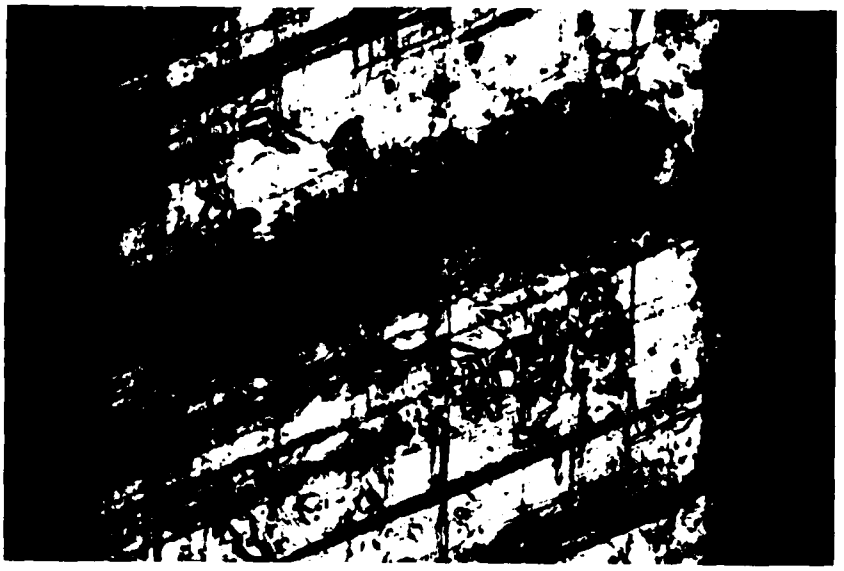

Figure 36. Shallow elongated pit on edge surface after 67 day exposure to Test IV environment (100X)

Figure 37. Pits on exterior surface of C-ring after 67 day exposure to Test IV environment (200X)

Figure 38. Large pit on exterior surface of C-ring after 67 days of exposure to the Test IV environment (200X)

Figure 39. Type A corrosion, large equiaxed pits, on exterior surface of C-ring after 90 days of exposure to the Test IV environment (200X)

A. 100X

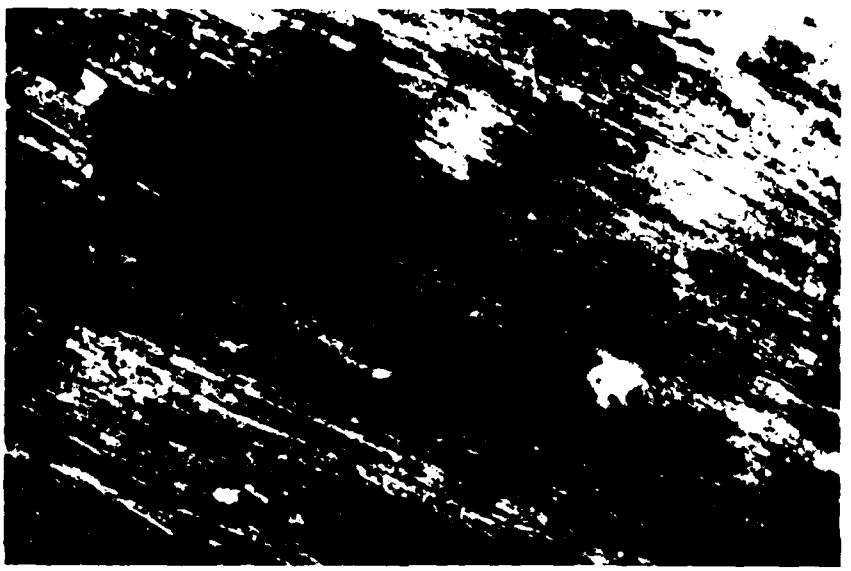

B. 100X

Figure 40. Severe shallow corrosion. A. Elongated pit on edge. B. Surface corrosion on edge of C-ring after 90 days of exposure to the Test IV environment

A. 100X

B. 200X

Figure 41. Intergranular cracks. A. 100X, B. 200X, C. 200X after 45 days of exposure to the Test IV environment (continued)

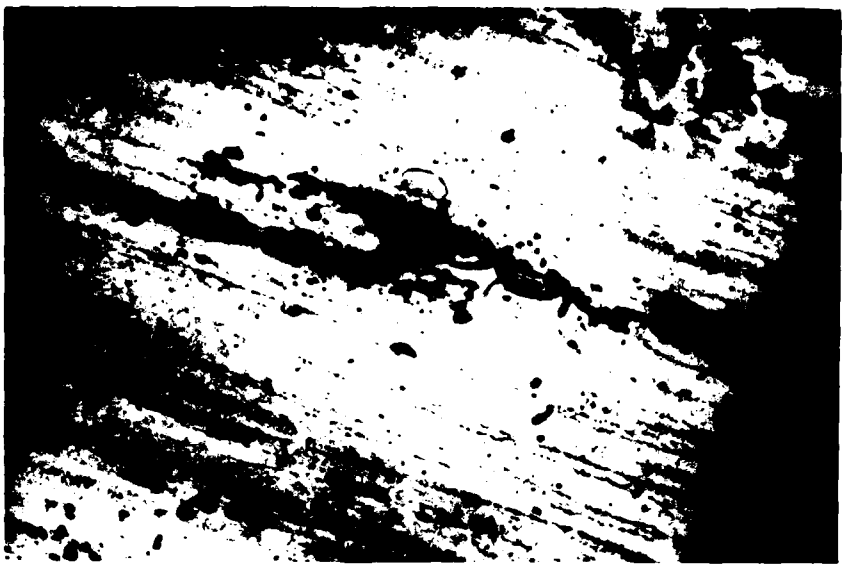

C. 200X

Figure 41. Intergranular cracks. A. 100X, B. 200X C. 200X after 45 days of exposure to the Test IV environment

Figure 42. Two pits with transgranular cracks after 45 days of exposure to the Test IV environment (200X)

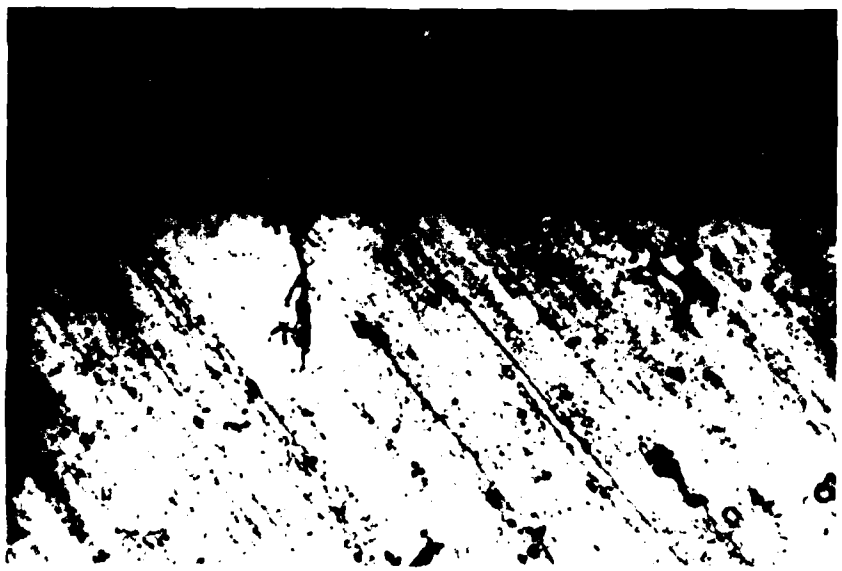

Figure 43. Two intergranular cracks initiated in very small pits in C-ring after 45 days of exposure to the Test IV environment (200X)

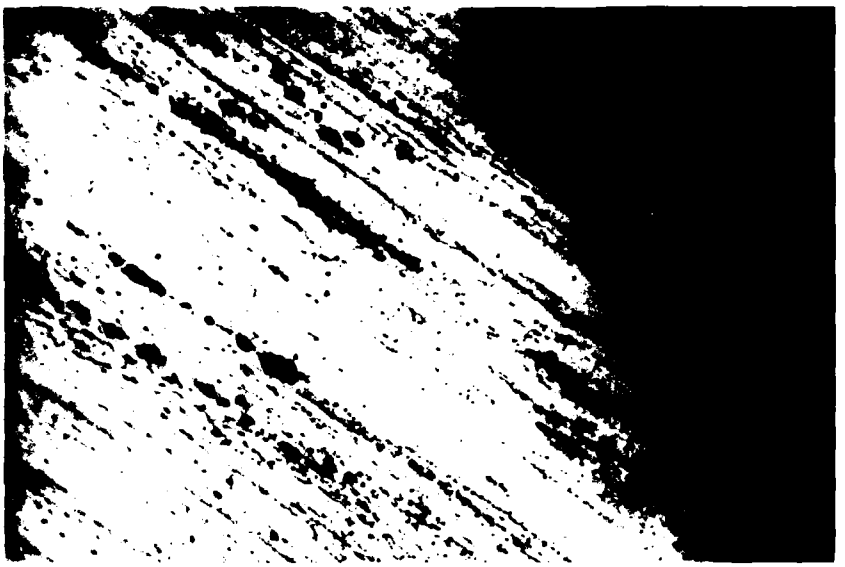

A. 200X

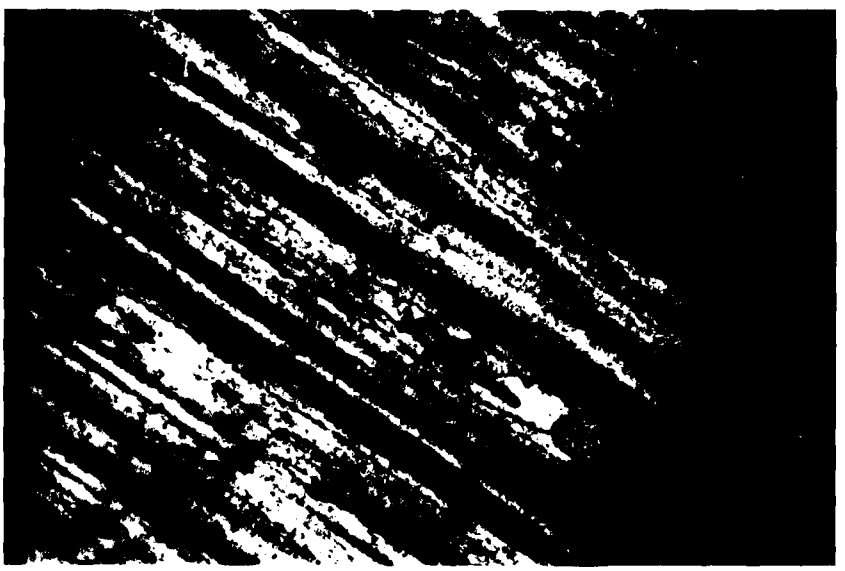

B. 200X

Figure 44. C-rings which were kept in a desiccator for 45 days

Figure 45. Large pit which may have originated from several pits and cracks in C-ring after 67 day exposure to Test IV environment (100X)

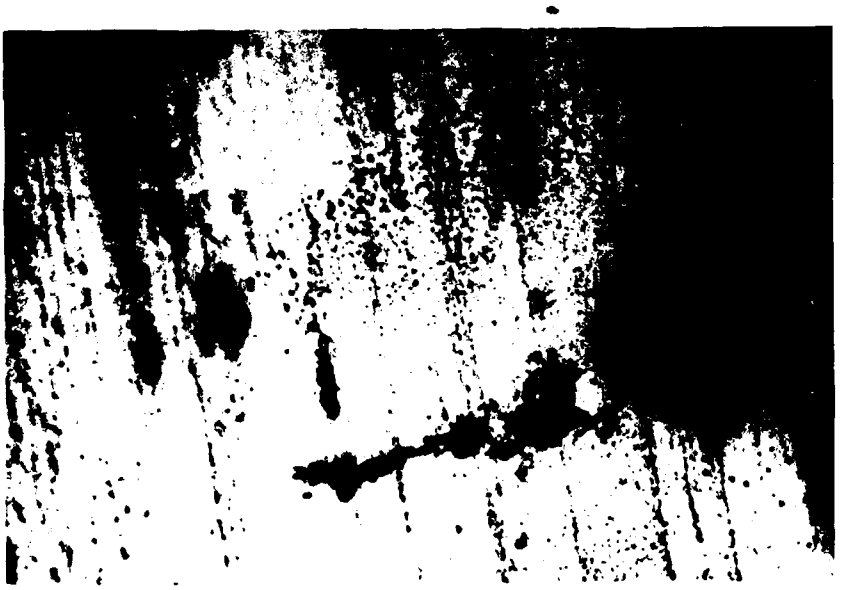

Figure 46. Transgranular pit caused by corrosion of transgranular crack in C-ring after 67 day exposure to Test IV environment (200X)

A. 200X

B. 200X

Figure 47. Intergranular cracking in C-ring after 67 day exposure to Test IV environment

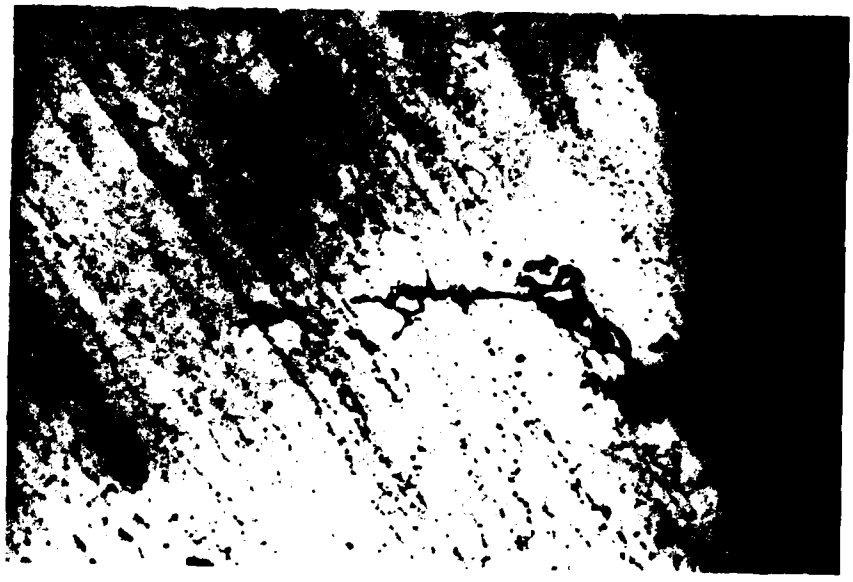

Figure 48. Crack which changed mode from intergranular to transgranular in C-ring after 67 day exposure to Test IV environment (500X)

Figure 49. Large pit in C-ring after 90 day exposure to Test IV environment (50X)

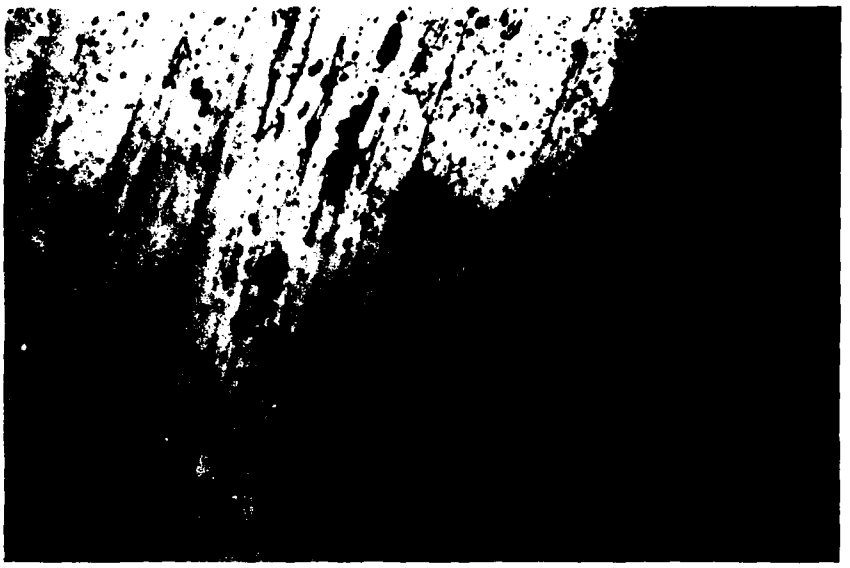

Figure 50. Transgranular pit in C-ring after 90 day exposure to Test IV environment (200X)

Figure 51. Transgranular pit and large pit which may have been caused by extensive corrosion of a transgranular crack in C-ring after 90 day exposure to Test IV environment (100X)

Figure 52. Small shallow pits on surface of flat specimen after 67 day exposure to Test IV environment (50X)

Figure 53. Pit on 90 day exposure flat specimen long pit on flat specimen after 90 day exposure to Test IV environment (100X)

Figure 54. Machined surface from tensile cutting operation before exposure to Test IV environment (100X)

A. 100X

B. 100X

Figure 55. Appearance of the machined surface from the tensile cutting operation after exposure to the Test IV environment. A. 67 days, B. 90 days (100X)

Figure 56. Shallow under surface corrosion in the process of creating a rough surface on the flat specimen after 90 day exposure to the Test IV environment (500X)

A. 500X

B. 200X

Figure 57. Pits. A. Small normal pit, and B. Shallow surface pit on flat specimens after 90 day exposure to Test IV environment

Figure 58. Pit on edge of specimen in tensile cut region after 90 day exposure to Test IV environment (200X)

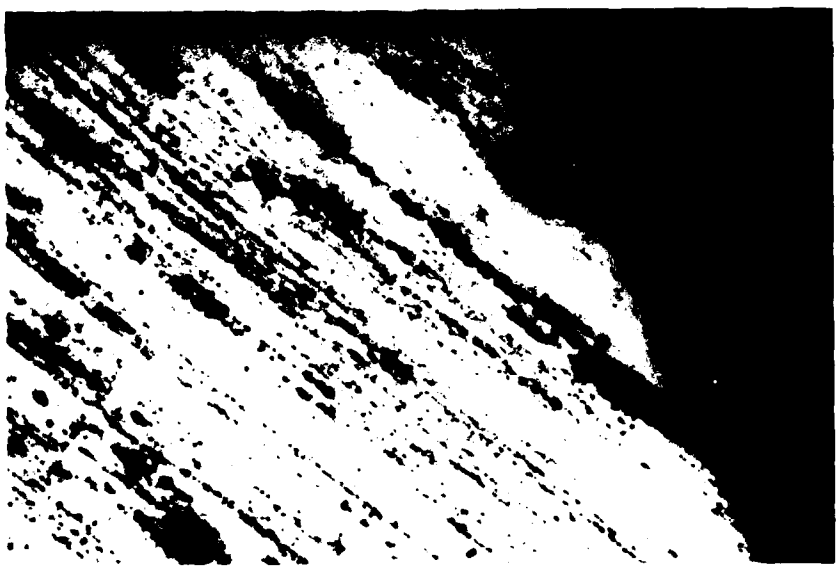

Figure 59. Pit and surface roughness which is indicative of shallow surface corrosion in C-ring in Test V

Figure 60. Shallow surface corrosion on C-ring in Test VI (Type D corrosion) (100X)

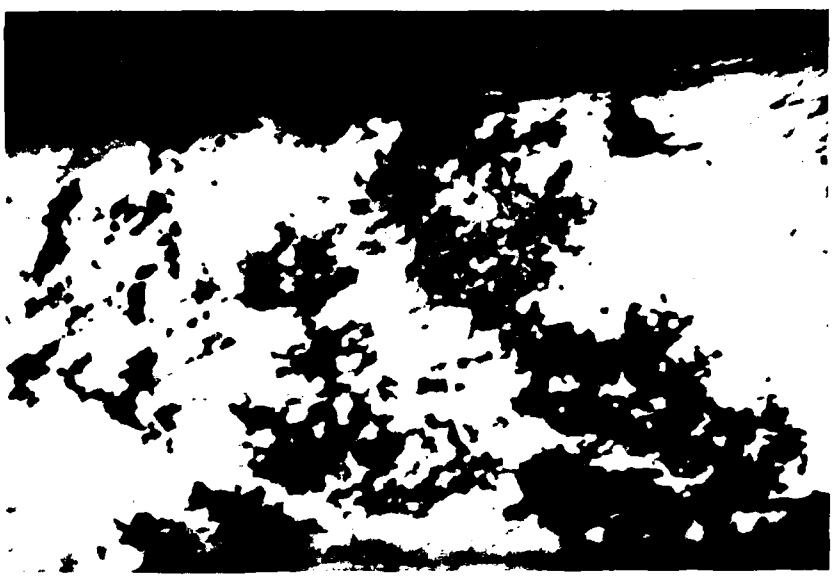

Figure 61. Shallow surface corrosion on edge of C-ring in Test VI (50X)

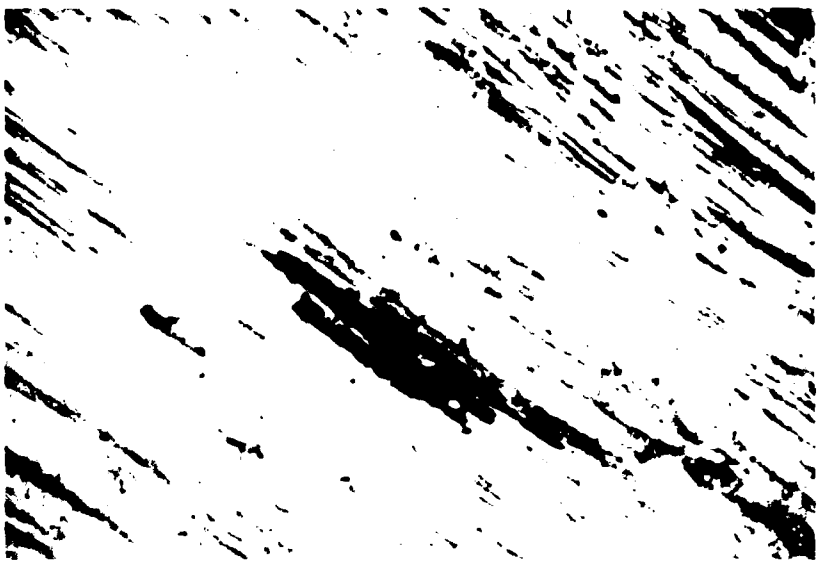

Figure 62. Shallow elongated pit on edge surface of C-ring after Test VI exposure (100X)

Figure 63. Severe pitting in surface of C-ring after Test VI exposure (200X)

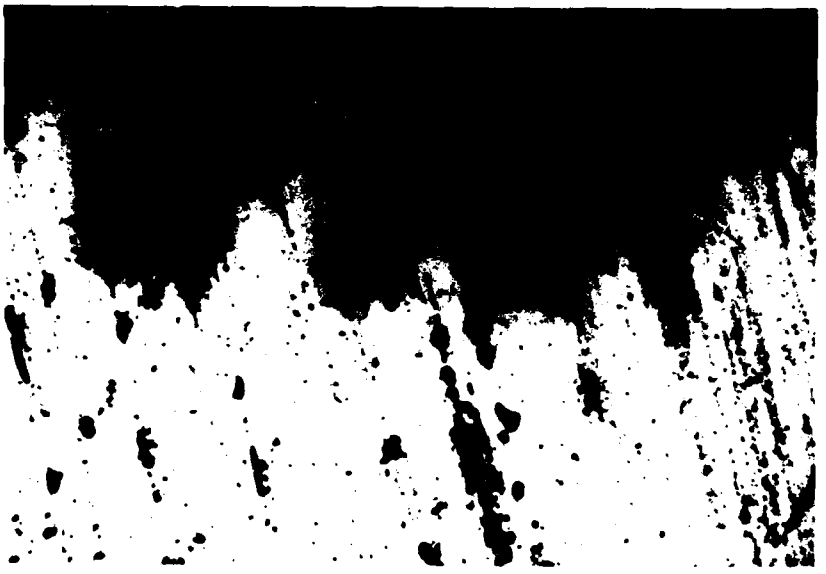

Figure 64. Pitting. The damage beneath the surface is hidden by a thin layer of surface metal on the C-ring after Test VI exposure (200X)

Figure 65. Typical surface of flat specimen. Lighter areas experienced more corrosion damage after Test VI exposure (100X)

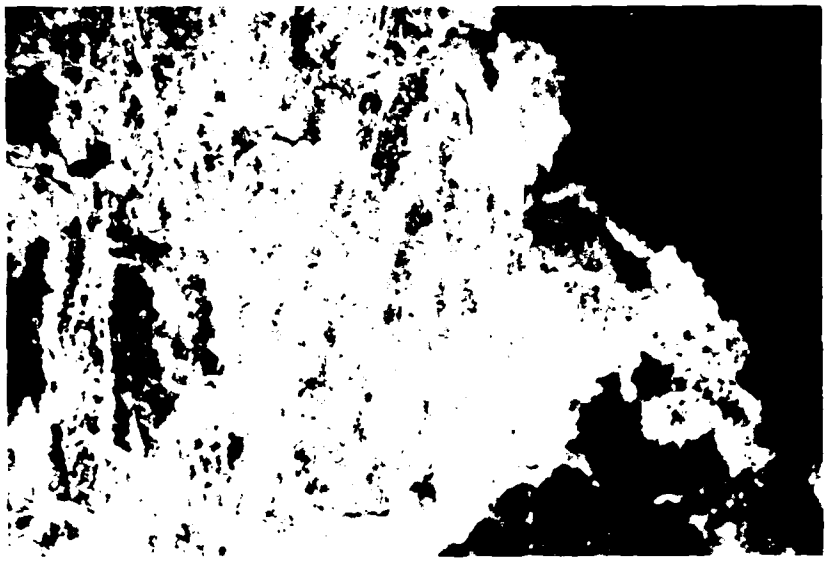

Figure 66. Surface which was beneath a microbiological colony on a flat specimen after exposure to Test VI environment (100X)

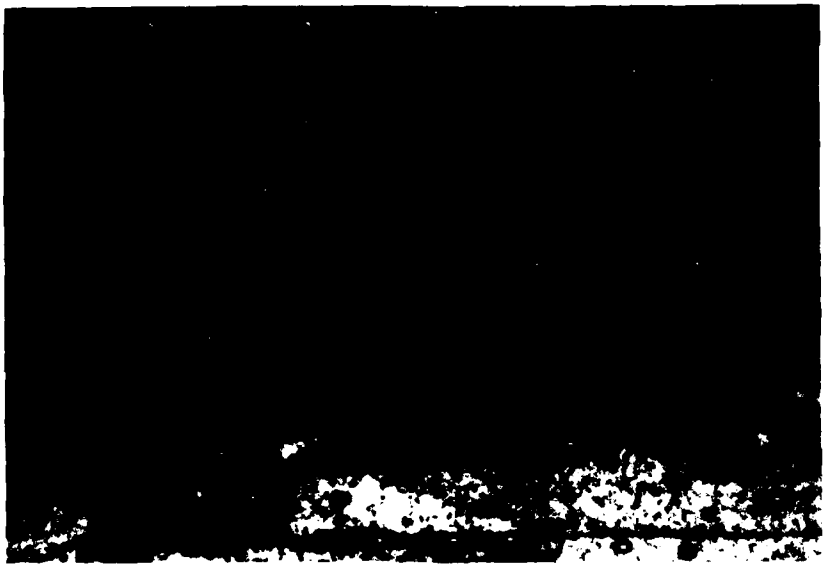

Figure 67. Pitting with areas of heavy localized attack on surface of flat specimen after Test VI exposure (200X)

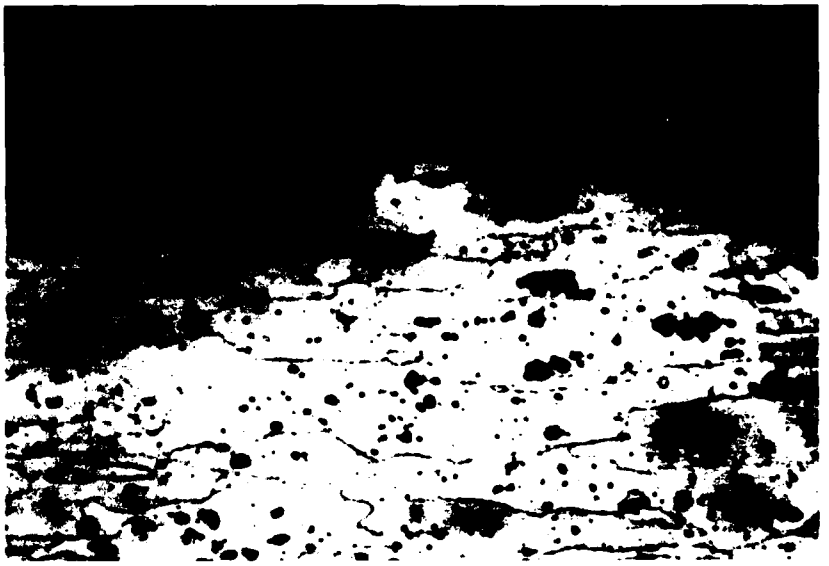

A. 200X

B. 200X

Figure 68. Pitting in a Test VI flat specimen. A. Majority of the damage is not visible from the surface. B. Most damage is visible.

Figure 69 Large pit on the flat specimen after Test VI exposure. Largest such pit seen on the flats (200X)

Figure 70. Pitting on edge of tensile bar which follows with the grain direction after Test VI exposure (500X)

Figure 71. Narrow pit in a C-ring after Test VII exposure (200X)

Figure 72. Large pit on the thin Test VII C-ring with cracks on the bottom (200X)

Figure 73. Surface with little evidence of surface attack on Test VIII C-ring after exposure (200X)

DISTRIBUTION FOR REPORT NO. 2461

DEPARTMENT OF DEFENSE

1 Director, Technical Information
Defense Advanced Research Projects Agency
1400 Wilson Blvd.
Arlington, VA 22209

1 Director
Defense Nuclear Agency
ATTN: TITL
Washington, DC 20305

2 Defense Technical Information Center
Cameron Station
ATTN: DTIC-FDAC
Alexandria, VA 22304-6145

DEPARTMENT OF THE ARMY

1 HQDA (DAMA-AOA-M)
Washington, DC 220310

1 HQDA (DALO-TSM)
Washington, DC 20314

1 HQDA (DAEN-RDL)
Washington, DC 20314

1 HQDA (DAEN-MPE-T)
Washington, DC 20314

1 Commander
US Army Missile Research & Development Command
ATTN: AMSMI-PR
Redstone Arsenal, AL 35809

1 Director
Army Materials and Mechanics Research Center
ATTN: AMXMR-RL Technical Library
Watertown, MA 02172-0001

1 Commander
Chemical Research R&D Center
ATTN: SMCCR-SPS (Tech Library)
Aberdeen Proving Ground, MD 21010-5423

1 Commander
US Army Aberdeen Proving Ground
ATTN: STEAP-MT-U (GE Branch)
Aberdeen Proving Ground, MD 21010

1 Director
US Army Materiel Systems Analysis Agency
ATTN: AMXSY-CM
Aberdeen Proving Ground, MD 21005-5071

1 Director
US Army Materiel Systems Analysis Agency
ATTN: AMXSY-MP
Aberdeen Proving Ground, MD 21005-5071

1 Director
US Ballistics Research Laboratory
ATTN: AMXBR-OD-ST (STINFO)
Aberdeen Proving Ground, MD 21005-5066

1 Director
US Army Engineer Waterways Eperiment Station
ATTN: Chief, Library Branch
Technical Information Center
Vicksburg, MS 39180

1 Commander
US Army Armament Research & Development Command
ATTN: SMCAR-TSS
Dover, NJ 07801-5001

1 Commander
US Army Troop Support & Aviation Materiel Readiness Command
ATTN: DRSTS-MES (1)
St. Louis, MO 63120

2 Director
Petrol & Fld Svc Dept
US Army Quartermaster School
Fort Lee, VA 23801

1 US Army Tank Automotive Command
ATTN: DRSTA-TSL
Warren, MI 48090

1 US Army Laboratory Command
ATTN: M. Levy SLCMT-MM
Materials Technology Laboratory
Watertown, MA 02172-0001

1 US Army Laboratory Command
ATTN: J. Wells SLCMT-MCZ
Materials Technology Laboratory
Watertown, MA 02172-0001

1 Commander
US Army Electronics Research & Development Command
ATTN: DELSD-L
Fort Monmouth, NJ 07703-5301

1 President
US Army Aviation Test Board
ATTN: STEBG-PO
Fort Rucker, AL 36360

1 US Army Aviation School Library
PO Drawer O
Fort Rucker, AL 36360

1 HQ 193D Infantry Brigade (Panama)
ATTN: AFZU-FE
APO Miami 34004

2 Special Forces Detachment, Europe
ATTN: PBO
APO New York 09050

2 Engineer Representative
USA Research & Standardization Group (Europe)
Box 65
FPO 09510

1 Commander
Rock Island Arsenal
ATTN: SARRI-LPL
Rock Island, IL 61299-7300

1 HQDA
ODCSLOG
DALO-TSE
Room 1E588, Pentagon
Washington, DC 20310-0561

1 Plastics Technical Evaluation Center
ARRADCOM, Bldg 3401
Dover, NJ 07801

1 Commandant
US Army Engineer School
ATZA-CDD
Fort Belvoir, VA 22060

1 US Army AMCCOM
ATTN: Joseph Menke
1032 N. Thornwood
Davenport, IA 52804

1 President
US Aviation Test Board
ATTN: STBEG-PO
Fort Rucker, AL 36360

1 Commander
Headquarters, 39th Engineer Bn (Cbt)
Fort Devens, MA 01433

1 President
US Army Airborne, Communications & Electronics
ATTN: STEBF-ABTD
Fort Bragg, NC 28307

1 President
US Army Armor and Engineer Board
ATTN: ATZK-AE-PD-E
Fort Knox, KY 40121

1 Commander and Director
USA FESA
ATTN: FESA-TS
Fort Belvoir, VA 22060

1 HQ, USAEUR & Seventh Army
Deputy Chief of Staff, Engineer
ATTN: AEAEN-MT-P
APO New York 09430

1 Director
US Army TRADOC
Systems Analysis Activity
ATTN: ATAA-SL (Tech Lib)
White Sands Missile Range, NM 88002

BELVOIR RD&E CENTER

1 Commander STRBE-Z
1 Deputy Commander STRBE-ZD
1 Technical Director STRBE-ZT
1 Assoc Tech Dir (E&A) STRBE-ZTE
1 Assoc Tech Dir (R&D) STRBE-ZTR
1 Executive Officer STRBE-ZX
1 Sergeant Major STRBE-ZM
1 Advanced Systems Concept Dir STRBE-H
1 Program Planning Div STRBE-HP
1 Foreign Intelligence Div STRBE-HF
1 Systems and Concepts Div STRBE-HC
1 STRBE-V
12 STRBE-VC
3 Tech Reports Ofc STRBE-BPG
3 Security Ofc (for liaison officers) STRBE-S
2 Tech Lib STRBE-BT
1 Public Affairs Ofc STRBE-I
1 Ofc of Chief Counsel STRBE-L

DEPARTMENT OF THE NAVY

1 Director
Physics Program (421)
Office of Naval Research
Arlington, VA 22217

2 Commander
Naval Facilities Engineering Command
Department of the Navy
ATTN: Code 032-B
062
200 Stovall Street
Alexandria, VA 22332

1 US Naval Oceanographic Office
Navy Library/NSTL Station
Bay St. Louis, MS 39522

1 Library (Code L08A)
Civil Engineering Laboratory
Naval Construction Battalion Center
Port Hueneme, CA 93043

1 Director
Earth Physics Program
Code 464
Office of Naval Research
Arlington, VA 22219

1 Naval Training Equipment Center
ATTN: Technical Library
Orlando, FL 32813

3 Naval Sea Systems Command
ATTN: P. Schneider PMS377J1
Wasington, DC 20362-5101

1 Naval Air Development Center
ATTN: V. S. Agarwala, Code 6062
Warminster, PA 18974

3 David W. Taylor Naval Ship
Research & Development Center
ATTN: A. G. S. Morton
Code 2813
Annapolis, MD 21402

DEPARTMENT OF THE AIR FORCE

1 HQ USAF/RDPT
ATTN: Commander
Washington, DC 20330

1 HQ USAF/PREEU
Chief, Utilities Branch
Washington, DC 20330

1 HQ Air Force Engineering & Services Ctr
Technical Library FL7050
Tyndall AFB, FL 32403

1 US Air Force
Warner Robins Air Logistics Center
WR-ALC/MMEM
Warner-Robins AFB, GA 31098

1 Chief, Lubrications Branch
Fuels & Lubrications Div
ATTN: AFWAL/POSL
Wright-Patterson AFB, OH 45433

OTHERS

1 Department of Transportation
Library, FOB 10A, M494-6
800 Independence Ave, SW
Washington, DC 20591

U.S. GOVERNMENT PRINTING OFFICE: 1988- 201-454/82353

END
DATED
FILM
8-88
DTIC